NASA TECHNICAL NOTE

NASA TN D-3076

CALIBRATION OF CONICAL PRESSURE PROBES FOR DETERMINATION OF LOCAL FLOW CONDITIONS AT MACH NUMBERS FROM 3 TO 6

by John D. Norris

Langley Research Center
Langley Station, Hampton, Va.

NATIONAL AERONAUTICS AND SPACE ADMINISTRATION • WASHINGTON, D. C. • NOVEMBER 1965

NASA TN D-3076

CALIBRATION OF CONICAL PRESSURE PROBES FOR DETERMINATION OF LOCAL FLOW CONDITIONS AT MACH NUMBERS FROM 3 TO 6

By John D. Norris

Langley Research Center
Langley Station, Hampton, Va.

NATIONAL AERONAUTICS AND SPACE ADMINISTRATION

For sale by the Clearinghouse for Federal Scientific and Technical Information
Springfield, Virginia 22151 – Price $3.00

CALIBRATION OF CONICAL PRESSURE PROBES FOR DETERMINATION OF LOCAL FLOW CONDITIONS AT MACH NUMBERS FROM 3 TO 6*

By John D. Norris
Langley Research Center

SUMMARY

A wind-tunnel investigation was conducted to study the characteristics of six cones, which varied in diameter and cone angle, for use as pressure probes in the determination of Mach number, total pressure, and flow angles. The cones had four equally spaced static-pressure orifices on the surface and a total-pressure orifice at the apex. Pressure measurements were taken at Mach numbers of 3.0, 4.5, and 6.0 and angles of pitch up to about 20°. The tests were conducted at a Reynolds number per foot (per 30.5 cm) of approximately 0.85×10^{6}.

The results indicate that Mach number can be determined within approximately ±3 percent and flow angles within about $\pm 0.5^{\circ}$. The possible error in determining total pressure increases with increasing Mach number. Total pressure can be determined within approximately ±5 percent at a Mach number of 3.0 and ±13 percent at a Mach number of 6.0. These quoted accuracies are for the instrumentation and techniques employed in this investigation and are not necessarily the limiting capability of the method itself. In general, an iterative procedure is usually required in order to obtain the best accuracy with this method.

INTRODUCTION

At supersonic speeds, the capability of measuring local flow conditions (Mach number, total pressure, and flow angularities) by the use of a conical-shaped pressure probe with four equally spaced static-pressure orifices on the surface and a total-pressure orifice at the apex has been fairly well

*Part of the material presented in this report is included as a part of a thesis, entitled "Use of a Conical Pressure Probe for Determination of Local Flow Conditions at M = 3 to 6," submitted in partial fulfillment of the requirements for the degree of Master of Mechanical Engineering, University of Virginia, Charlottesville, Virginia, June 1965.

established up to a Mach number of 2.46. (See refs. 1 to 3.) With increased emphasis on higher speeds, it has become desirable to extend this capability of determining local flow conditions to hypersonic Mach numbers. If a conical pressure probe can be calibrated to determine Mach number, total pressure, and flow angularity at these higher speeds it could then be used to measure local flow conditions in the vicinity of hypersonic wing and body configurations. Knowledge of the local flow parameters would allow a better understanding of three-dimensional interferences in particular regions and also be of assistance in positioning and sizing of hypersonic inlets.

The present investigation was initiated to determine the feasibility of using a conical pressure probe with four equally spaced static-pressure orifices on the cone surface and a total-pressure orifice at the apex to measure local flow conditions at hypersonic speeds. A principal objective was to ascertain the accuracy with which Mach number, total pressure, and flow angularity could be determined from the five measured pressures. Considerations deemed important in selection of any probe may be enumerated and it is observed that some conflicts exist which may be expected to lead to compromise. Most of the considerations were given in reference 3 but are repeated herein together with additional items of special importance for hypersonic testing:

(1) A large cone included angle will delay flow separation to large flow angles.

(2) A large cone angle should provide maximum angle sensitivity because of the greater pressure difference between diametrically opposed orifices.

(3) A small cone angle and probe diameter should minimize the probe-induced disturbances.

(4) A large cone angle will provide cone surface pressures of large magnitude compared with that of the stream static pressure but will not necessarily give any substantial increase in the Mach number sensitivity of the device unless for the higher pressures greater instrument measurement accuracy can be achieved.

The present investigation included, therefore, measurement of the characteristics of several different conical probes varying in diameter from 0.125 inch to 0.500 inch and with cone half-angle from 15° to 25°. The test conditions were: Mach number range, from 3 to 6; angle-of-pitch range, up to approximately 20°; and roll-angle range, through 360°. The angle ranges permitted simulation of a broad range of effective downwash and sidewash flow combinations.

SYMBOLS

C_p surface pressure coefficient, $\frac{p_s - p_l}{q_l}$

M_1 Mach number ahead of normal shock wave at cone apex (local stream Mach number)

$\bar{p}_A$ arithmetic mean of four cone surface static pressures, $\frac{1}{4}\left(p_{s,a} + p_{s,b} + p_{s,c} + p_{s,d}\right)$

p_s static pressure on cone surface

$p_{t,1}$ total pressure ahead of normal shock wave at cone apex (local stream total pressure)

$p_{t,2}$ total pressure measured behind normal shock wave at cone apex (pitot pressure)

p_1 static pressure ahead of normal shock at cone apex (local stream static pressure)

$\left(\frac{\Delta p}{q_1}\right)_\epsilon$ difference in pressures between orifices c and a, $\frac{p_{s,c} - p_{s,a}}{q_1}$ (see fig. 2)

$\left(\frac{\Delta p}{q_1}\right)_\sigma$ difference in pressures between orifices d and b, $\frac{p_{s,d} - p_{s,b}}{q_1}$ (see fig. 2)

q_1 dynamic pressure ahead of normal shock at cone apex (local stream dynamic pressure)

u,v,w velocities in the X-, Y-, and Z-directions, respectively (see fig. 2)

V_1 velocity ahead of normal shock wave at cone apex, local stream velocity

X,Y,Z body axes (see fig. 2)

α angle of attack (see fig. 2)

β angle of sideslip (see fig. 2)

ϵ angle of downwash (see fig. 2)

θ angle of pitch of cone axis (see fig. 2)

σ angle of sidewash (see fig. 2)

ϕ angle of roll (see fig. 2)

Subscripts:

a,b,c,d	position of orifices on cone surface (see fig. 2)
θ	quantity at angle of pitch
$\theta=0$	quantity at zero angle of pitch

MODELS

Probes

Principal details of six cone-cylinder probes, which varied in cone diameter from 0.125 in. (0.318 cm) to 0.500 in. (1.27 cm) and in cone half-angle from 15° to 25°, are shown in figure 1 and table I. Four static-pressure orifices were circumferentially located 90° apart on the cone surface (fig. 2) and a total-pressure orifice was located at the cone apex.

Model Support

The conical pressure probes were mounted on a wedge-shaped strut that extended horizontally and on the tunnel center line across the tunnel test section as shown in figure 1(b). The strut had a 15° half-angle and provisions were made for mounting the probe models so that the static-orifice locations would be 2.15 in. (5.46 cm) ahead of the sharp-wedge leading edge. Three cones were mounted simultaneously for testing at the three indicated positions. The strut was pitched about an axis which passed through the station of the static-pressure orifices of the probes. Provisions were made to roll the probes about their longitudinal axis of symmetry which when coupled with pitch angle would permit simulation of different combinations of downwash and sidewash.

TESTS, INSTRUMENTATION, AND PRECISION

The tests were conducted in the 2-foot hypersonic facility at the Langley Research Center (ref. 4) at Mach numbers of 3, 4.5, and 6 and a Reynolds number per foot (per 30.5 cm) of approximately 0.85×10^6. Pressure measurements were obtained up to about ±20° angle of pitch and through 360° angle of roll. The investigation was conducted in such a way that each roll angle required a separate run.

Measurements of the pressures indicated by the five orifices on each probe were obtained by means of 2-psia (13.79-kN/m^2) transducers referenced to zero pressure. These pressure transducers were calibrated three times during the testing period and no changes in calibration sensitivities were noted. The total pressure of the tunnel was measured by a precision electromanometer. Also employed during the investigation was a radiation-type pressure-sensing instrument used to measure the static pressure in the tunnel test section.

The Mach number was set by using the appropriate ratio of the tunnel static pressure to the tunnel total pressure. Since both pressures were measured by high accuracy instrumentation all the tests were conducted under identical conditions. The Mach number was also checked from the ratio of the tunnel total pressure to the pitot pressure sensed by the pressure probe at zero angle of attack.

The approximate uncertainties of the test data and conditions, as estimated on the basis of random scatter and deviations from mean values, are as follows:

C_p	±0.030
$\bar{p}_A/p_{t,2}$	±0.003
$\Delta p/q_1$	±0.020
M_1	±0.010
θ, deg	±0.15
ϕ, deg	±0.15

These estimates are believed to afford reasonable indications of the instrumentation errors although it does not preclude the possibility of any unknown systematic errors or represent the maximum possible error that could occur. The angle settings are referenced to the tunnel center line.

PRESENTATION OF RESULTS AND METHODS

The basic data are presented in detail for probe 1 in figures 3 to 7. Typical data for all six different conical probes employed in this investigation have been presented in the form of plots of static-pressure differences against angle of pitch for representative test conditions. These data are shown in figures 7 to 12. The data for probe 1 appeared more consistent than those for the smaller tested probes and were used to prepare detailed analysis charts (figs. 13 and 14) from the results of figure 7. The problems encountered with the small probes were considered to be primarily of mechanical nature. These difficulties included ability to set and adjust pitch and roll angles with inadequate auxiliary devices and to achieve adequately settled pressures for the small orifice sizes and relatively large response chambers in the available measurement instrumentation. The inadequacies of testing technique should not be construed to mean that accurate data cannot be obtained with small probes, rather that sufficient care should be exercised in the selections of technique and instrumentation to insure satisfactory results.

From the basic data figures and analysis charts of probe 1 the Mach number, total pressure, and flow angles of previously undefined flow can be determined from the five probe pressure measurements. The general iterative procedure, discussed in detail in the following section, is as follows:

(1) Assume that the conical pressure probe is at zero angle of pitch and that from the ratio of arithmetic mean surface static pressures to the measured

pitot pressure $\bar{p}_A/p_{t,2}$ an approximate Mach number can be obtained from figure 4.

(2) From this initial Mach number and the measured pitot pressure $p_{t,2}$, the actual stream total pressure $p_{t,1}$ can be obtained from the theoretical total-pressure ratio across a normal shock. Next, from the total pressure and Mach number, the dynamic pressure q_1 can be obtained by using the isentropic relations.

(3) From the difference in pressures across the two sets of diametrically opposed orifices, the factor $\Delta p/q_1$ can be employed along with figures 13 and 14 to determine the flow angles.

(4) With the flow angularities known, a correction can be applied to $\bar{p}_A/p_{t,2}$ from step 1 to convert it to a zero angle-of-pitch value (fig. 5). Steps 1 and 2 are then repeated to obtain corrected values of Mach number and total pressure. A numerical example of this procedure is presented in the appendix.

DISCUSSION OF RESULTS

In order to assess the capability of the conical probe to determine the flow properties of an unknown flow field the experimental data are discussed to show how the particular desired property is influenced. Also, the iteration procedure is explained in further detail with regards to application and the resulting inaccuracies.

Cone Pressure Distribution

Figure 3 illustrates the pressure distribution around the surface of probe 1 for the three test Mach numbers and various angles of pitch. This figure demonstrates the approximate symmetry of the data at equivalent geometrical locations on opposite sides of the cone. Illustrated also is the expected result that at nominally zero angle of pitch the surface pressures are essentially constant and increasing angle of pitch increases the surface pressure on the windward surface and decreases the pressure on the leeward surface. Although all the pressure coefficients are positive, this trend would indicate that either further increases in the angle of pitch or decreases in the included cone half-angle would induce negative pressure coefficients on the leeward surface.

Determination of Mach Number

The determination of Mach number using a conical pitot-static pressure probe depends on the ratio of the surface static pressure to the pitot pressure and on the flow inclination (angles of pitch and roll). At zero angle of pitch

the Mach number can be computed from the ratio of the surface static pressure to the pitot pressure which in this investigation would be equivalent to $\bar{p}_A/p_{t,2}$. Figure 4 presents the experimental results of this condition for probe 1 and also the theoretical values (ref. 5) for a sharp-nose cone (no pitot-pressure orifice). The experimental results were lower than the theoretical values and it appeared that the experimental value at $M_1 = 4.5$ was relatively higher than the experimental values at $M_1 = 3$ and $M_1 = 6$ when compared with their corresponding theoretical values. Although not shown, this same result occurred to a lesser degree for the other five probes tested.

At angles of pitch, large variations in the static pressure occur around the circumference of the cone as previously shown in figure 3. It would be desirable to be able to combine the four measured pressures on the cone surface in such a manner as to provide a pressure which is essentially invariant to changes in angle of pitch. The results of references 1 and 2, which were restricted to Mach numbers near 1.60, indicate that for low angles of pitch the arithmetic average of the four static pressures is nearly constant. Reference 3 indicates that for $M_1 = 1.95$ the arithmetic average is constant up to angles of pitch of approximately 15°; for $M_1 = 2.46$, only up to about 8°. The variation of the ratio of the arithmetically averaged static pressures to the pitot pressure $\bar{p}_A/p_{t,2}$ with angle of pitch is presented in figure 5 for probe 1. For convenience $\bar{p}_A/p_{t,2}$ has been normalized to the zero pitch value. Geometrically similar roll angles were grouped together inasmuch as the averaged static pressures would be expected to be the same because of symmetry. The data indicate that increasing Mach number decreases the pitch range in which the ratio of the arithmetically averaged static pressures to the pitot pressure was constant. At $M_1 = 3$, $\bar{p}_A/p_{t,2}$ was constant within 1 percent up to approximately 5° of pitch; whereas, at $M_1 = 6$, $\bar{p}_A/p_{t,2}$ was constant within 1 percent only up to 2° or 3° of pitch. Figure 5 illustrates that angle of roll does not have a large effect on $\bar{p}_A/p_{t,2}$ although there is a slight decrease in $\bar{p}_A/p_{t,2}$ in going from $\phi = 0^\circ$ to $\phi = 40^\circ$ and from $\phi = 90^\circ$ to $\phi = 50^\circ$.

In general, the procedure for determining Mach number is first to assume $\theta = 0$. A first approximation of the Mach number M_1 is then obtained from figure 4 for the measured value of $\bar{p}_A/p_{t,2}$. The flow angles θ and ϕ are then determined by the method described in the section "Determination of Flow Angles." When θ and ϕ are known along with the first approximation of M_1, a correction factor for $\bar{p}_A/p_{t,2}$ is obtained from figure 5 and an equivalent value of $\bar{p}_A/p_{t,2}$ corresponding to $\theta = 0$ is calculated by a division of the measured value by this correction factor. In some cases better accuracy can be obtained by an interpolation between the Mach number curves in figure 5. For example, if the first approximated Mach number is 3.2 then the $M_1 = 3$ curve can be satisfactorily used but if the first approximated Mach number happened to be 5.25 then an average between the $M_1 = 4.5$ and $M_1 = 6.0$ curves would give a more accurate correction factor.

A second approximation of the Mach number can be obtained from figure 4 by using the equivalent $\bar{p}_A/p_{t,2}$ value for $\theta = 0$. Generally a second iteration is required but a third iteration would be unnecessary. If θ was found to be small so that the correction factor is near unity then the first approximation is sufficient.

Figure 4 shows that the slope of the curve of $\bar{p}_A/p_{t,2}$ plotted against Mach number decreases with increasing Mach number. This result is detrimental to the ability to determine Mach number accurately in that any small uncertainty in $\bar{p}_A/p_{t,2}$ could introduce a significant error in Mach number at the higher Mach numbers. This technique or procedure would therefore be of limited usefulness at higher hypersonic speed ranges. Also shown in figure 4 is the ratio of free-stream static pressure to pitot pressure behind a normal shock, which illustrates the relative magnitude of the cone surface pressure to the free-stream static pressure.

The error in determining Mach number with probe 1 by use of figures 4 and 5 was estimated to be ± 0.06 at $M = 3$, ± 0.12 at $M = 4.5$, and ± 0.20 at $M = 6.0$.

Determination of Total Pressure

The total pressure $p_{t,1}$ is a function of pitot pressure $p_{t,2}$, Mach number M_1, and angle of pitch. The assumption is made that at zero angle of pitch the ratio of the pitot pressure to the total pressure is equal to the theoretical total-pressure ratio across a normal shock wave. Once the Mach number is known from the preceding section, $p_{t,2}/p_{t,1}$ can be found for that Mach number using the theoretical tables of reference 6. The total pressure can then be obtained since the measured pitot pressure is known.

The effect of Mach number and angle of pitch on the measured pitot pressure is shown in figure 6 for probe 1. The results indicate that, for $M_1 = 3$ and $M_1 = 4.5$, the angle-of-pitch range tested had a negligible effect on the measured pitot pressure, or that at $\theta = 20^\circ$ the probe measured the same pitot pressure as it would have at $\theta = 0$. At Mach number 6, however, the measured pitot pressure is no longer independent of pitch angle and above $\theta = 14^\circ$ the pitot pressure must be divided by an appropriate correction factor from the calibration using figure 6 in order to obtain an equivalent value of $p_{t,2}$ at $\theta = 0$.

Since the ability to determine total pressure depends on Mach number, it is evident from the preceding discussion of Mach number that the accuracy of determining total pressure diminishes with increasing Mach number. The estimated possible error in determining total pressure is 5 percent at $M_1 = 3.0$, 10 percent at $M_1 = 4.5$, and 13 percent at $M_1 = 6.0$.

Determination of Dynamic Pressure

Since the dynamic pressure q_1 is calculated from Mach number and total pressure it would appear that the errors associated with M_1 and $p_{t,1}$ would be accumulative and the factor $\Delta p/q_1$ could not be used with any degree of confidence in determining flow angles. However, this is not so in that any errors in Mach number and total pressure will counterbalance each other in the calculation of the dynamic pressure and in actuality q_1 can be determined within 1/2 percent.

The fact that q_1 can be determined with a high degree of accuracy suggests the possibility of one further iteration using $q_1/p_{t,2}$ to get a better indication of Mach number and in turn total pressure. This however is not practical because $q_1/p_{t,2}$ is less sensitive than $\bar{p}_A/p_{t,2}$ (fig. 4) to Mach number.

Determination of Flow Angles

The flow angles can be determined from the pressure differences across diametrically opposed orifices. The variation of the difference in static-pressure coefficient across opposed orifices with angle of pitch for the various Mach numbers are presented in figures 7 to 12 for probes 1 to 6, respectively. Because of wind-tunnel stream angularity, support misalinement, and probe asymmetry all the curves do not pass through the origin. Comparing probe 1 (fig. 7), probe 2 (fig. 8), and probe 3 (fig. 9) indicates the expected result that increasing the included cone angle causes an increase in the pressure difference between the sets of diametrically opposed orifices. The curves were approximately linear at $M = 3$ but as the Mach number increased to 6 some curvature is shown.

In order to facilitate the determination of θ and ϕ from measurements of $\left(\frac{\Delta p}{q}\right)_\epsilon$ and $\left(\frac{\Delta p}{q}\right)_\sigma$, the results of figure 7 have been combined in figure 13 to give plots of $\left(\frac{\Delta p}{q_1}\right)_\epsilon$ against $\left(\frac{\Delta p}{q_1}\right)_\sigma$ for various values of θ and ϕ for probe 1. The curves of figure 7 were first adjusted to eliminate the effects of tunnel stream angularity, support misalinement, and probe asymmetry.

Because of symmetry, curves which represent an average of the data are shown in one quadrant only. Information for the other quadrants can then be determined from this figure provided the proper sign convention is used as indicated.

The downwash ϵ and sidewash σ can be determined directly from their relation with angle of pitch θ and angle of roll ϕ which is

$$\tan \epsilon = -\tan \theta \cos \phi$$

$$\tan \sigma = \tan \theta \sin \phi$$

Figure 14 is the trigonometric conversion from figure 13 and presents $\left(\frac{\Delta p}{q_1}\right)_\epsilon$ plotted against $\left(\frac{\Delta p}{q_1}\right)_\sigma$ for various angles of downwash ϵ and angles of sidewash σ. Comparison of figures 14(a), 14(b), and 14(c) demonstrates a marked similarity between the charts for the three Mach numbers.

The procedure for determining flow angles is to find the difference between the measured surface static pressures and with the calculated value of dynamic pressure q_1 the factors $\left(\frac{\Delta p}{q_1}\right)_\epsilon$ and $\left(\frac{\Delta p}{q_1}\right)_\sigma$ can be obtained. Using these factors along with figures 13 and 14, the values of θ, ϕ, ϵ, and σ can be found. Any necessary correction can then be applied as previously discussed. The error in determining flow angles is estimated to be $\pm 0.5^\circ$.

CONCLUDING REMARKS

A wind-tunnel investigation was conducted to study the characteristics of six different conical probes for use in determining local flow conditions. Charts were prepared for one of the probes that enable the determination of local Mach number, total pressure, and flow angularity from probe-indicated pressures. Pressure measurements were taken at Mach numbers of 3.0, 4.5, and 6.0 and at angles of pitch up to about 20°.

The results indicate that Mach number can be determined within approximately ± 3 percent and flow angles within about $\pm 0.5^\circ$. The possible error in determining total pressure, however, increases with increasing Mach number. Total pressure can be determined within approximately ± 5 percent at a Mach number of 3.0 and ± 13 percent at a Mach number of 6.0. These quoted accuracies are for the instrumentation and techniques employed in this investigation and are not necessarily the limiting capability of the method itself. In general an iterative procedure is usually required in order to obtain the best accuracy with this method.

Langley Research Center,
National Aeronautics and Space Administration,
Langley Station, Hampton, Va., June 25, 1965.

APPENDIX

NUMERICAL EXAMPLE

The procedure used in determining the Mach number, total pressure, and flow directions of a previously unknown flow field from the measured pitot pressure and four static pressures on the cone surface is illustrated by the following numerical example. The measured pressures are

$$p_{s,a} = 10.0 \text{ mm Hg}$$

$$p_{s,b} = 11.22 \text{ mm Hg}$$

$$p_{s,c} = 26.7 \text{ mm Hg}$$

$$p_{s,d} = 25.52 \text{ mm Hg}$$

$$p_{t,2} = 97.16 \text{ mm Hg}$$

Step 1: The arithmetic mean of the four static pressures is

$$\bar{p}_A = \frac{1}{4}\left(p_{s,a} + p_{s,b} + p_{s,c} + p_{s,d}\right) = 18.36 \text{ mm Hg}$$

The ratio of this arithmetic mean static pressure to the pitot pressure is

$$\frac{\bar{p}_A}{p_{t,2}} = \frac{18.36}{97.16} = 0.189$$

Assuming that $\theta = 0$, the first approximated Mach number of 3.75 is obtained from figure 4.

Step 2: For $\theta = 0$, the total pressure ratio $p_{t,2}/p_{t,1}$ is given by the theoretical normal shock-wave relations tabulated in reference 6. For $M_1 = 3.75$,

$$\frac{p_{t,2}}{p_{t,1}} = 0.1717$$

Therefore,

$$p_{t,1} = \frac{\left(p_{t,2}\right)_\theta}{\left(\frac{p_{t,2}}{p_{t,1}}\right)_{\theta=0}} = \frac{97.16}{0.1717} = 566 \text{ mm Hg}$$

The dynamic pressure q_1 is obtained from the theoretical isentropic flow relation $q_1/p_{t,1}$ which is also tabulated in reference 6. For $M_1 = 3.75$,

$$\frac{q_1}{p_{t,1}} = 0.09098$$

and the dynamic pressure q_1 is

$$q_1 = \frac{q_1}{p_{t,1}} p_{t,1} = (0.09098)(566) = 51.5 \text{ mm Hg}$$

Step 3: Dividing the measured static-pressure difference across both pairs of orifices by the dynamic pressure gives

$$\left(\frac{\Delta p}{q_1}\right)_\epsilon = \frac{p_{s,c} - p_{s,a}}{q_1} = \frac{26.7 - 10}{51.5} = 0.324$$

$$\left(\frac{\Delta p}{q_1}\right)_\sigma = \frac{p_{s,d} - p_{s,b}}{q_1} = \frac{25.52 - 11.22}{51.5} = 0.278$$

The downwash and sidewash angles can now be obtained from figure 14 by using the factors $\left(\frac{\Delta p}{q_1}\right)_\epsilon$ and $\left(\frac{\Delta p}{q_1}\right)_\sigma$. Since $M_1 = 3.75$, however, it is not immediately evident whether the figure for $M_1 = 3$ or $M_1 = 4.5$ would provide the better results. It is subsequently shown that any angle-of-pitch effects cause the initial approximated Mach number to be low; therefore, when figure 14(b) for $M = 4.5$ is used,

$$\epsilon = -7.8^\circ$$

$$\sigma = 6.4^\circ$$

Also in order to correct the Mach number for flow angularity effects, the angles of pitch and roll must be known. From figure 13(b),

$$\phi = 40^\circ$$

$$\theta = 10^\circ$$

Step 4: Once the pitch and roll angles are known, the correction factor can be obtained from figure 5. Interpolating between the curves for $M = 3$ and $M = 4.5$, the correction factor is

$$\frac{\left(\frac{\bar{p}_A}{p_{t,2}}\right)_\theta}{\left(\frac{\bar{p}_A}{p_{t,2}}\right)_{\theta=0}} = 1.04$$

The corrected value of $\bar{p}_A/p_{t,2}$ corresponding to $\theta = 0$ is

$$\frac{\bar{p}_A}{p_{t,2}} = \frac{\left(\frac{\bar{p}_A}{p_{t,2}}\right)_\theta}{\frac{\left(\frac{\bar{p}_A}{p_{t,2}}\right)_\theta}{\left(\frac{\bar{p}_A}{p_{t,2}}\right)_{\theta=0}}} = \frac{0.189}{1.04} = 0.182$$

Now knowing the corrected value of $\bar{p}_A/p_{t,2}$ and using figure 4, the iterated Mach number is found to be 4.0.

Step 5: Using the second approximation for Mach number, step 2 is repeated. From reference 6 at $M_1 = 4.0$,

$$\frac{p_{t,2}}{p_{t,1}} = 0.1388$$

Therefore,

$$p_{t,1} = \frac{97.16}{0.1388} = 700 \text{ mm Hg}$$

Had it been found that the air speed was around $M_1 = 6$ with large flow angles then $p_{t,2}$ would have had to be corrected to $(p_{t,2})_{\theta=0}$ using figure 6 before being used to determine $p_{t,1}$. When the new values of Mach number and total pressure are used the corrected dynamic pressure is

$$q_1 = \left(\frac{q_1}{p_{t,1}}\right)p_{t,1} = (0.07376)(700) = 51.6 \text{ mm Hg}$$

Since there was little change in dynamic pressure the previously determined flow angles need no correction. Consequently from the five conical probe pressure measurements the local flow-field properties are

$$M_1 = 4.0$$

$$p_{t,1} = 700 \text{ mm Hg}$$

$$\epsilon = -7.8^\circ$$

$$\sigma = 6.4^\circ$$

REFERENCES

1. Cooper, Morton; and Webster, Robert A.: The Use of an Uncalibrated Cone for Determination of Flow Angles and Mach Numbers at Supersonic Speeds. NACA TN 2190, 1951.

2. Davis, Theodore: Development and Calibration of Two Conical Yawmeters. Meteor Rept. UAC-43, United Aircraft Corp., Oct. 1949.

3. Centolanzi, Frank J.: Characteristics of a 40° Cone for Measuring Mach Number, Total Pressure, and Flow Angles at Supersonic Speeds. NACA TN 3967, 1957.

4. Stokes, George M.: Description of a 2-Foot Hypersonic Facility at the Langley Research Center. NASA TN D-939, 1961.

5. Sims, Joseph L.: Tables for Supersonic Flow Around Right Circular Cones at Zero Angle of Attack. NASA SP-3004, 1964.

6. Ames Research Staff: Equations, Tables, and Charts for Compressible Flow. NACA Rept. 1135, 1953. (Supersedes NACA TN 1428.)

TABLE I.- CONE DESIGNATION

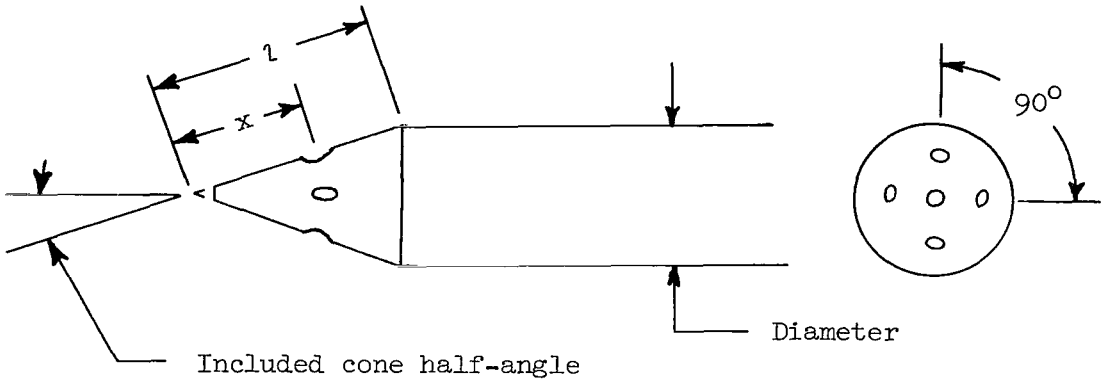

Probe	Diameter,		Included cone half-angle, deg	x/l	Orifice diameter,		Position tested on strut (fig. 1(a))
	in.	cm			in.	cm	
1	0.50	1.27	20	0.603	0.052	0.132	2
2	.50	1.27	15	.590	.052	.132	1
3	.50	1.27	25	.614	.052	.132	3
4	.25	.64	15	.629	.025	.064	1
5	.25	.64	20	.655	.025	.064	3
6	.125	.318	20	.760	.0135	.0343	2

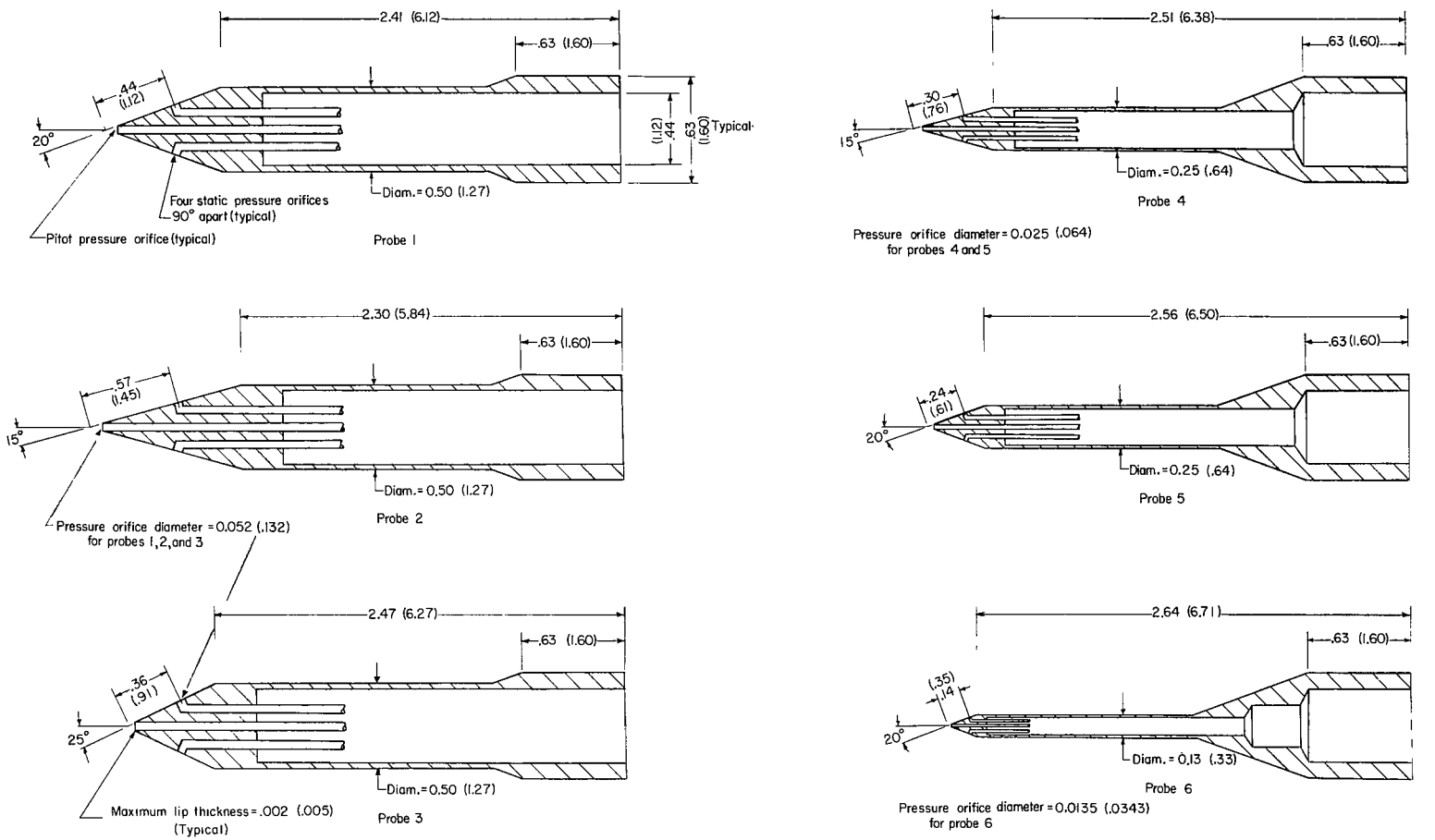

(a) Conical pressure probe models.

Figure 1.- Test apparatus. All dimensions are in inches (centimeters) unless otherwise noted.

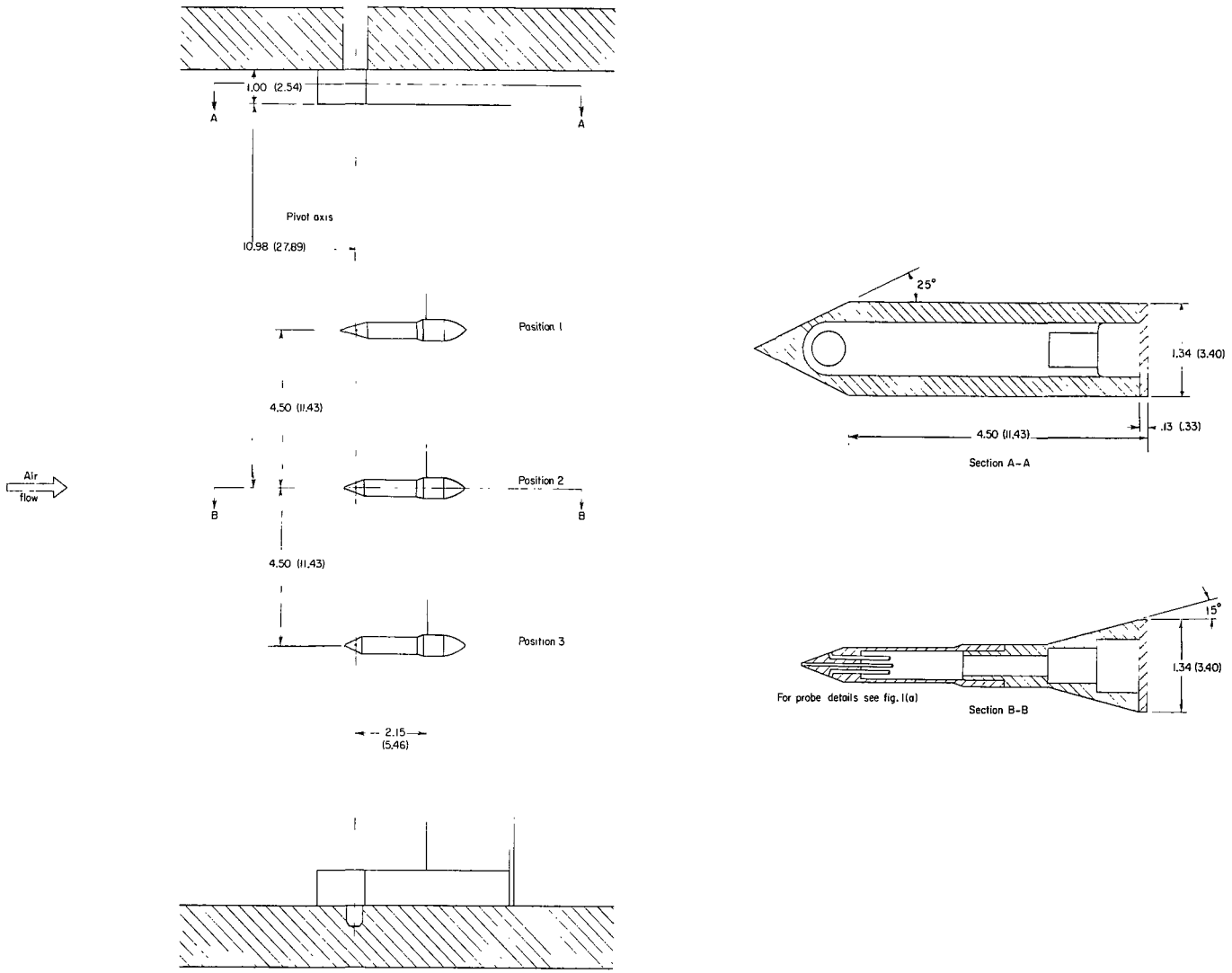

(b) Model support assembly.

Figure 1.- Concluded.

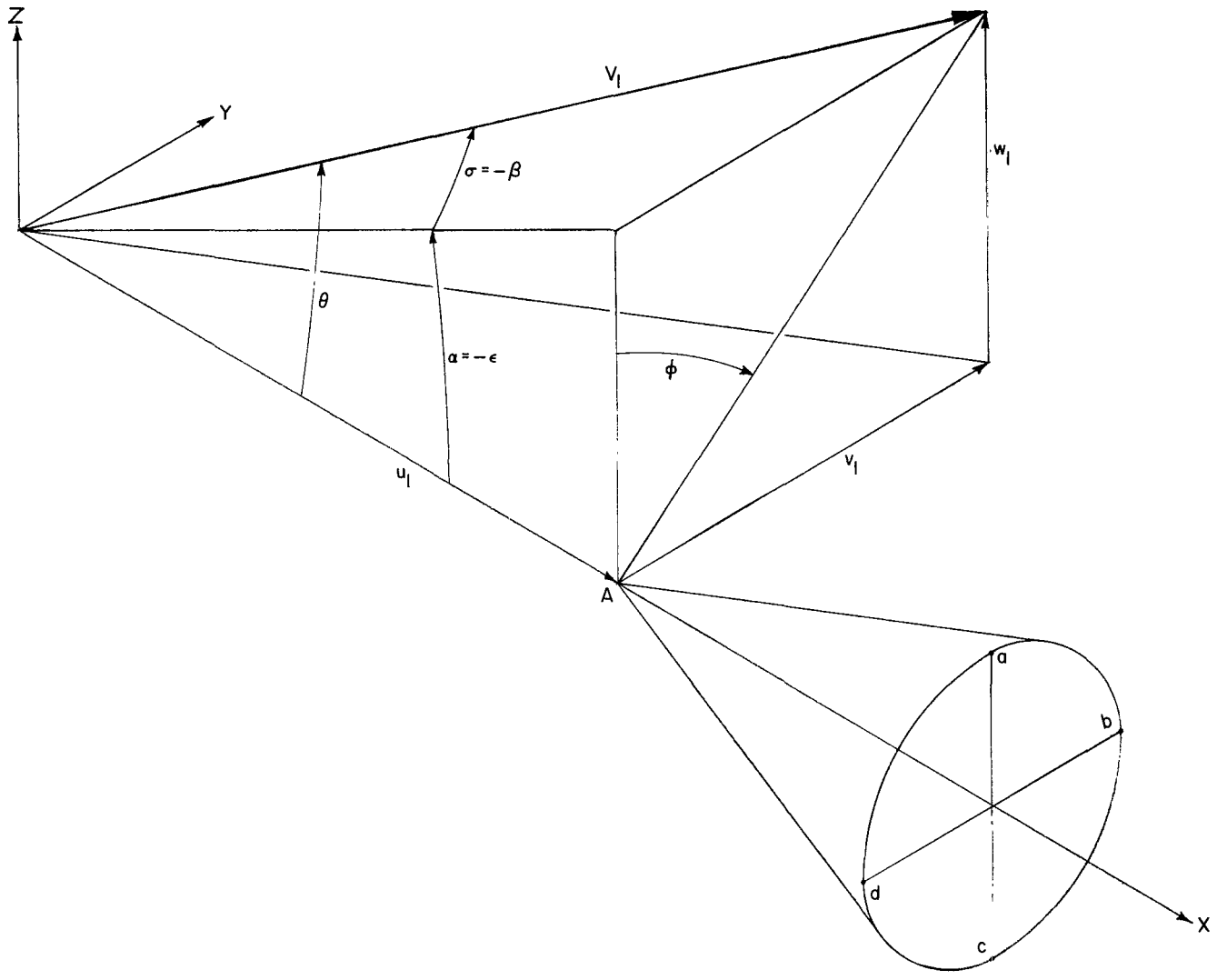

Figure 2.- Orifice designation and angle notation.

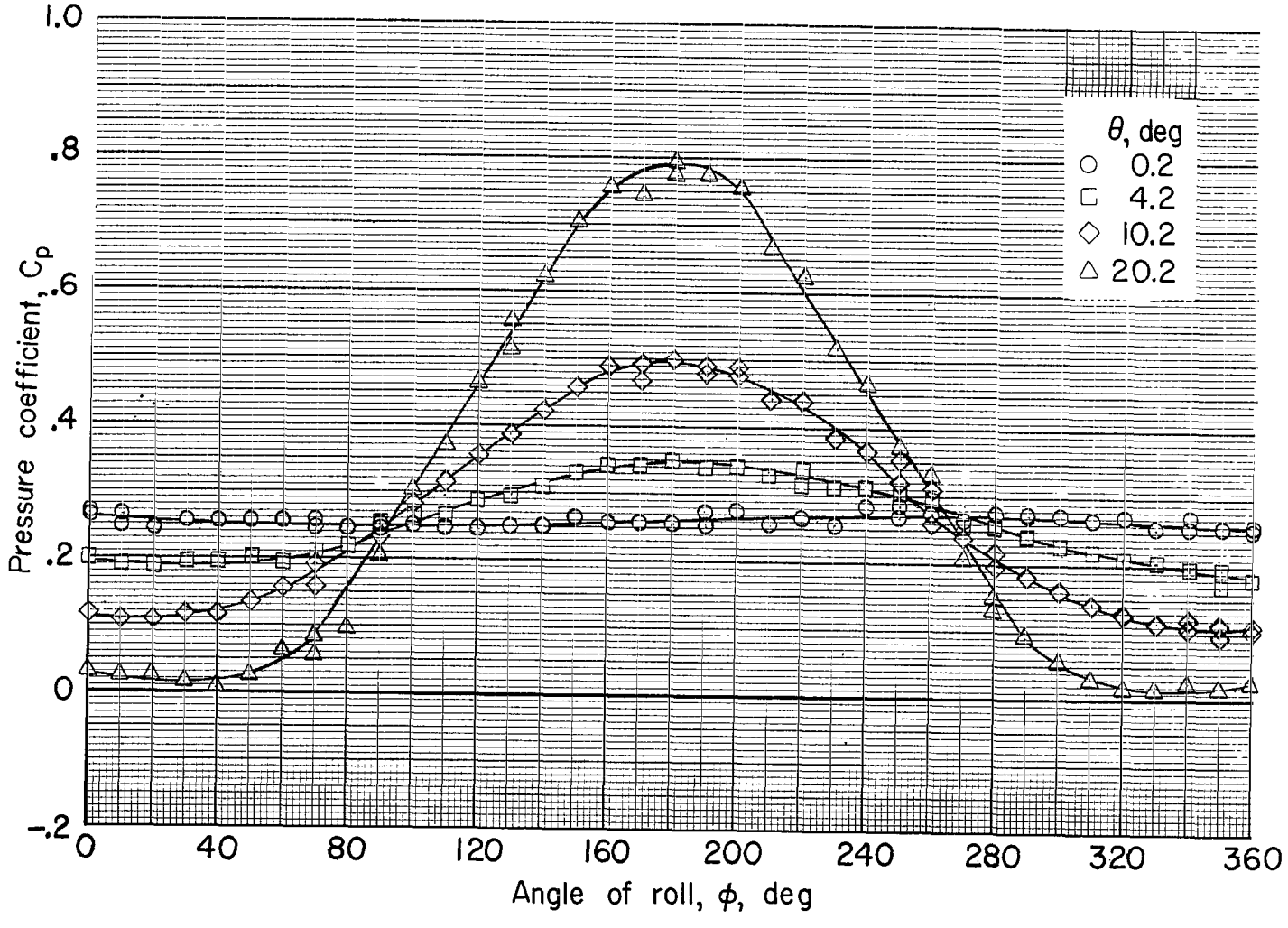

(a) $M_1 = 3.0$.

Figure 3.- Circumferential pressure distribution on surface of cone. Probe 1.

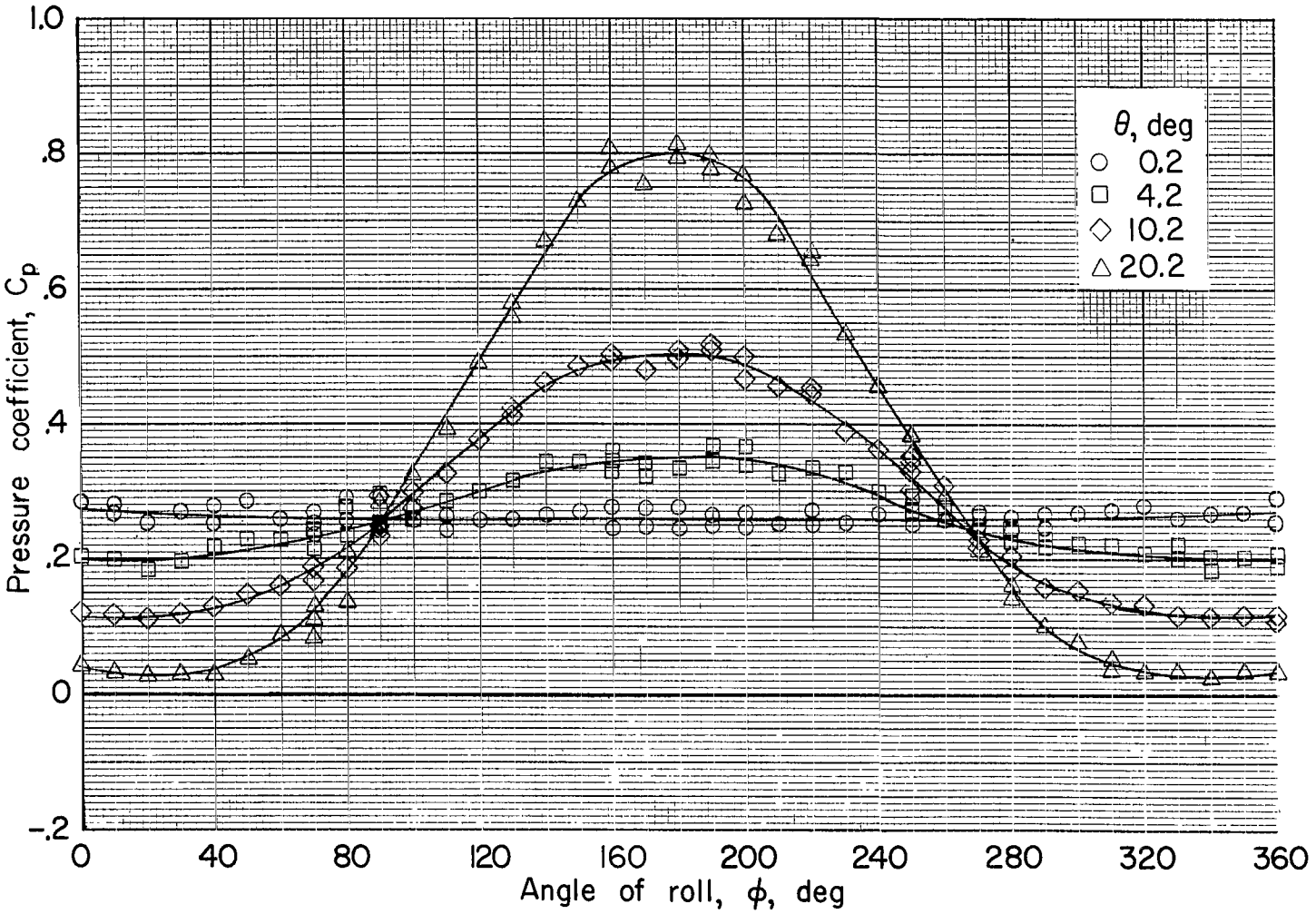

(b) $M_1 = 4.5$.

Figure 3.- Continued.

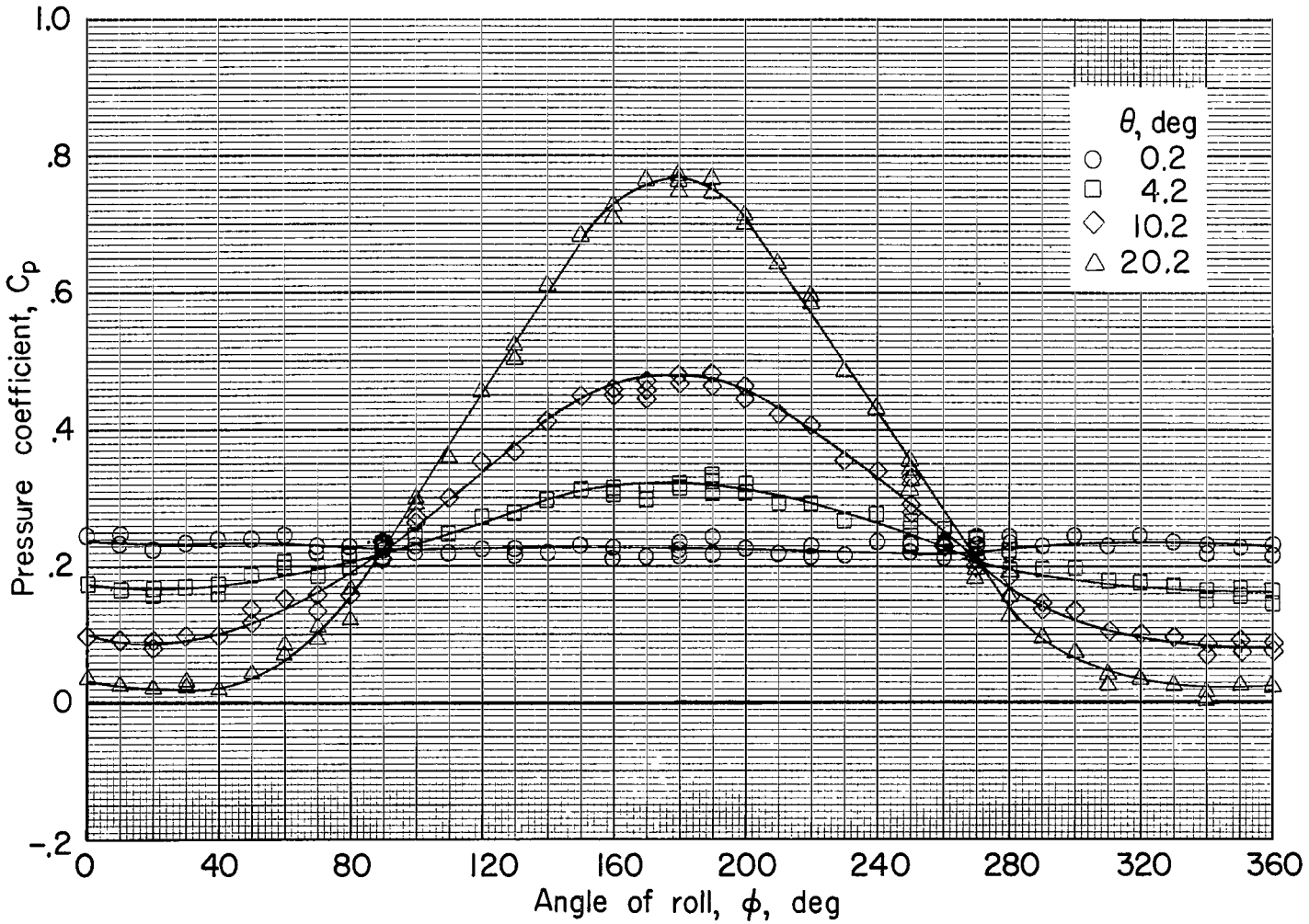

(c) $M_1 = 6.0$.

Figure 3.- Concluded.

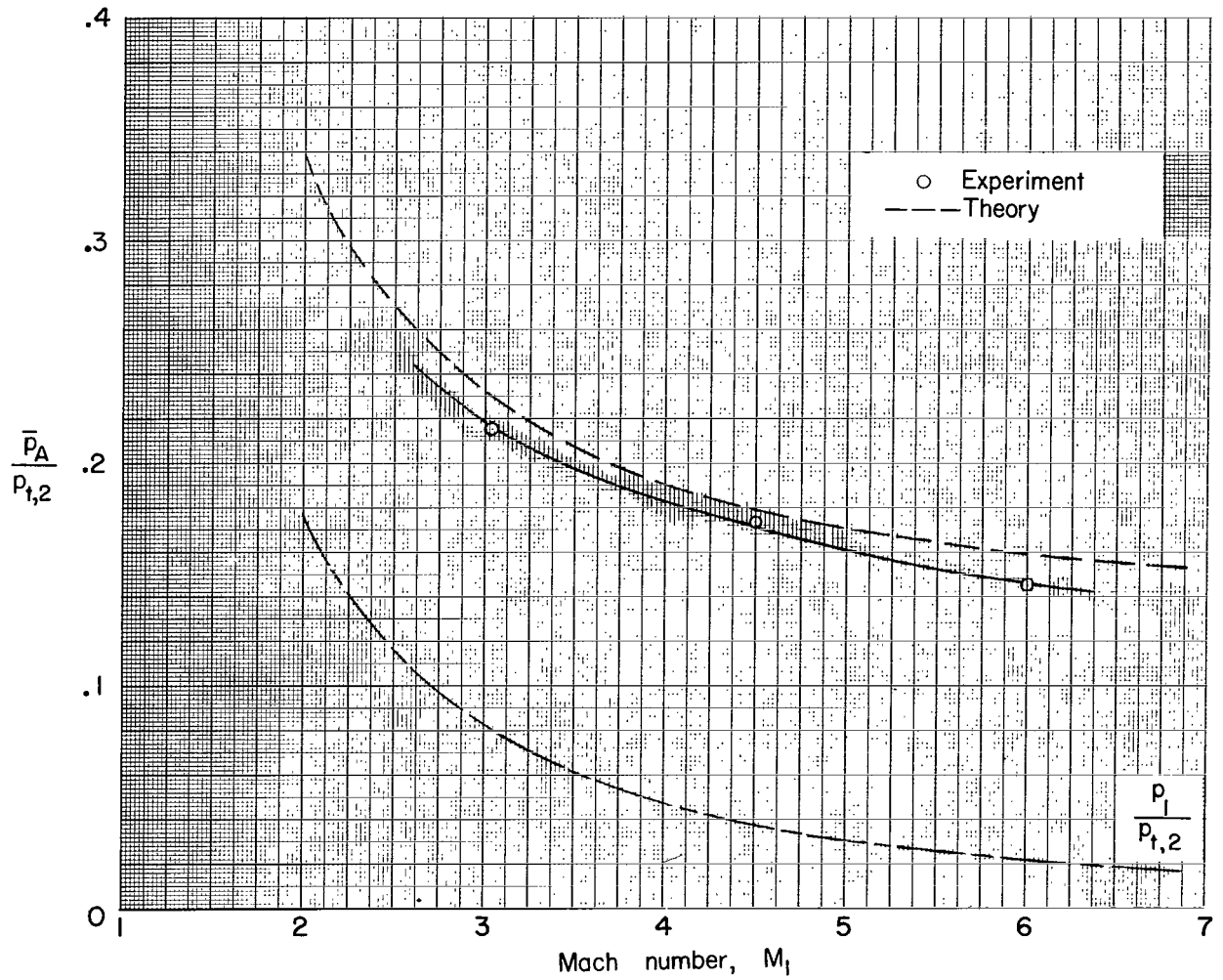

Figure 4.- Variation of static-to-pitot pressure ratio with Mach number at zero angle of pitch. Probe 1.

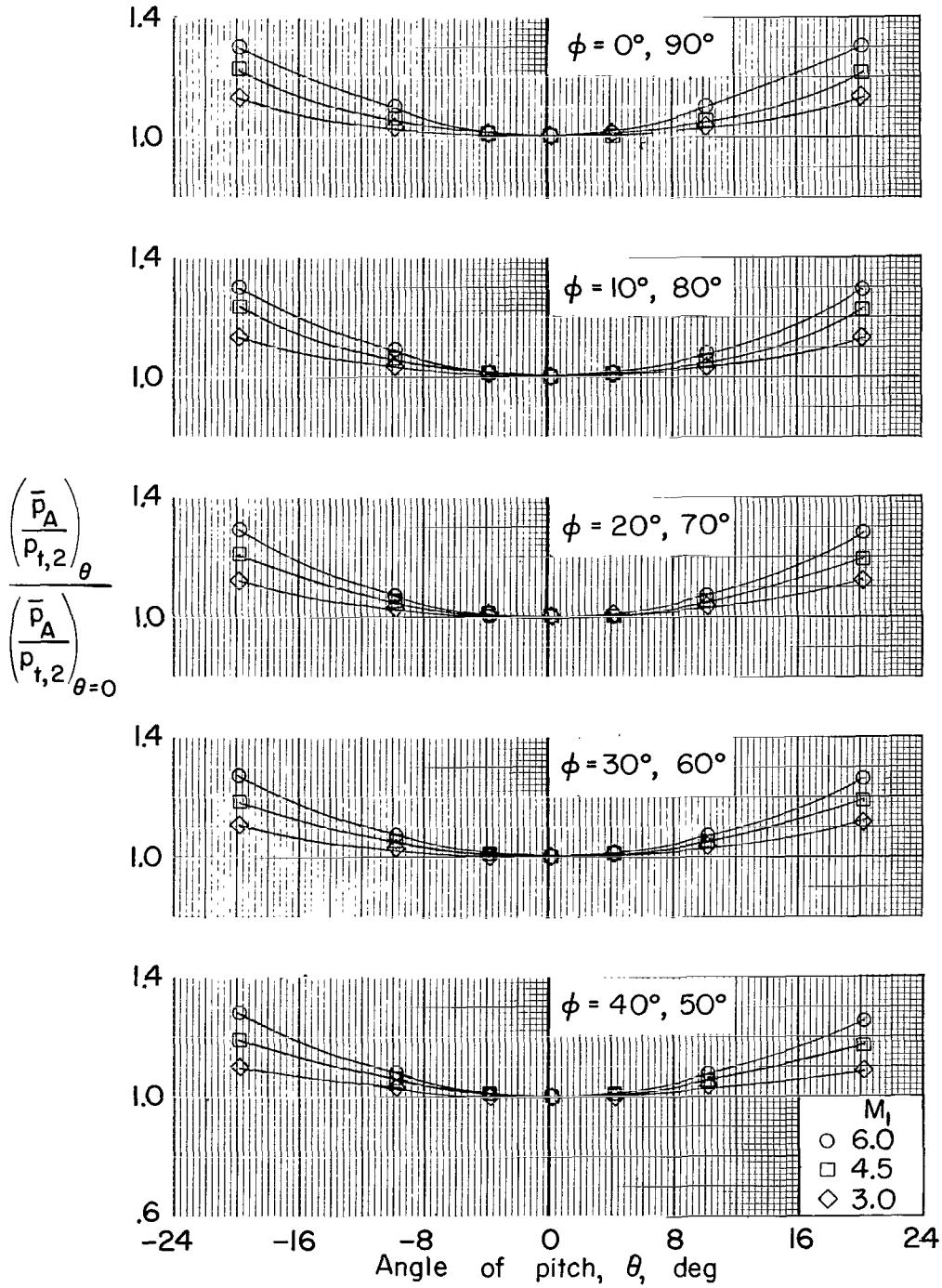

Figure 5.- Effect of angle of pitch on ratio of average static pressure to pitot pressure. Probe 1.

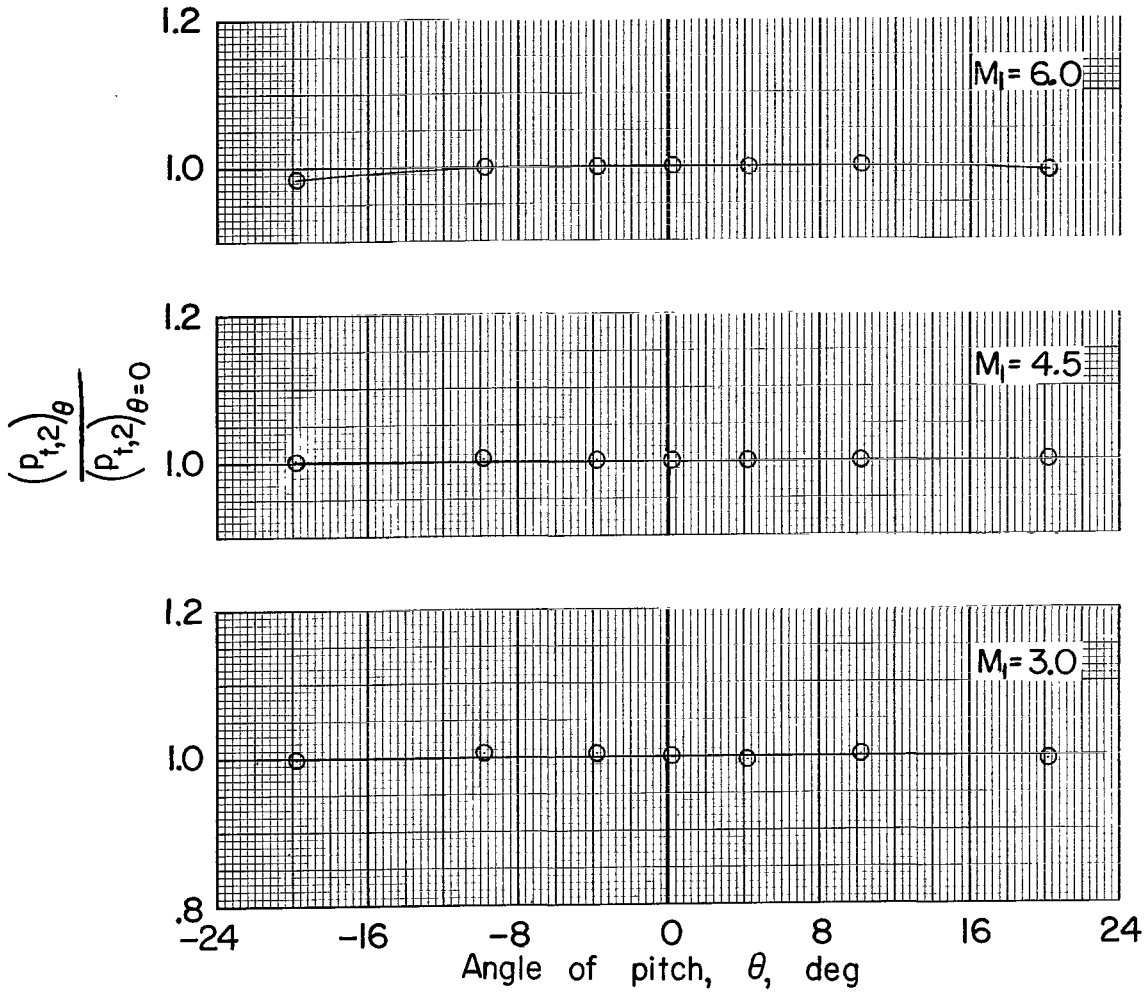

Figure 6.- Effect of angle of pitch on pitot pressure. Probe 1.

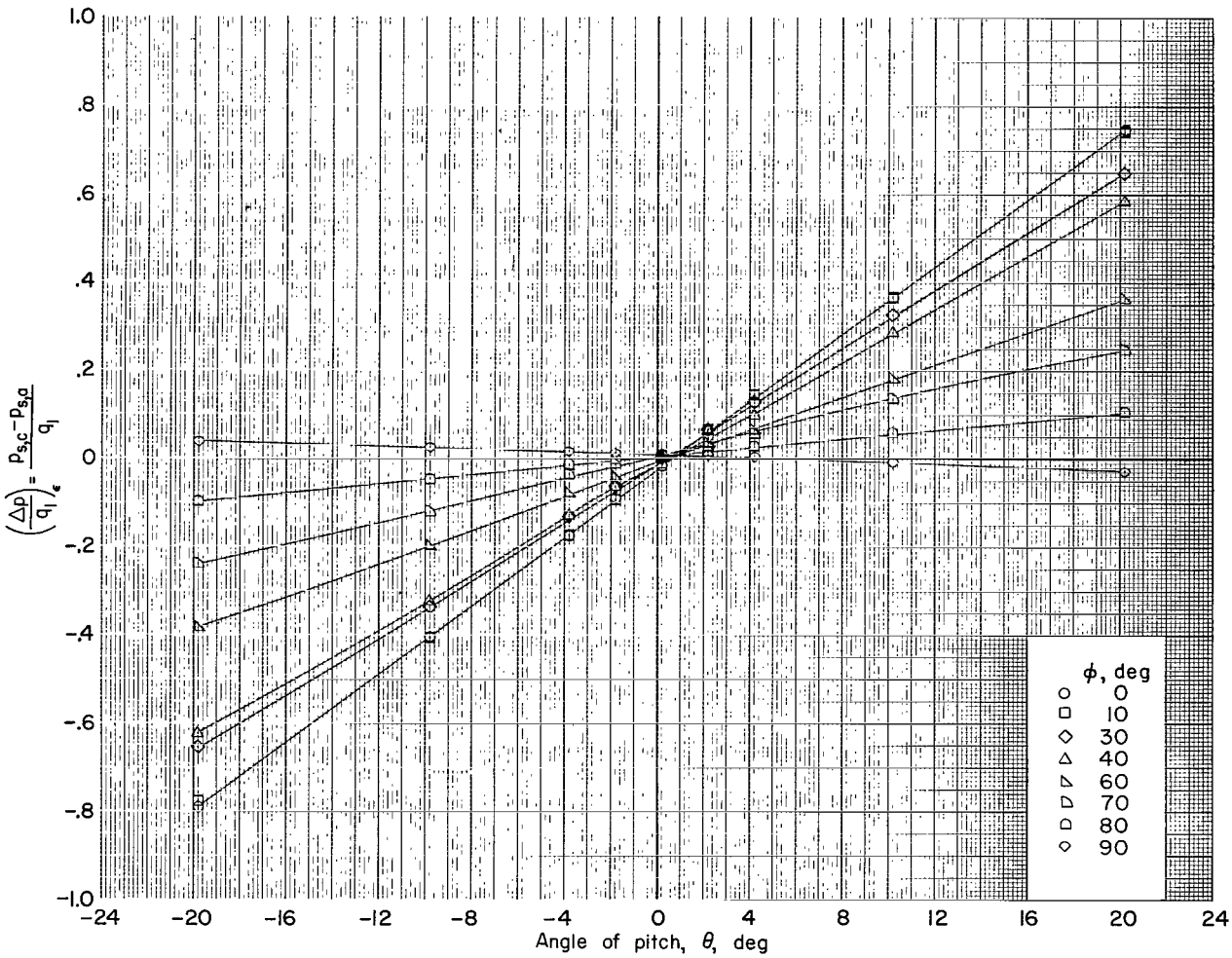

(a) $M_1 = 3.0$; orifices a and c.

Figure 7.- Variation of static pressure differences with angle of pitch. Probe 1.

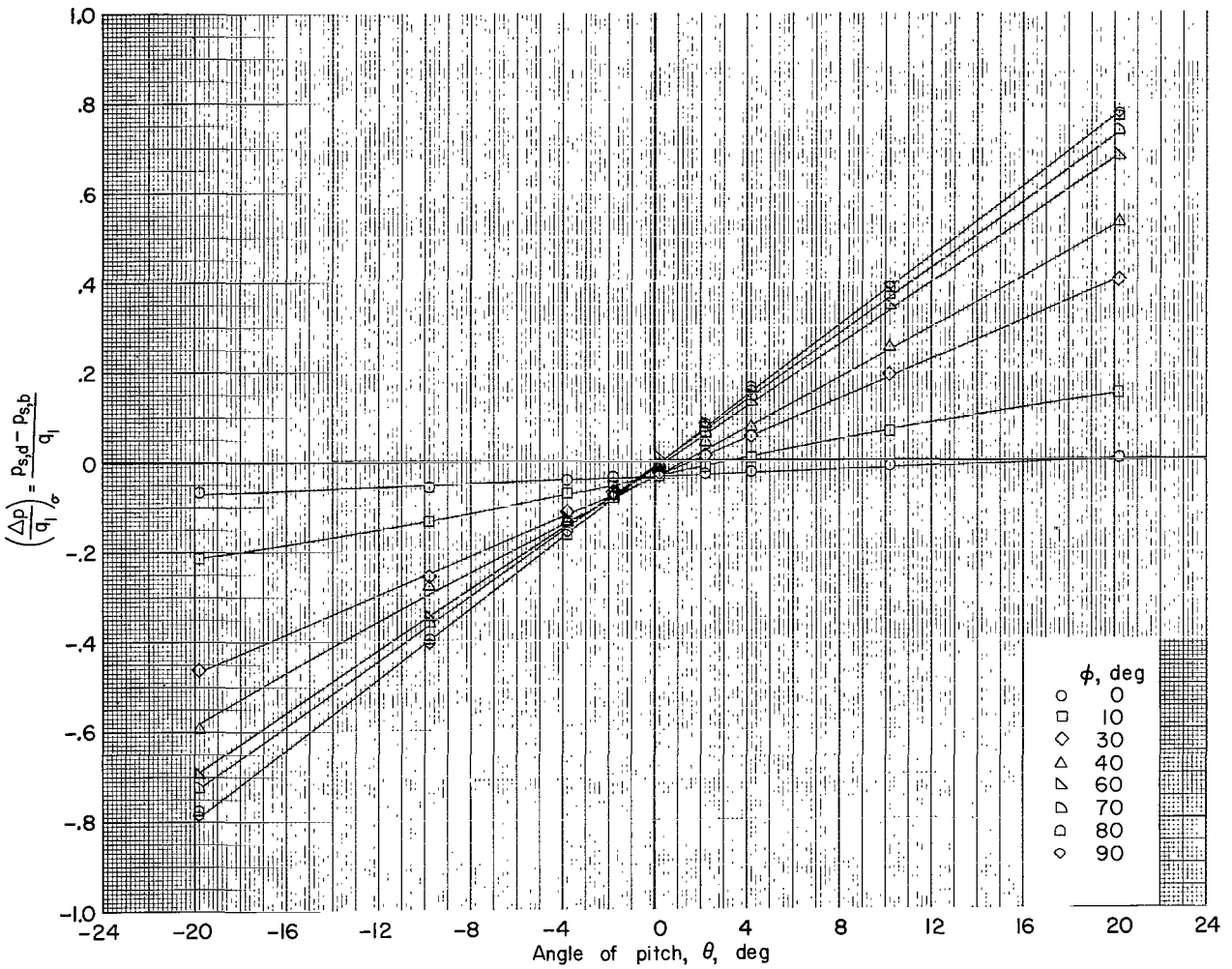

(b) $M_1 = 3.0$; orifices b and d.

Figure 7.- Continued.

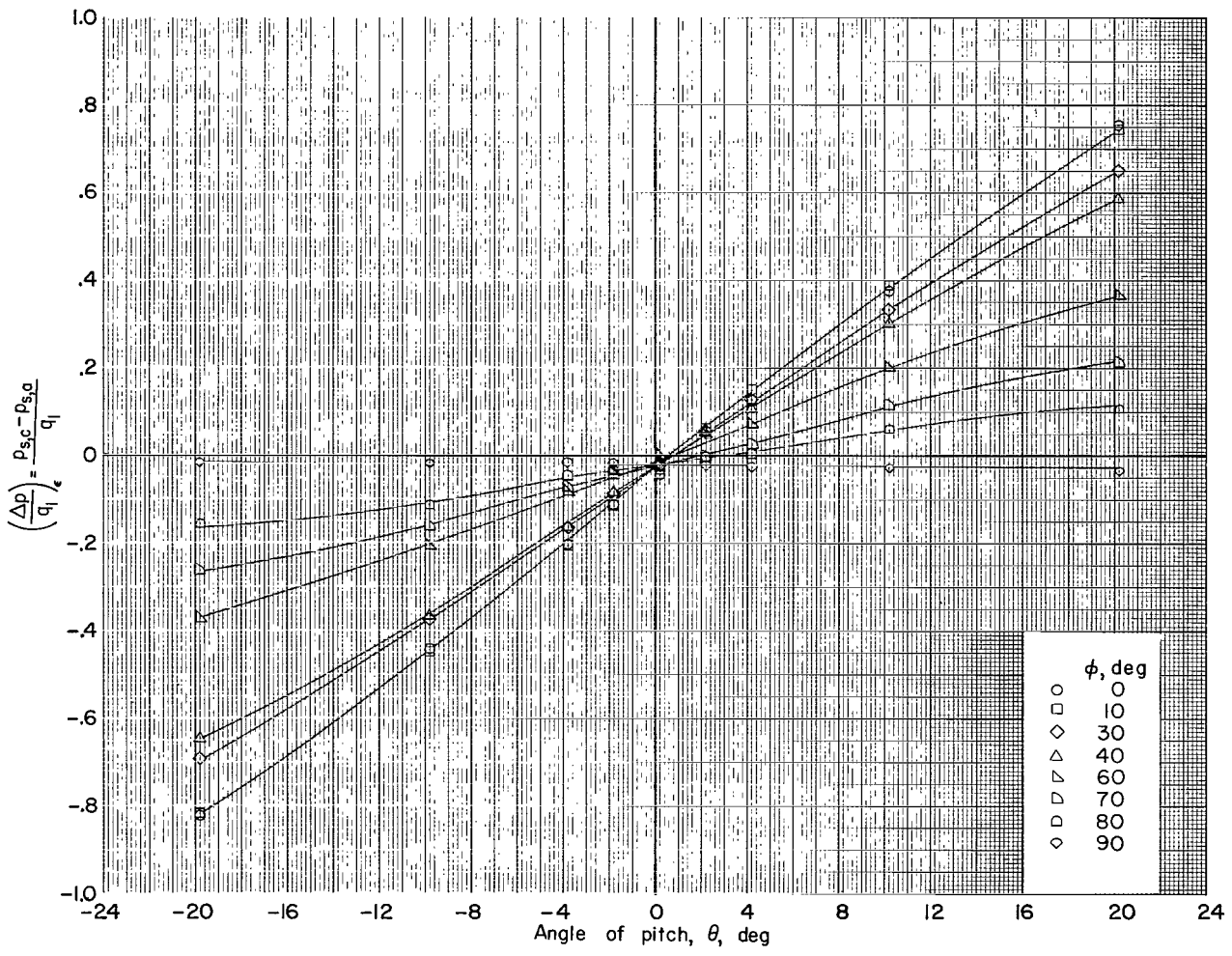

(c) M_1 = 4.5; orifices a and c.

Figure 7.- Continued.

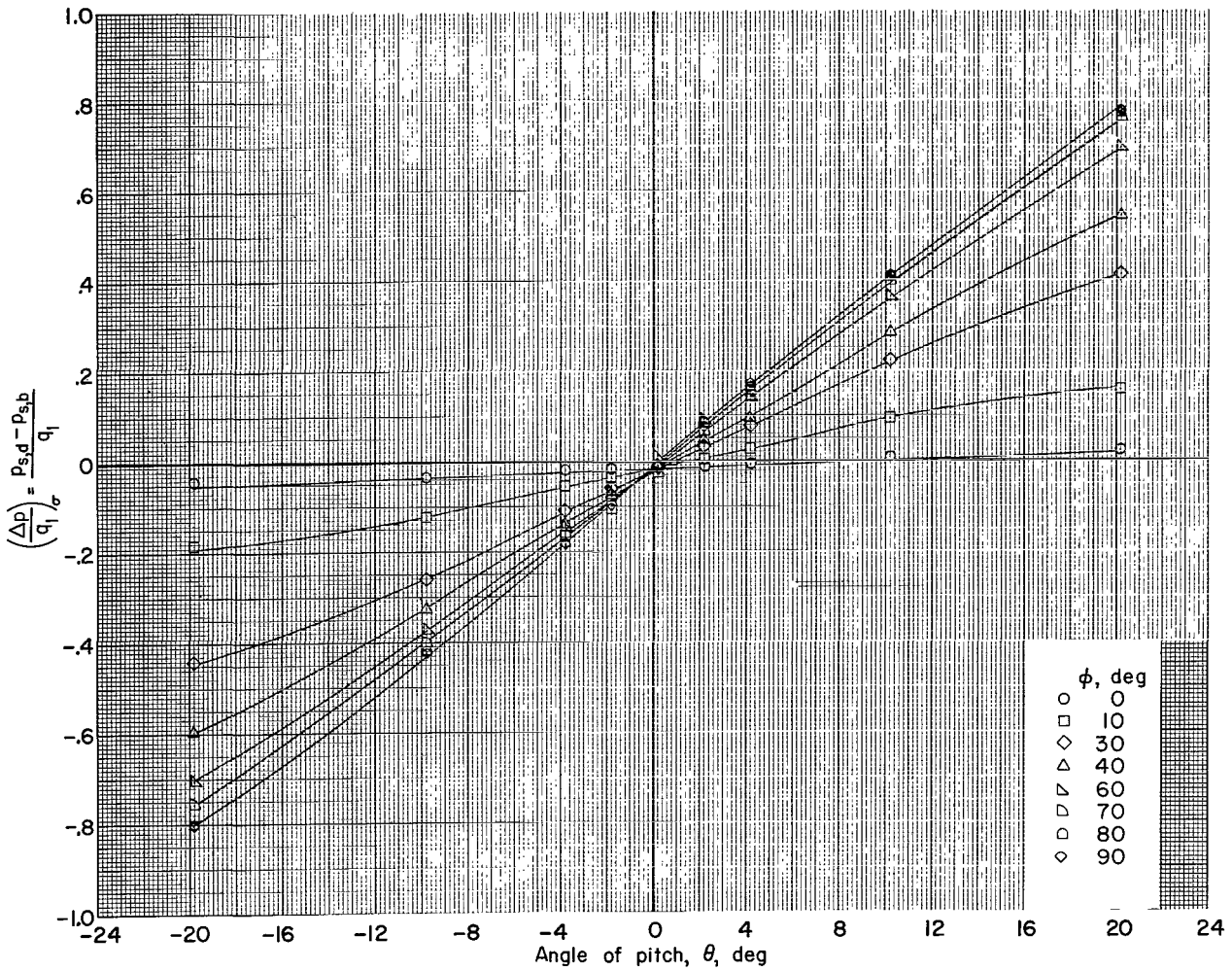

(d) M_1 = 4.5; orifices b and d.

Figure 7.- Continued.

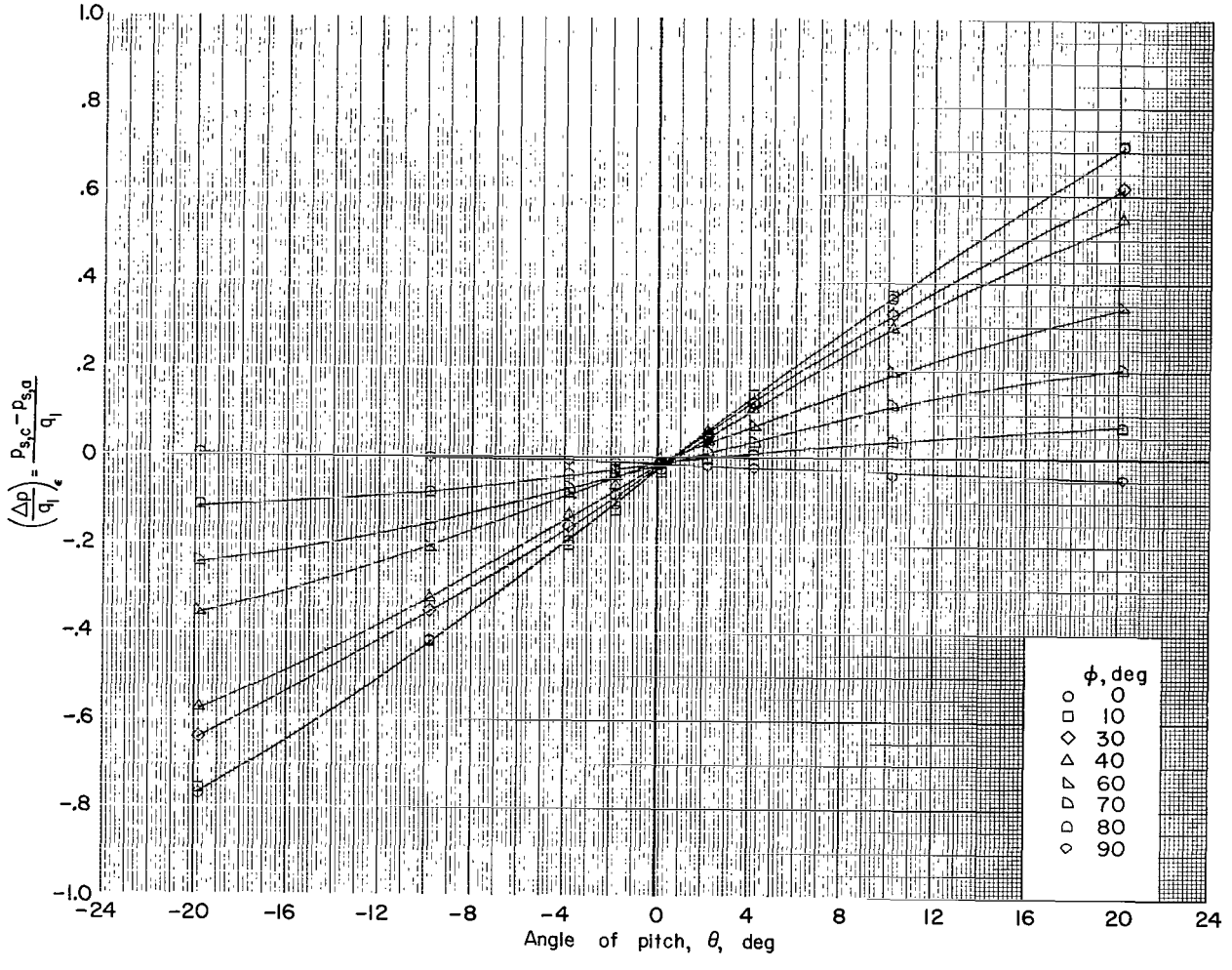

(e) $M_1 = 6.0$; orifices a and c.

Figure 7.- Continued.

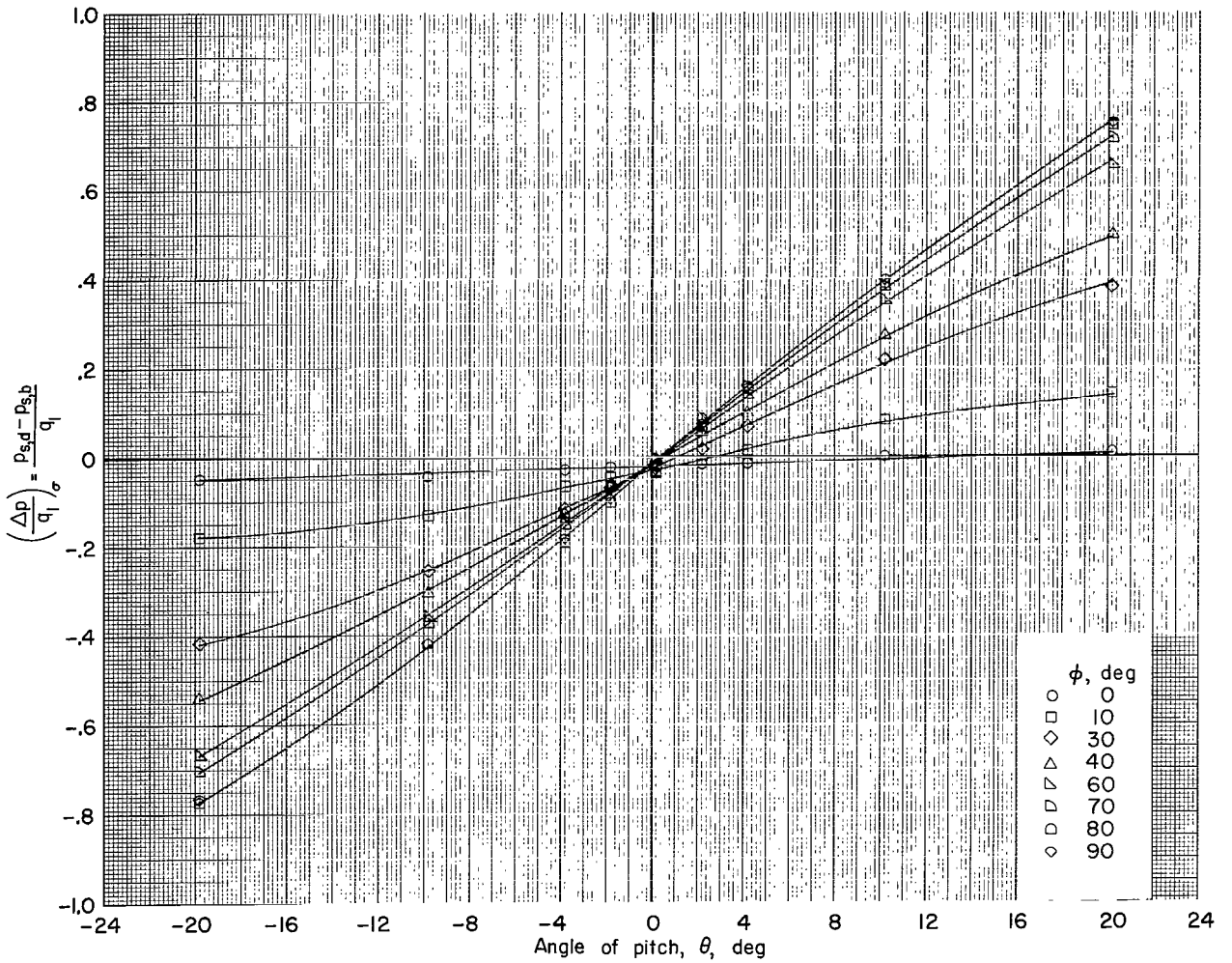

(f) M_1 = 6.0; orifices b and d.

Figure 7.- Concluded.

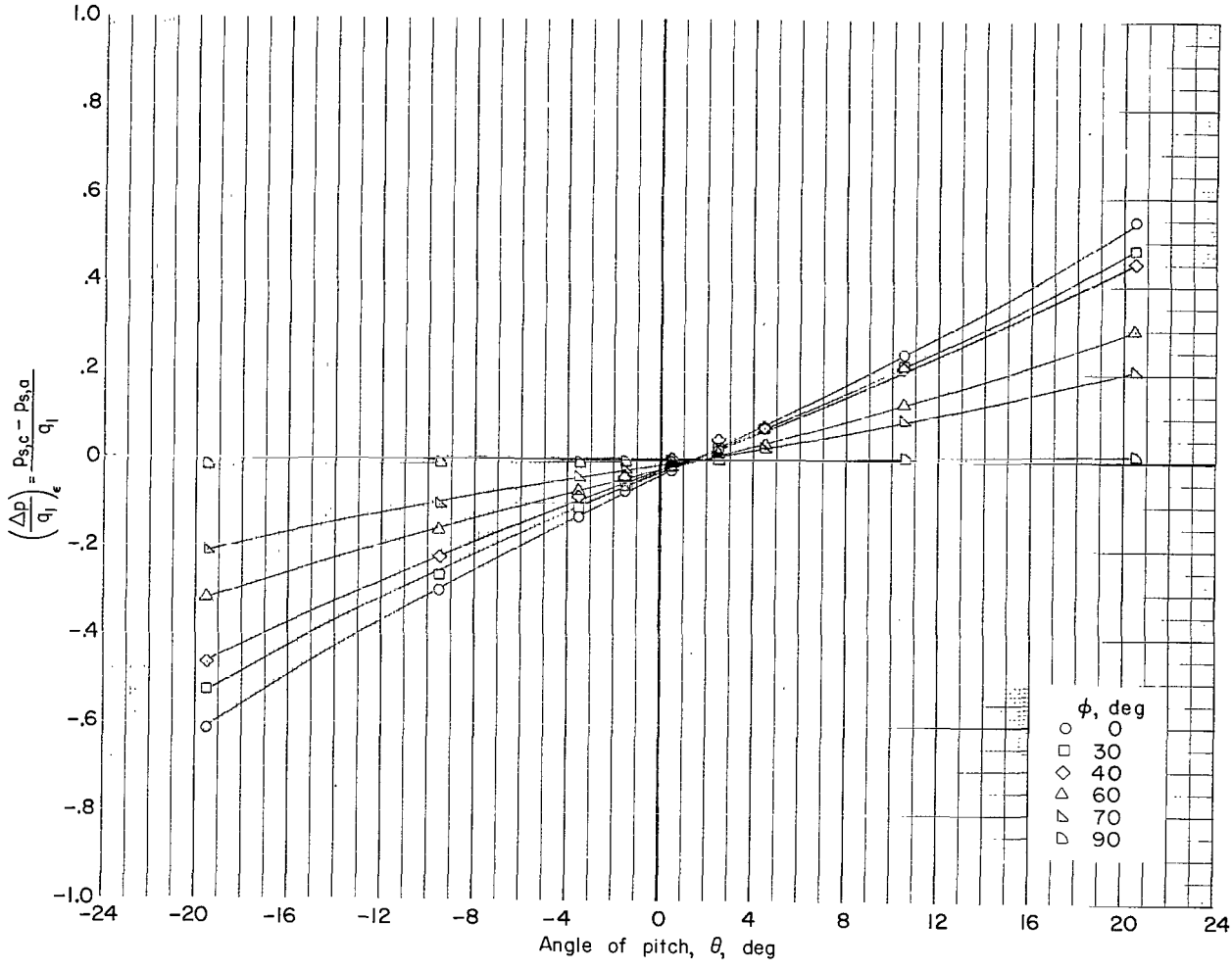

(a) $M_1 = 3.0$; orifices a and c.

Figure 8.- Variation of static pressure differences with angle of pitch. Probe 2.

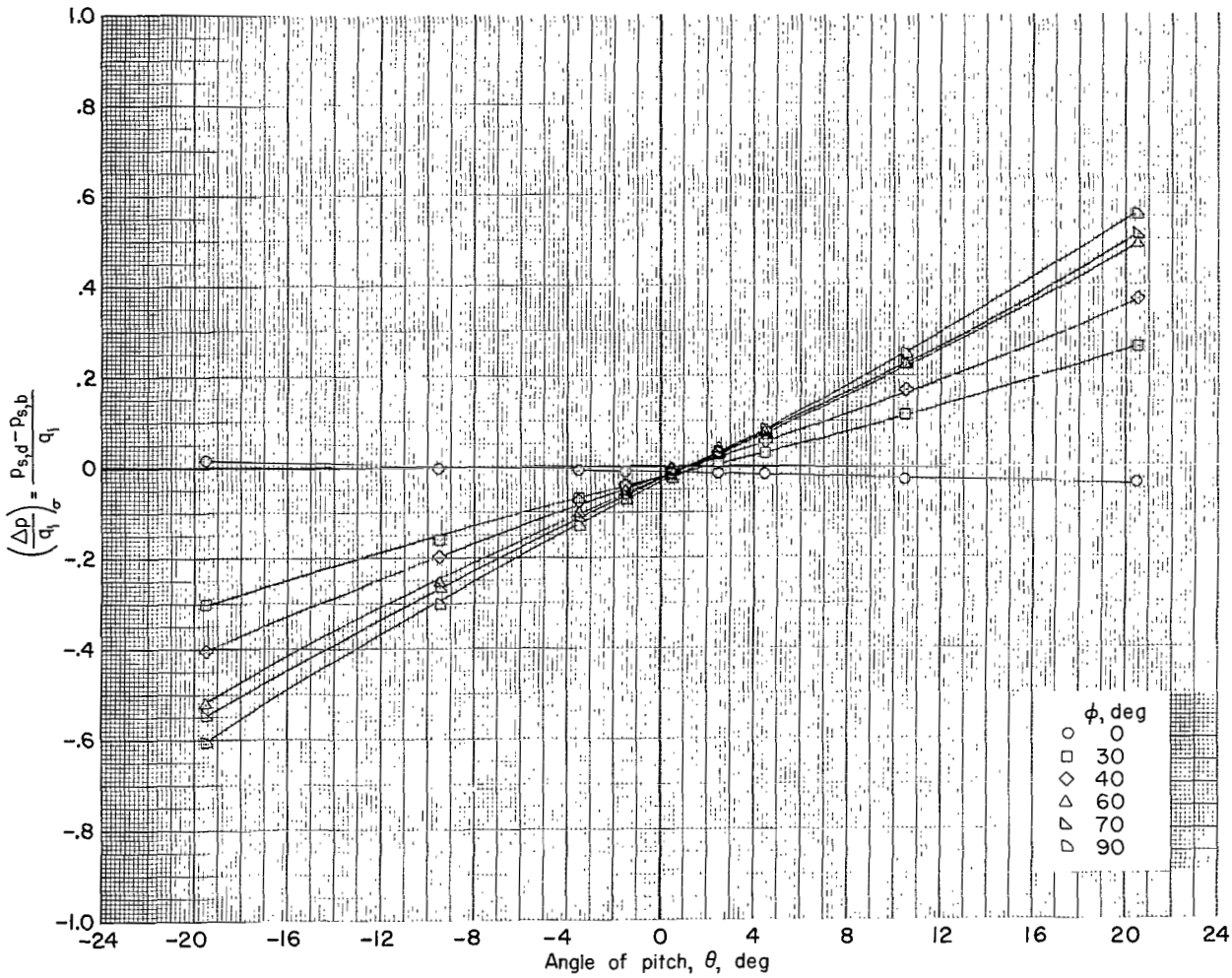

(b) M_1 = 3.0; orifices b and d.

Figure 8.- Continued.

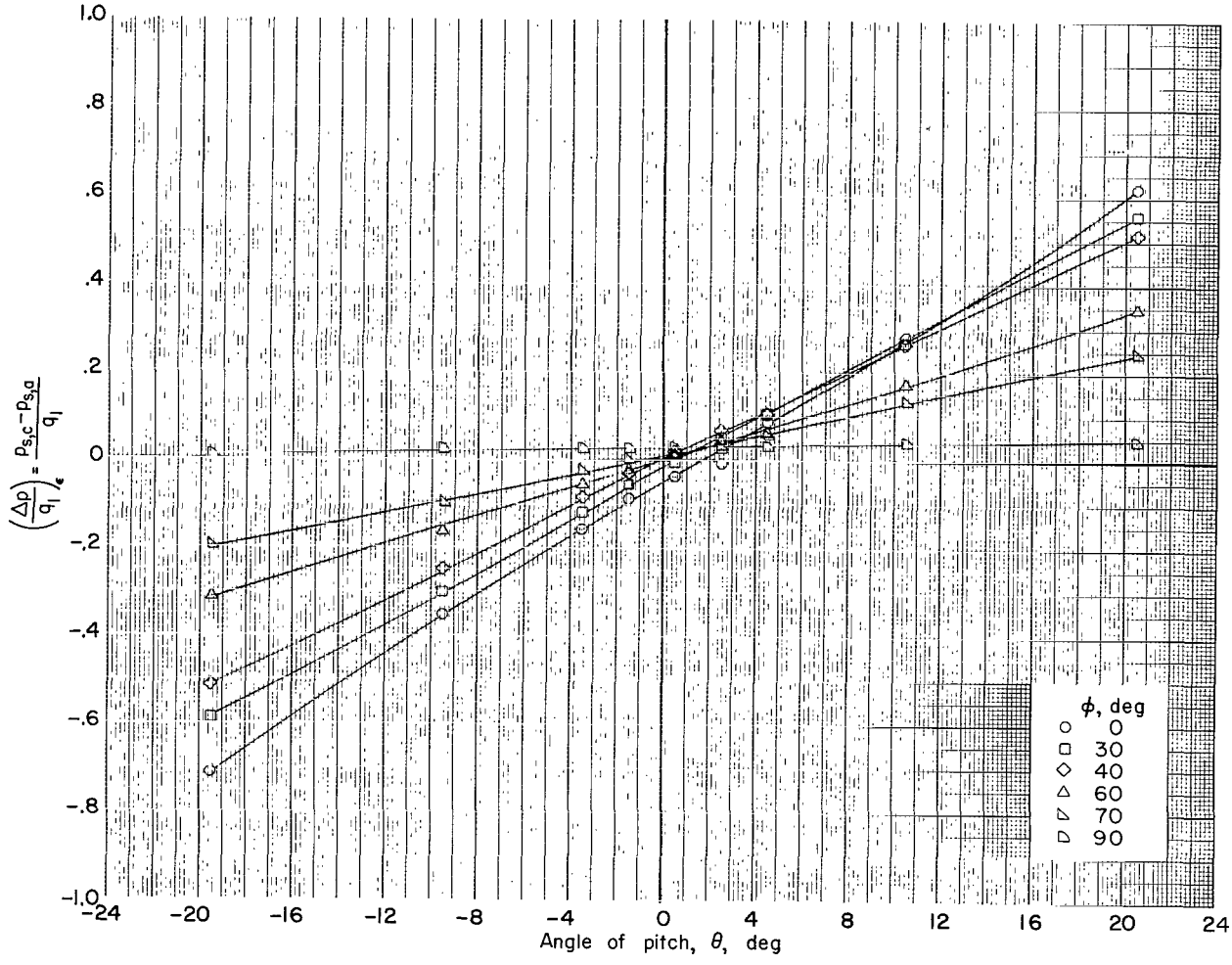

(c) $M_1 = 4.5$; orifices a and c.

Figure 8.- Continued.

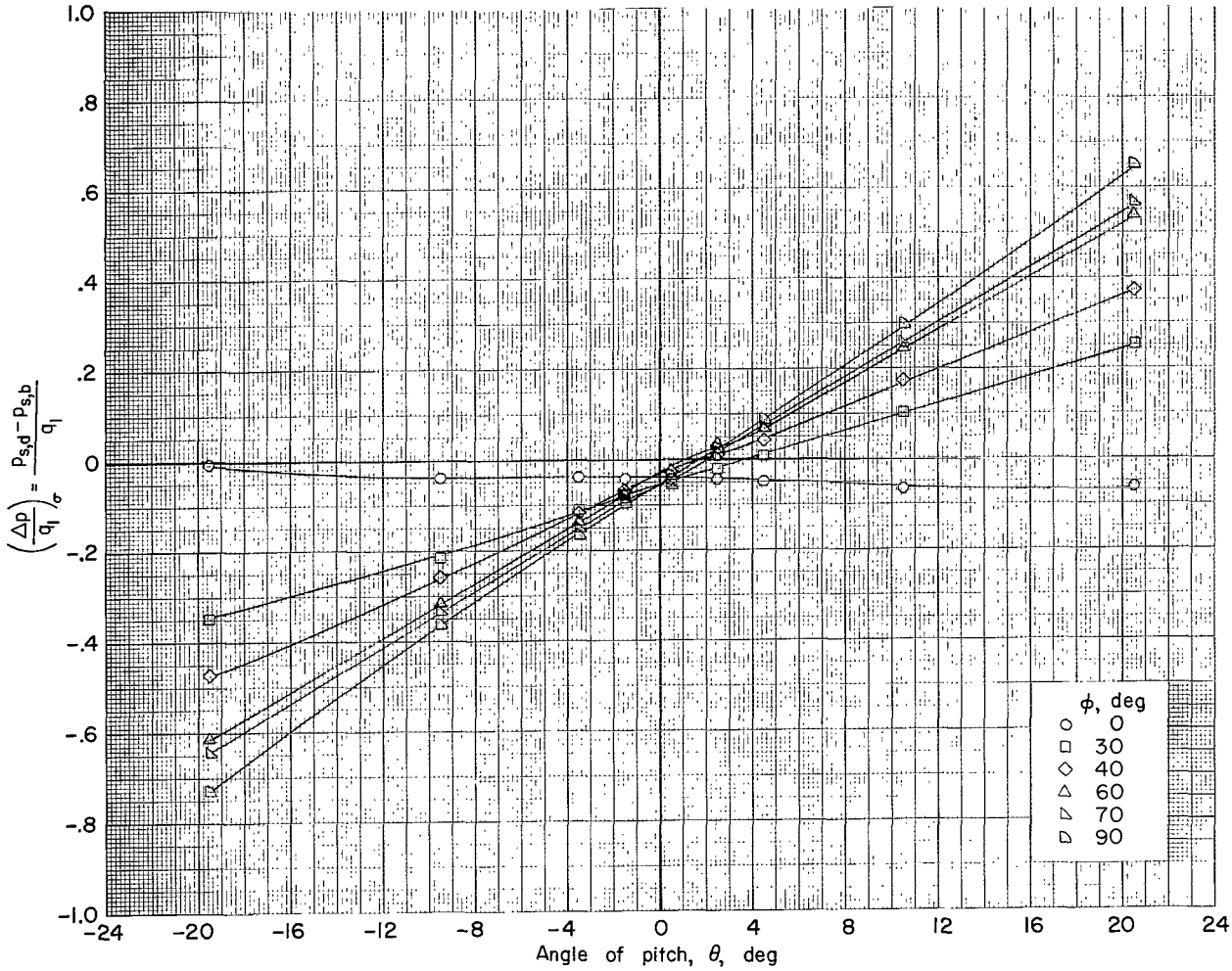

(d) $M_1 = 4.5$; orifices b and d.

Figure 8.- Continued.

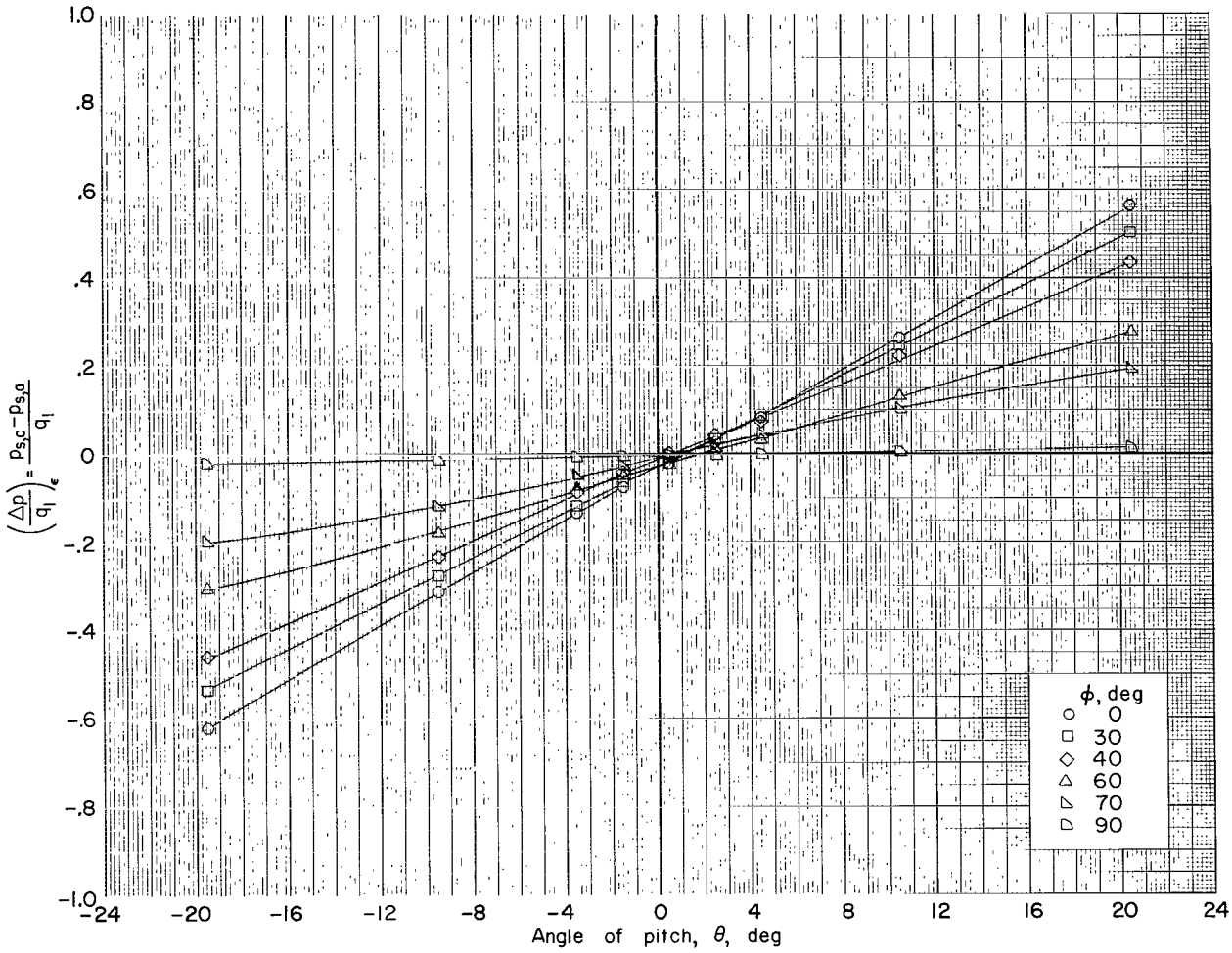

(e) M_1 = 6.0; orifices a and c.

Figure 8.- Continued.

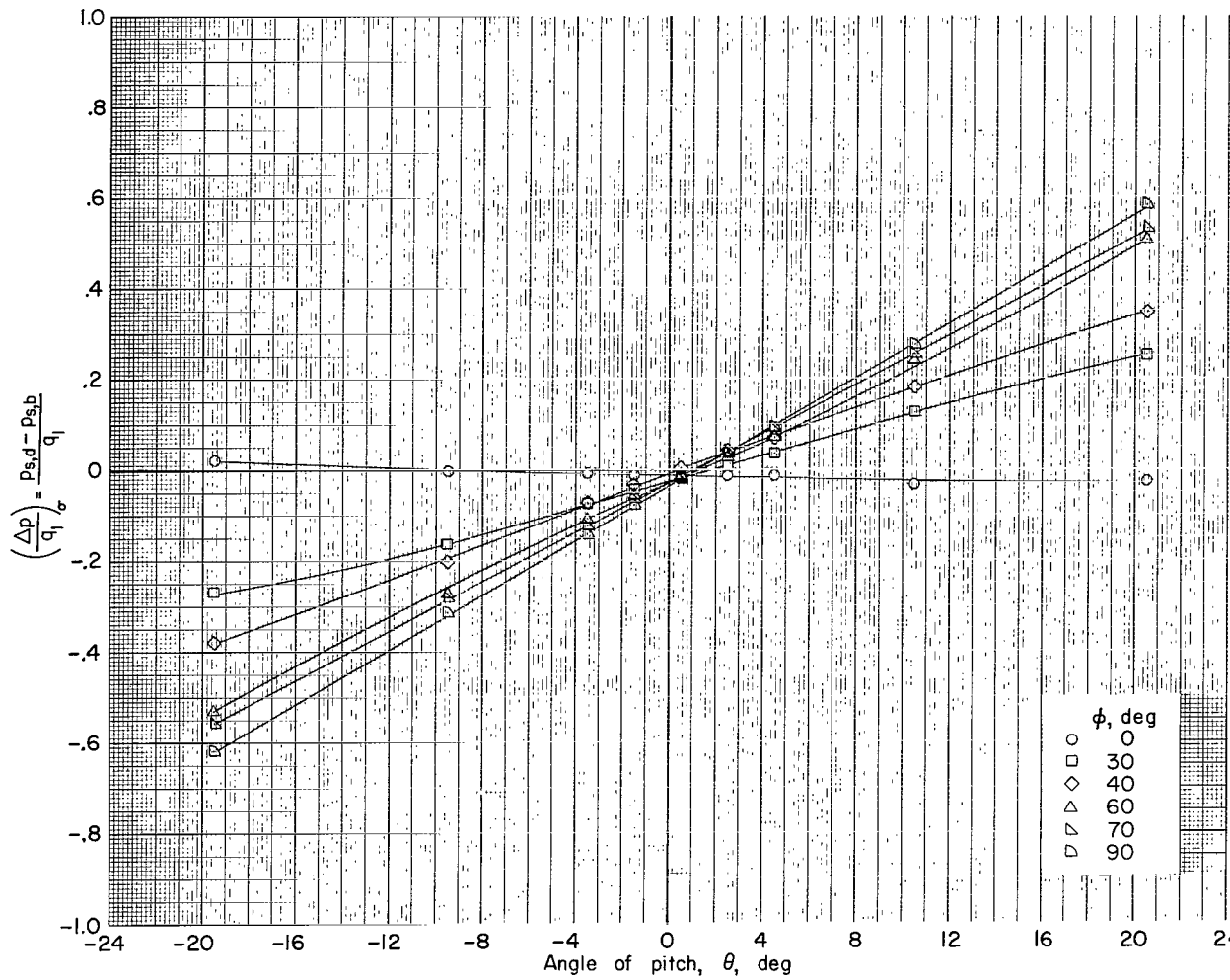

(f) M_1 = 6.0; orifices b and d.

Figure 8.- Concluded.

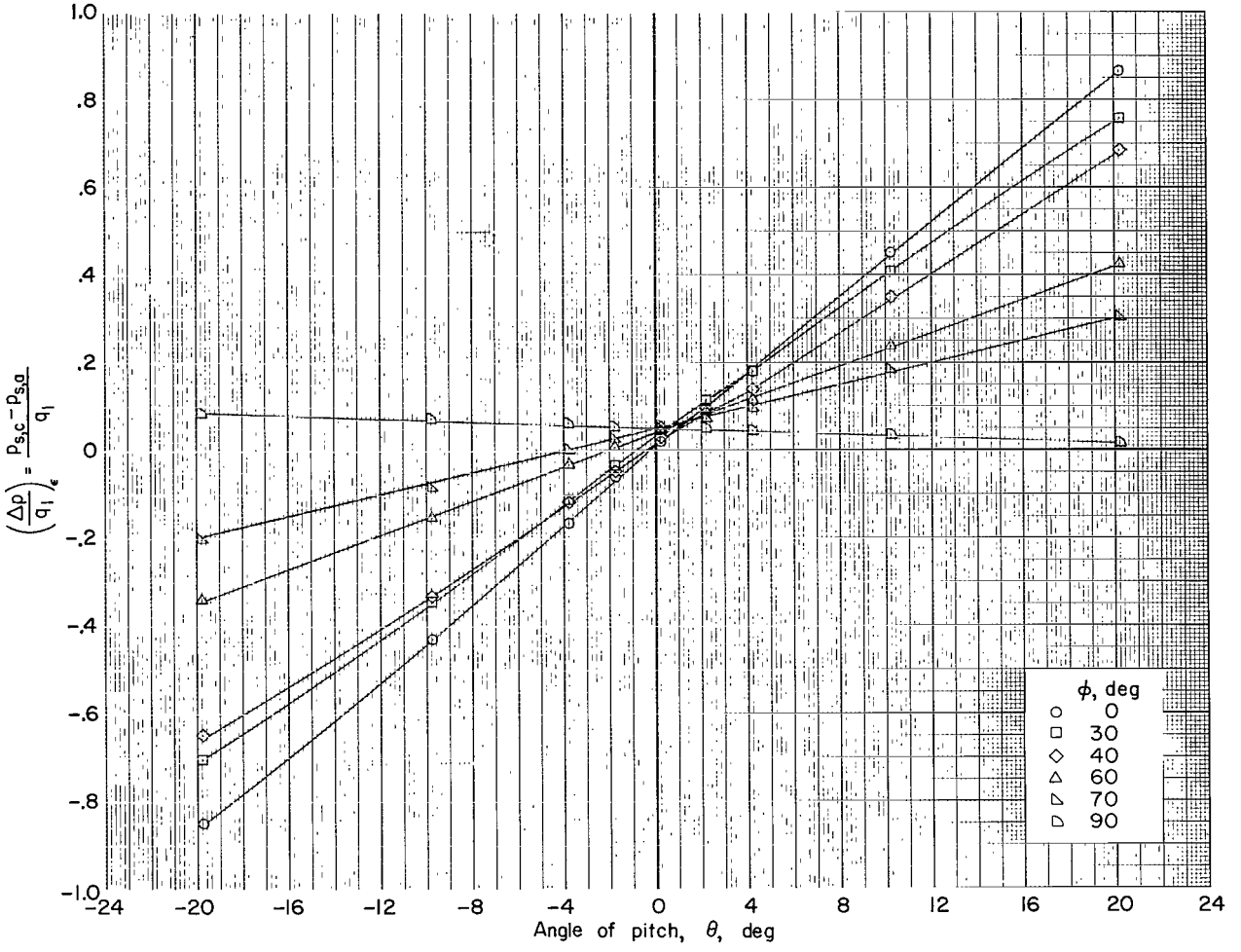

(a) M_1 = 3.0; orifices a and c.

Figure 9.- Variation of static pressure differences with angle of pitch. Probe 3.

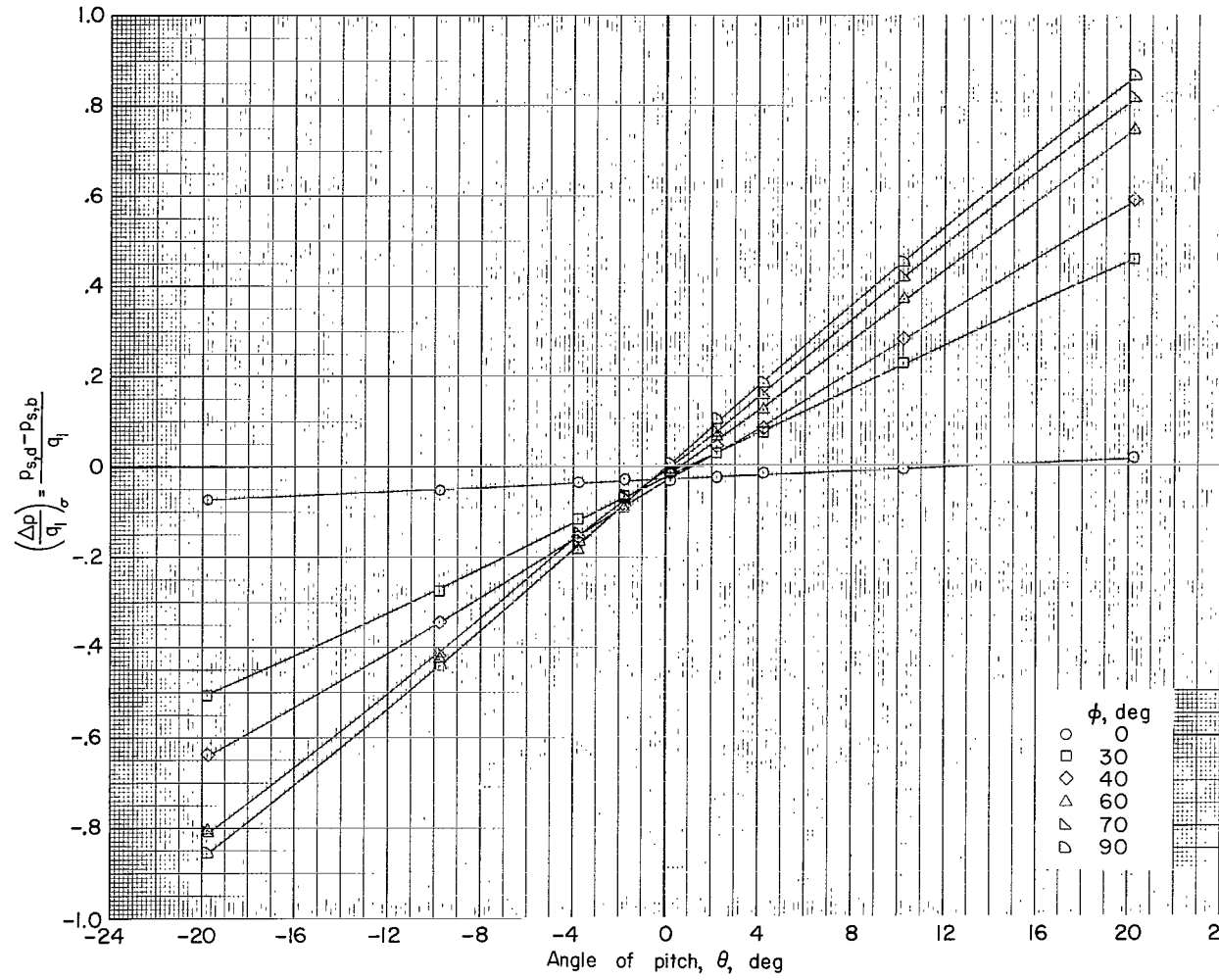

(b) M_1 = 3.0; orifices b and d.

Figure 9.- Continued.

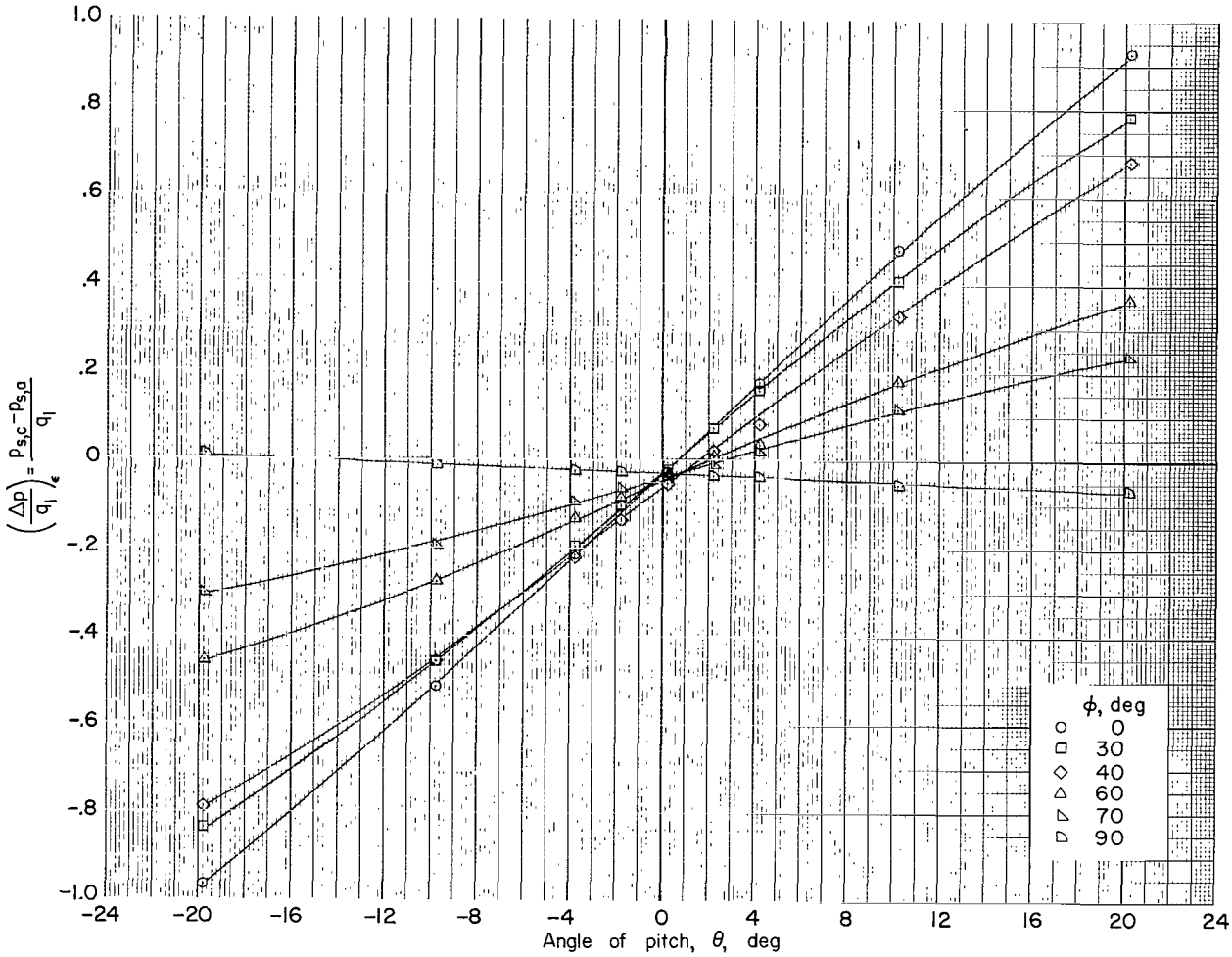

(c) M_1 = 4.5; orifices a and c.

Figure 9.- Continued.

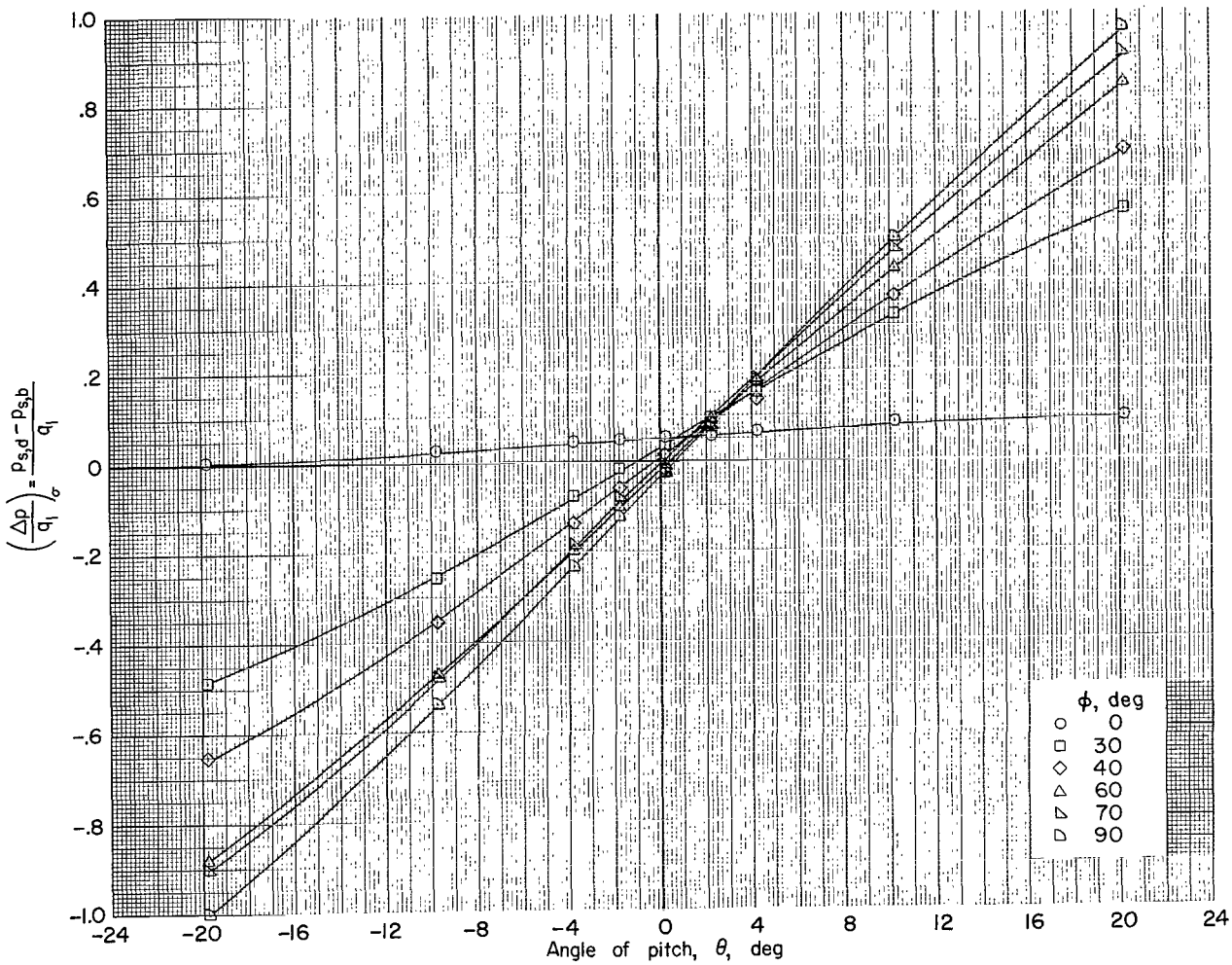

(d) M_1 = 4.5; orifices b and d.

Figure 9.- Continued.

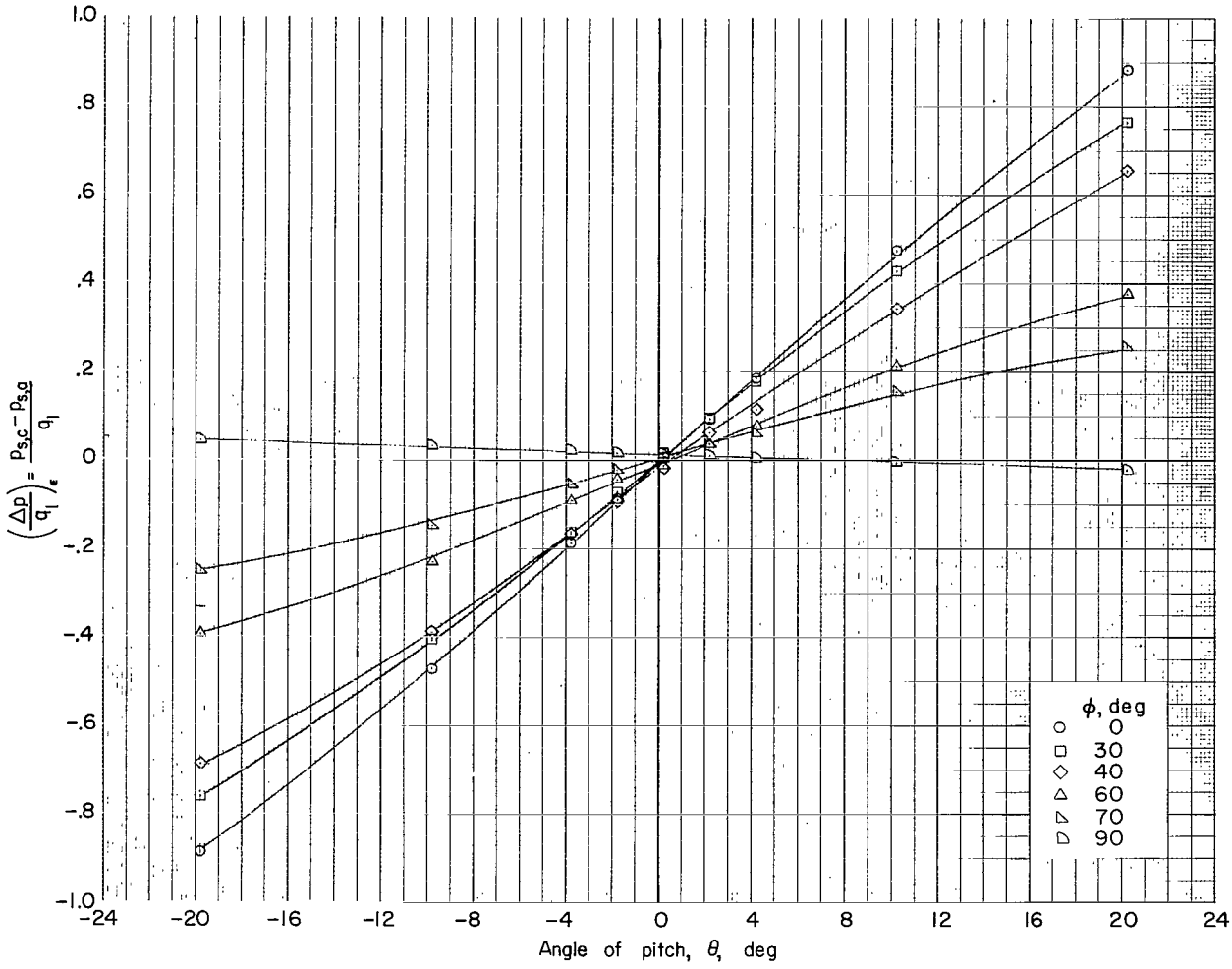

(e) $M_1 = 6.0$; orifices a and c.

Figure 9.- Continued.

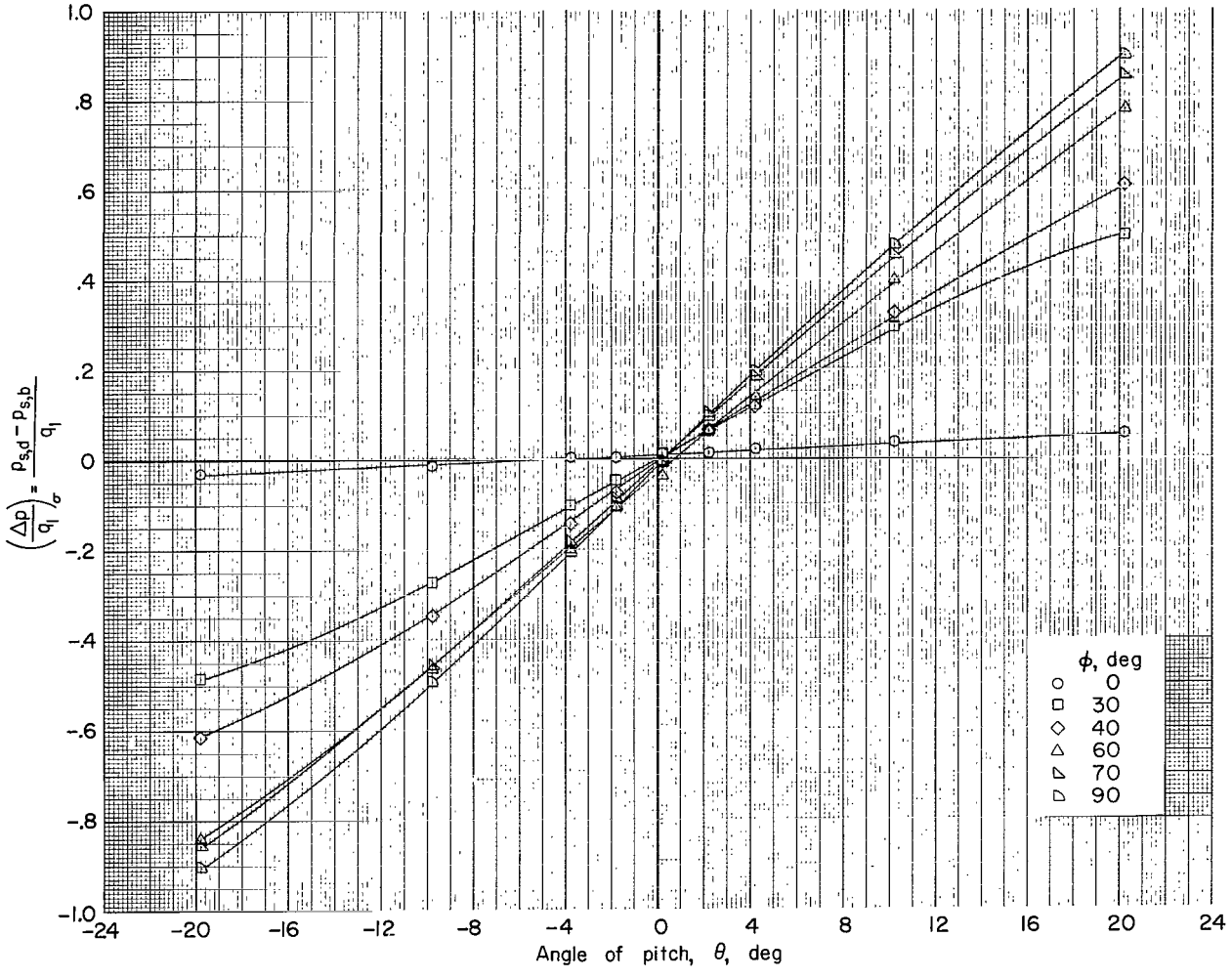

(f) M_1 = 6.0; orifices b and d.

Figure 9.- Concluded.

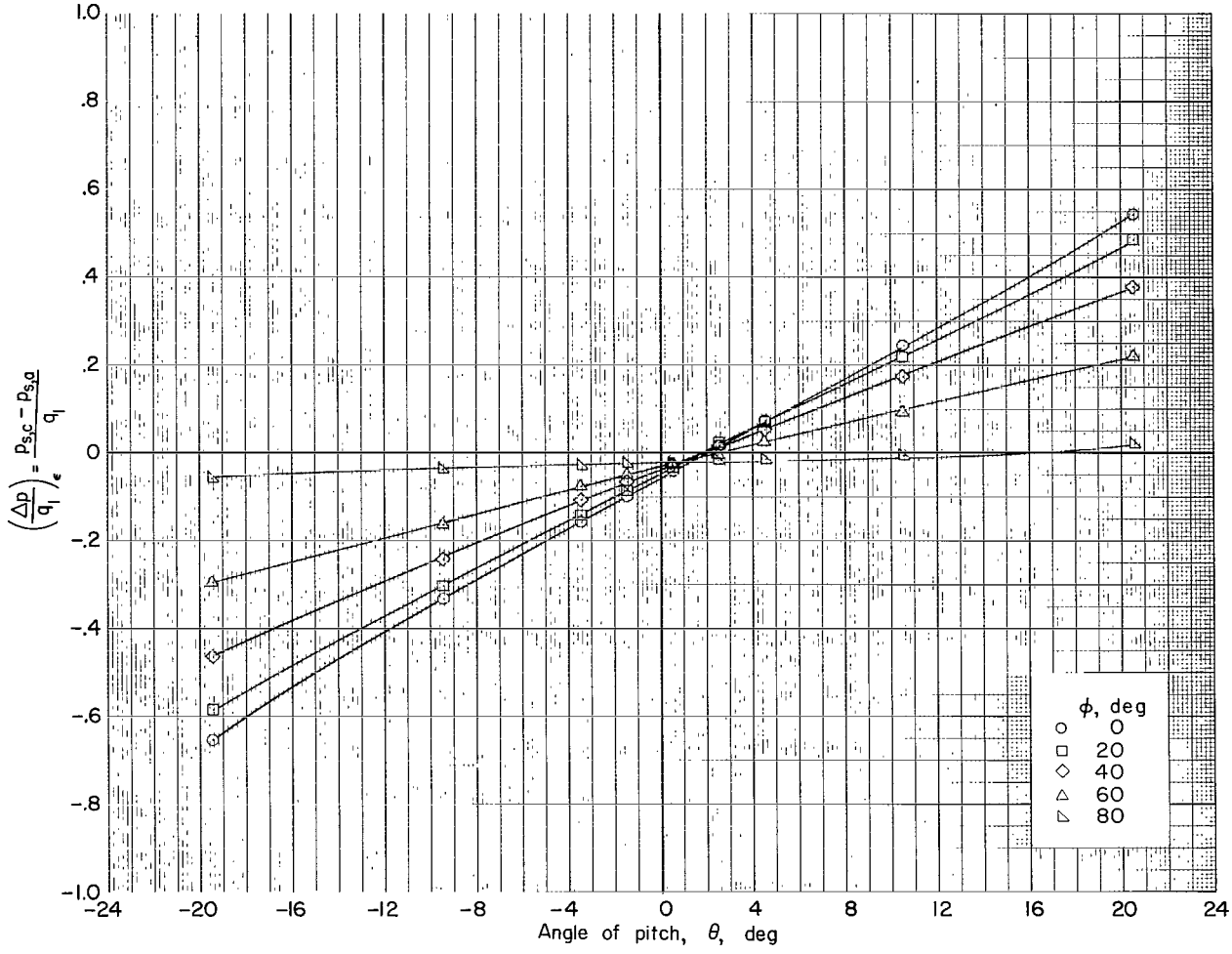

(a) M_1 = 3.0; orifices a and c.

Figure 10.- Variation of static pressure differences with angle of pitch. Probe 4.

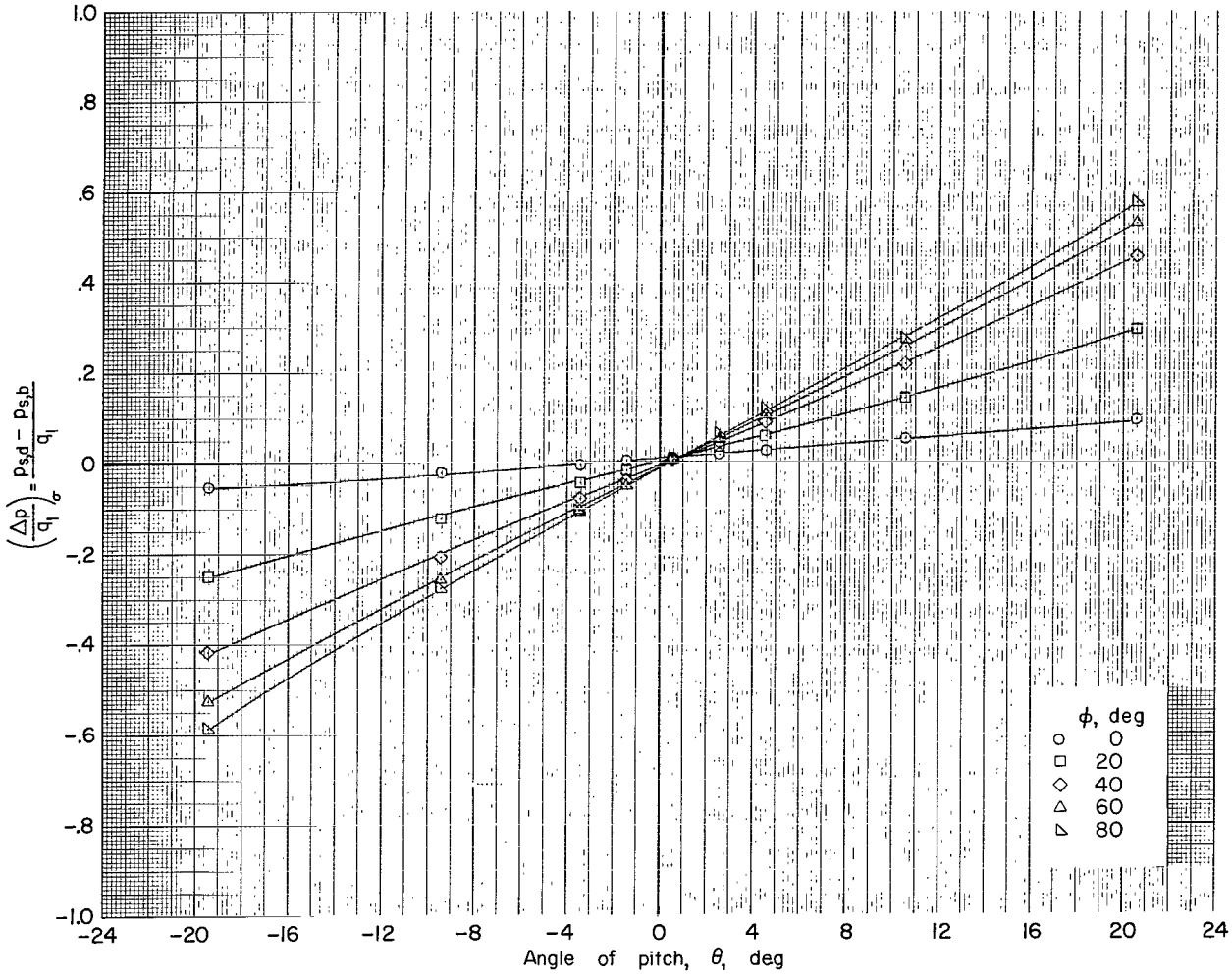

(b) M_1 = 3.0; orifices b and d.

Figure 10.- Continued.

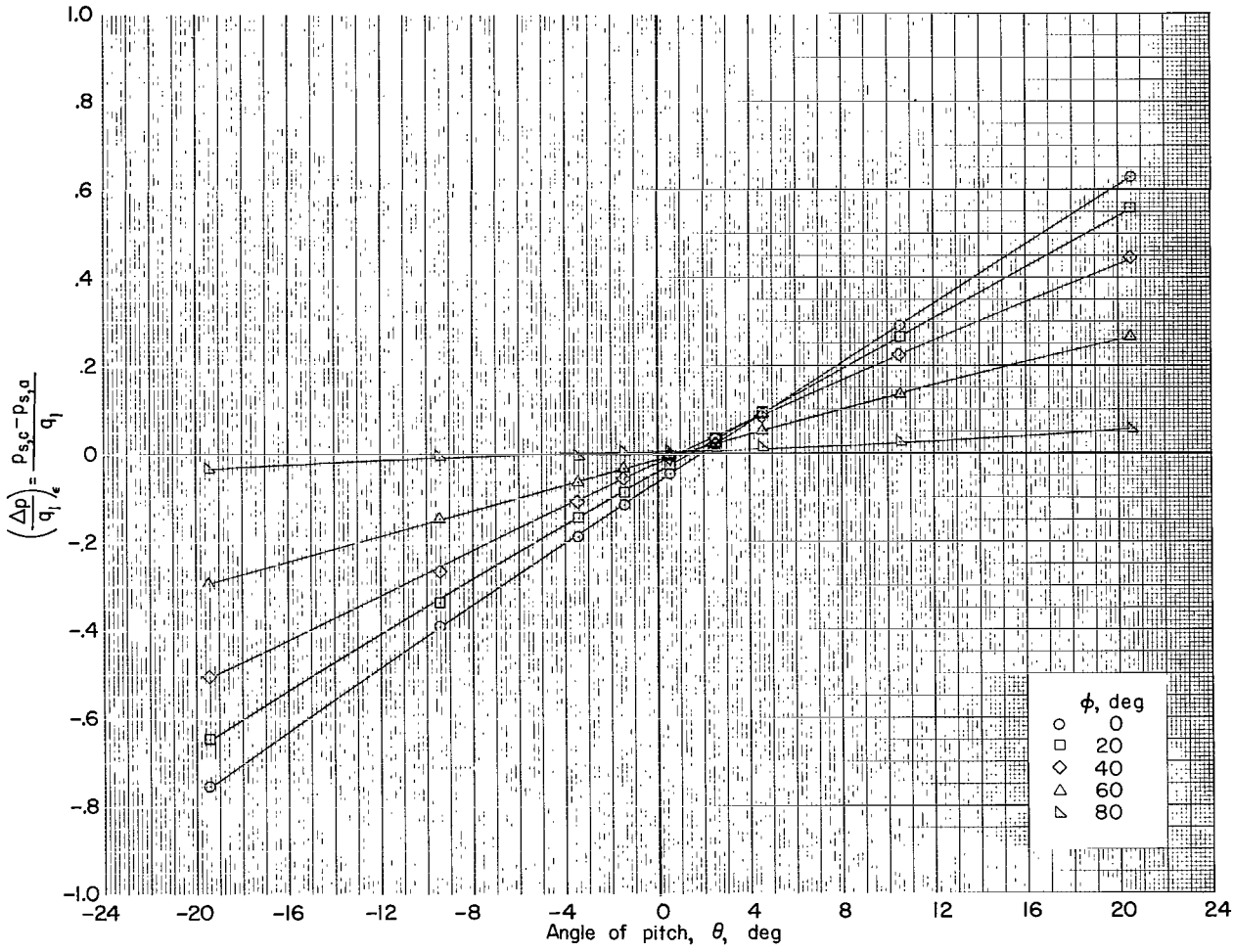

(c) M_1 = 4.5; orifices a and c.

Figure 10.- Continued.

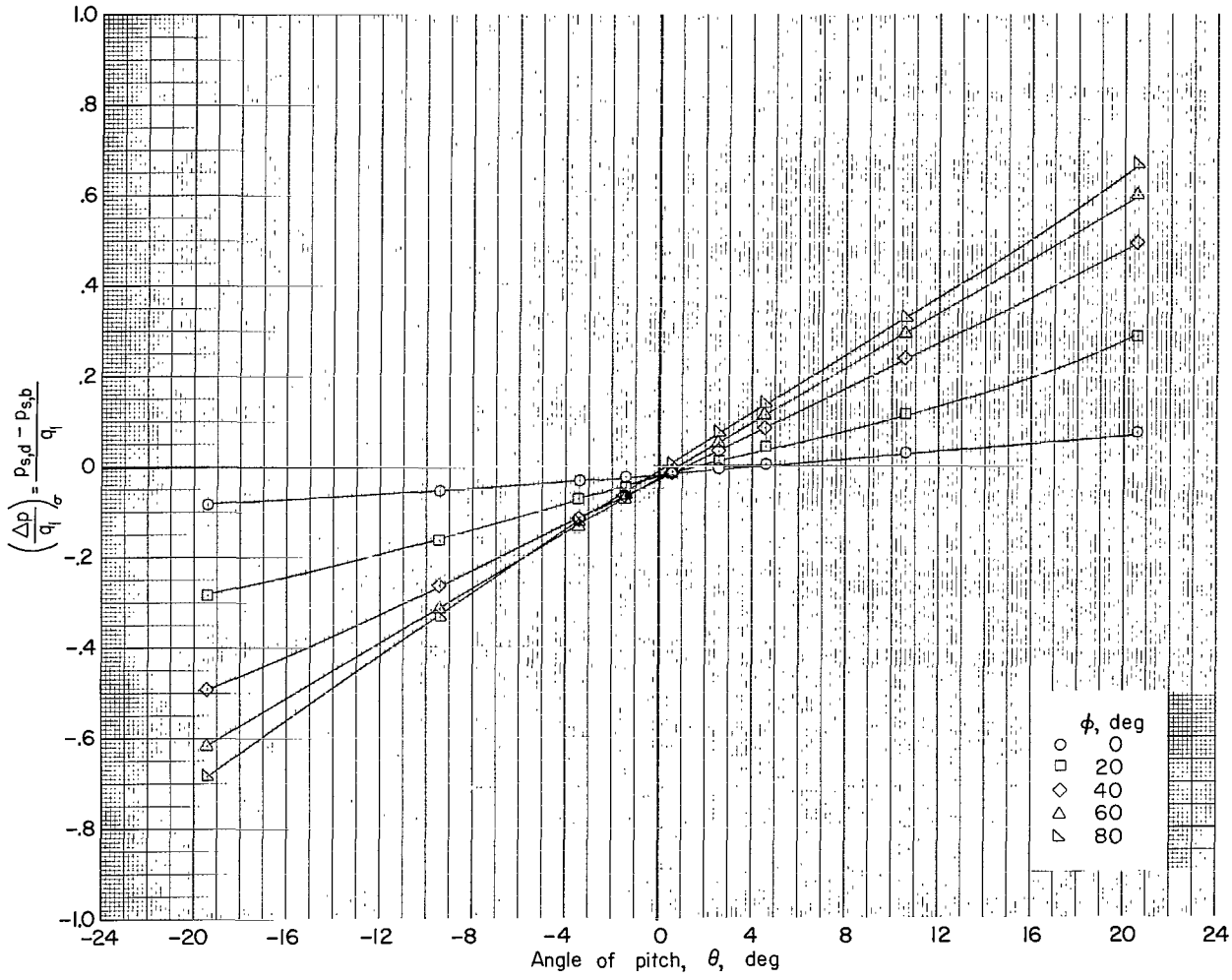

(d) M_1 = 4.5; orifices b and d.

Figure 10.- Continued.

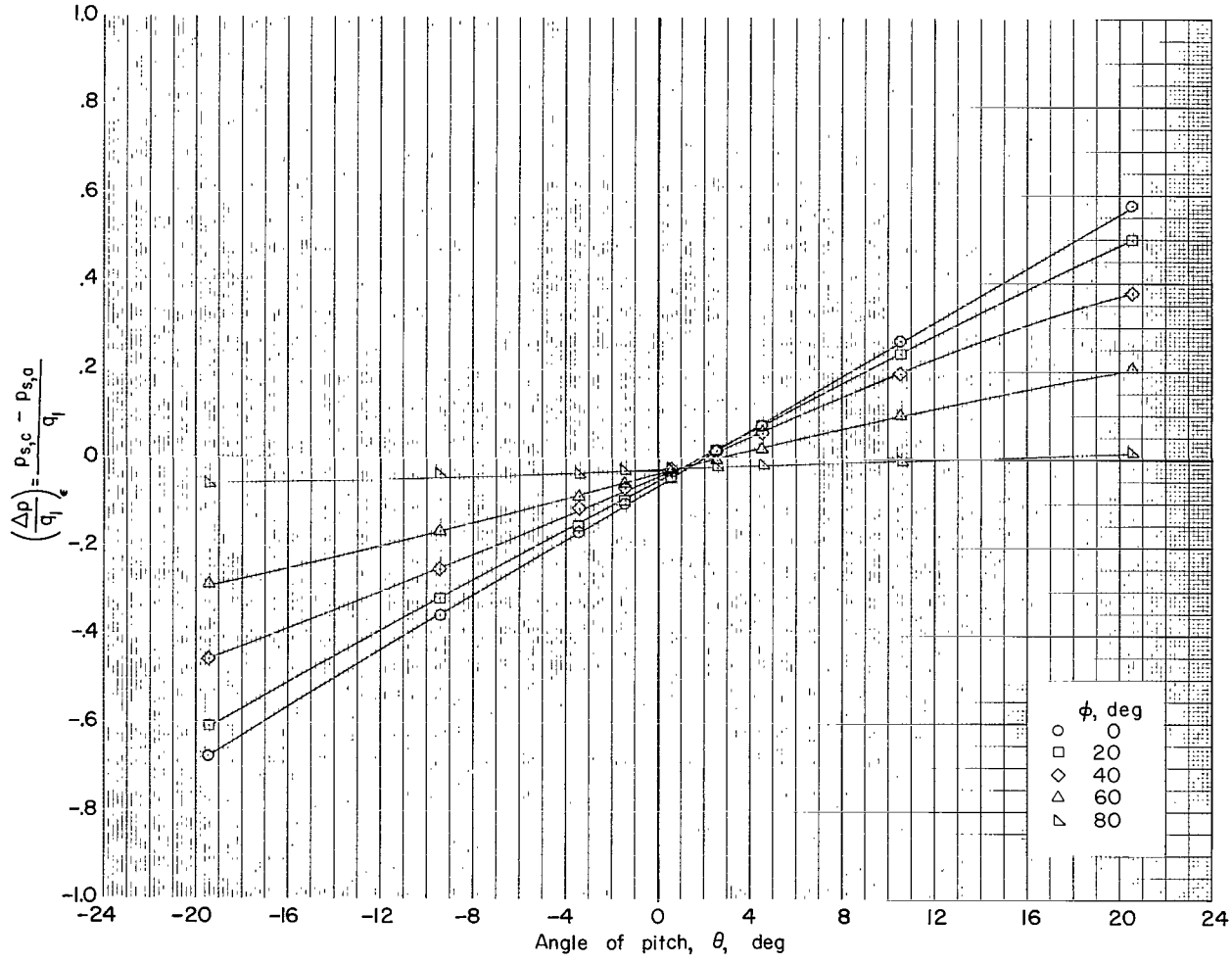

(e) M_1 = 6.0; orifices a and c.

Figure 10.- Continued.

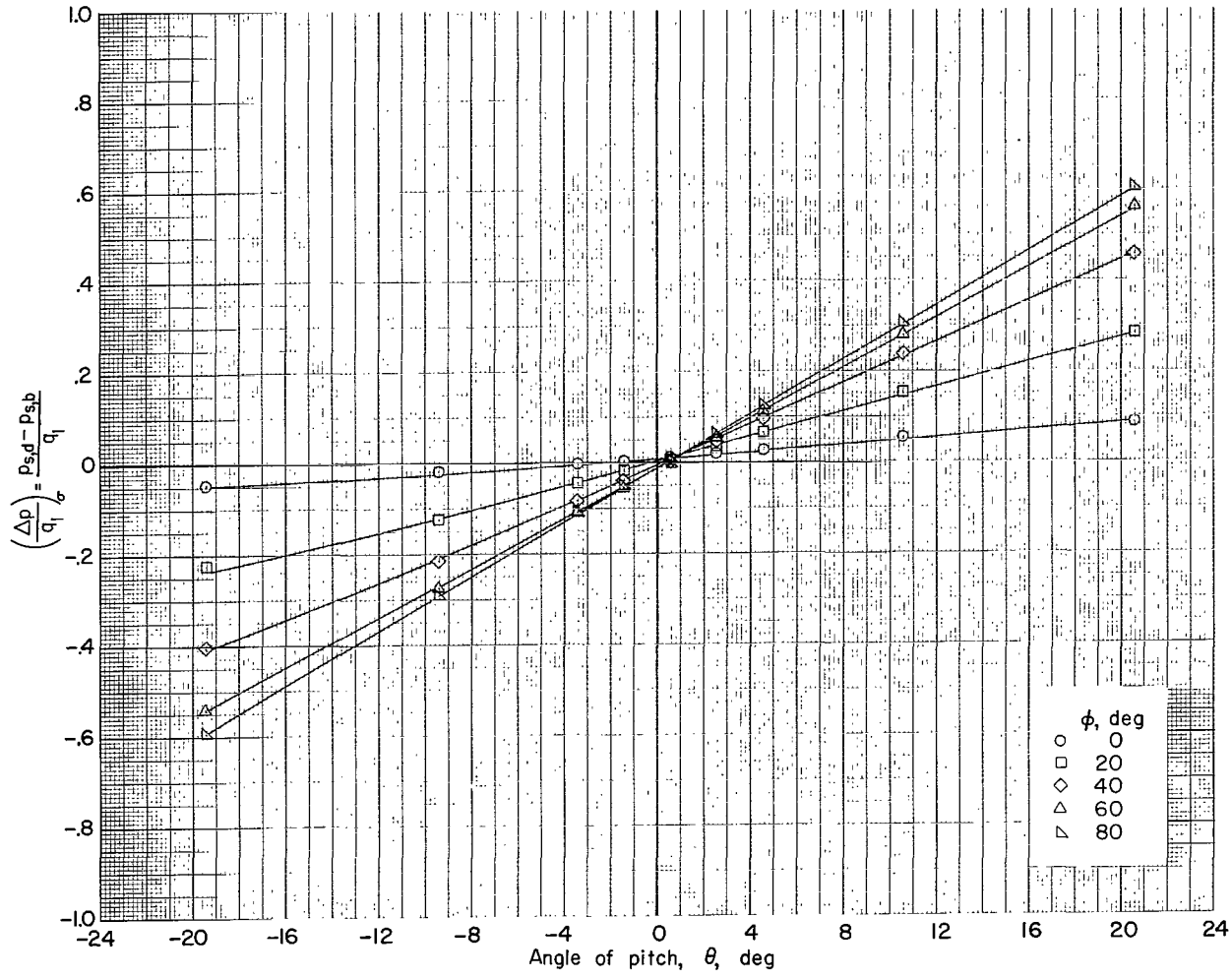

(f) M_1 = 6.0; orifices b and d.

Figure 10.- Concluded.

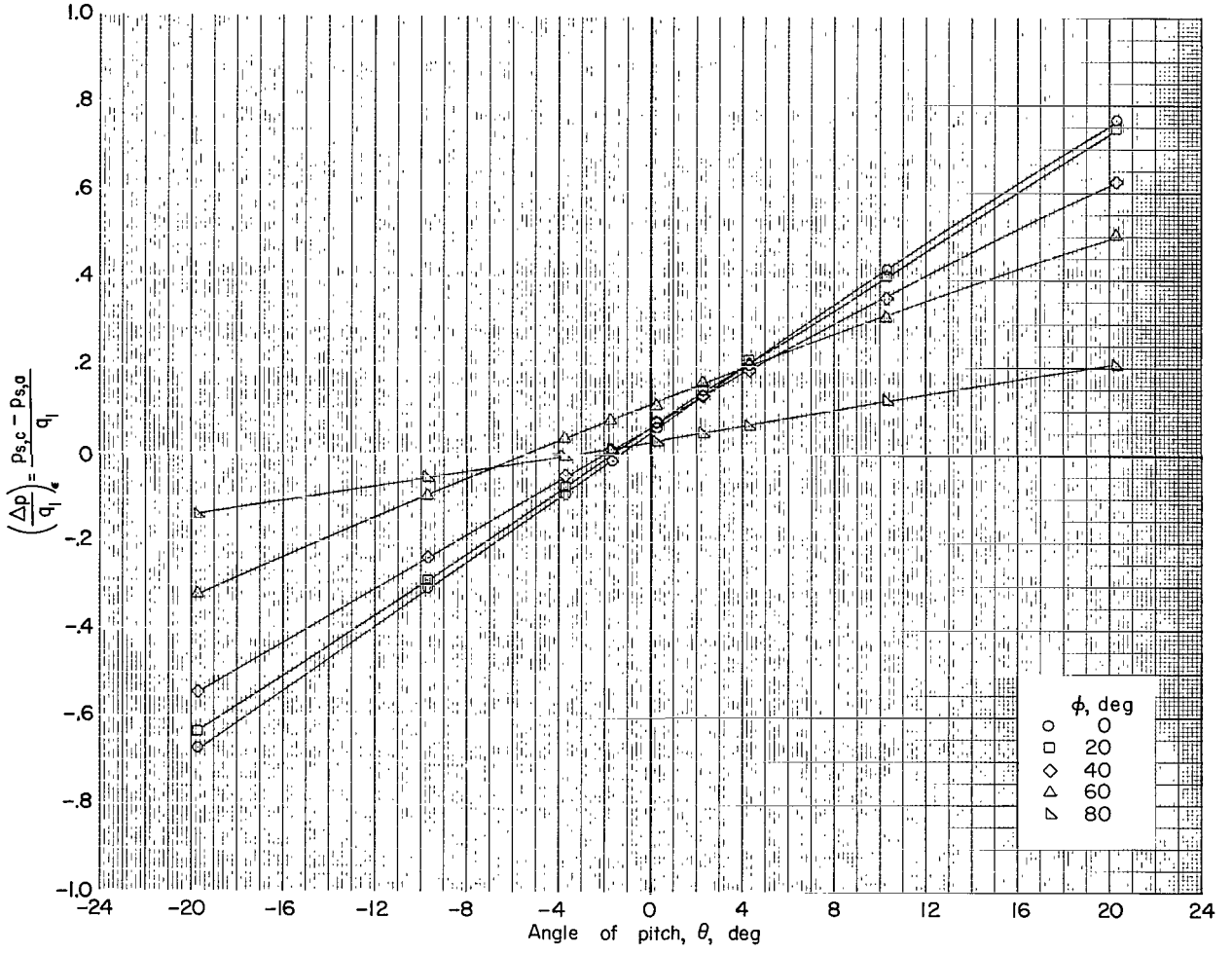

(a) M_1 = 3.0; orifices a and c.

Figure 11.- Variation of static pressure differences with angle of pitch. Probe 5.

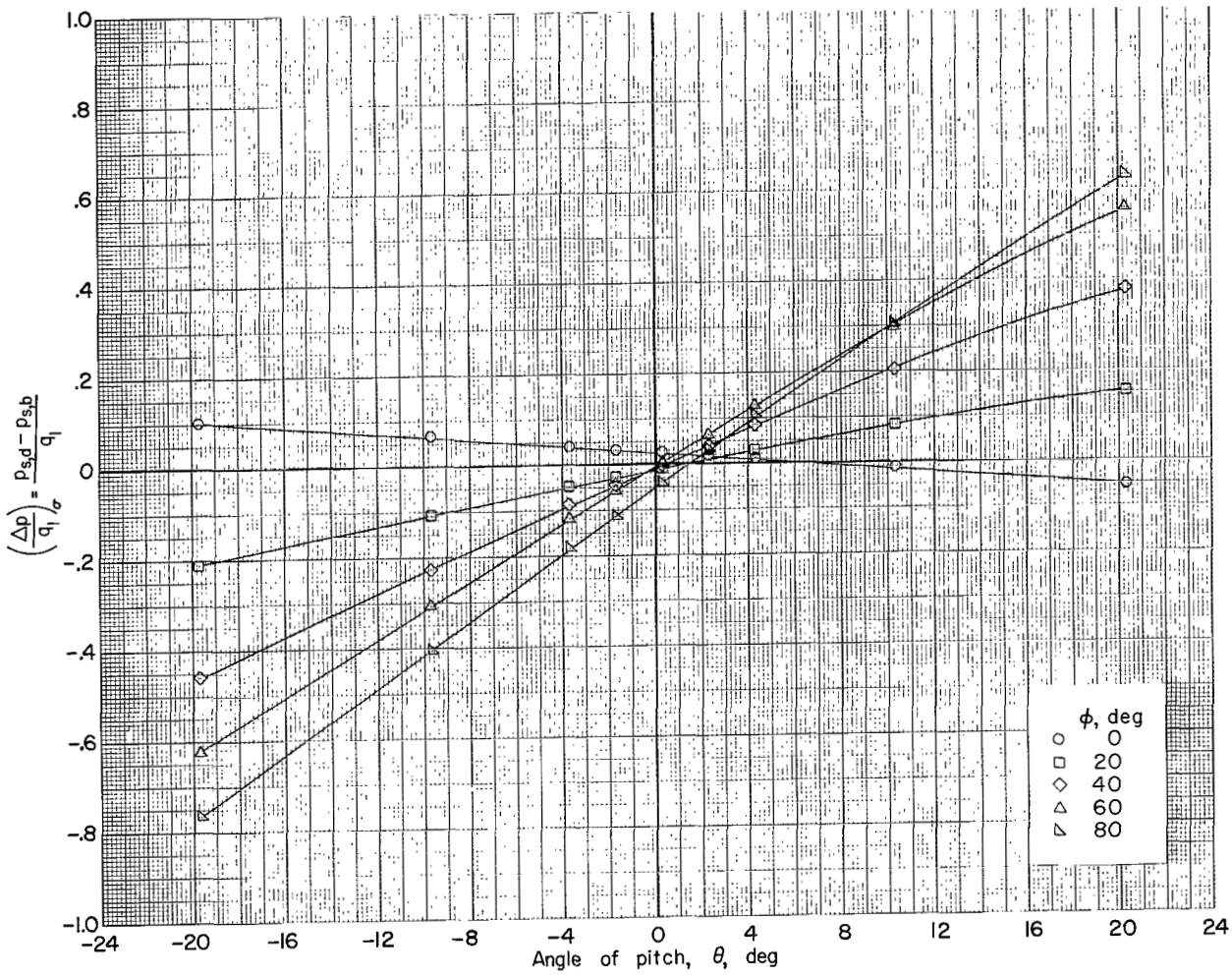

(b) $M_1 = 3.0$; orifices b and d.

Figure 11.- Continued.

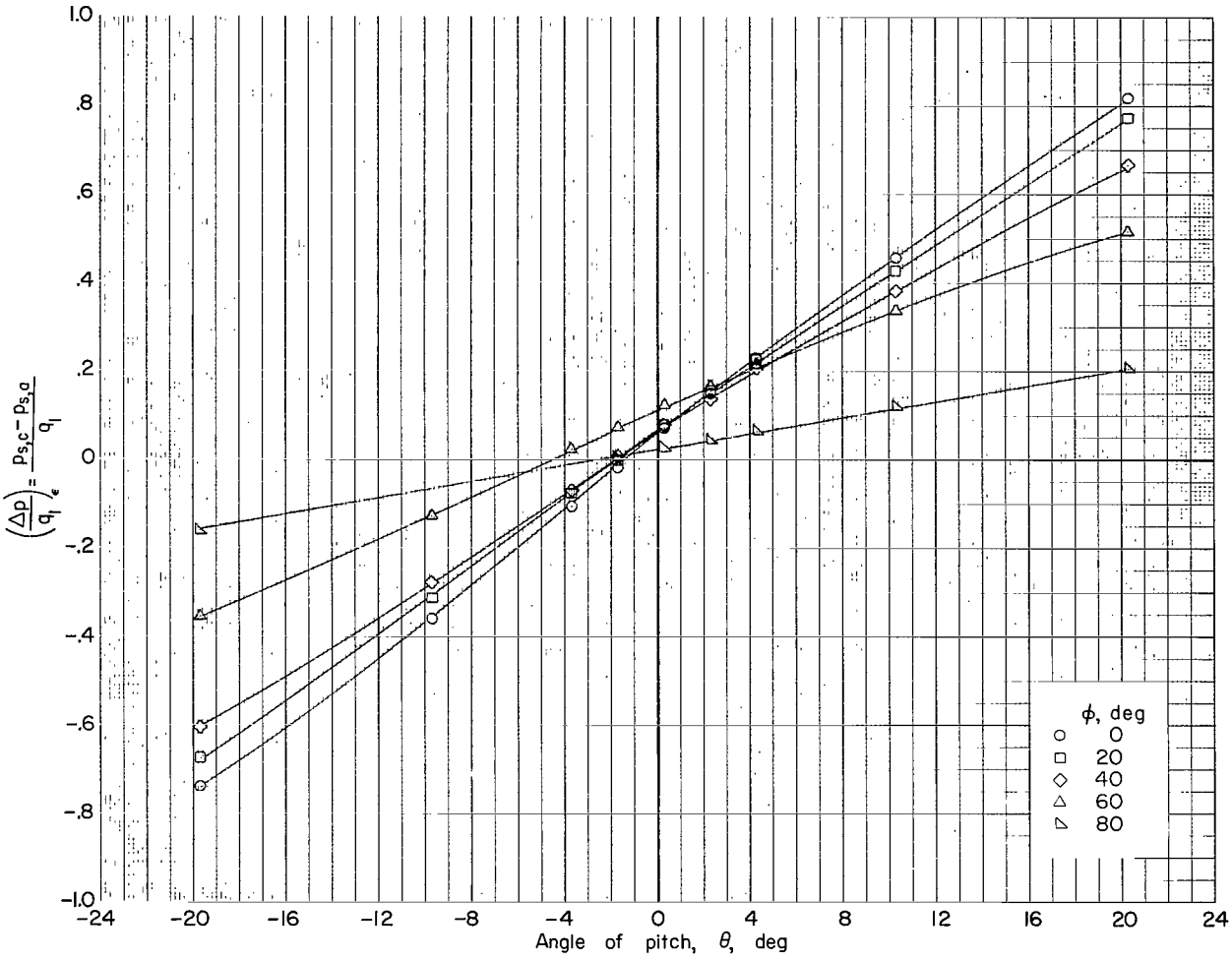

(c) M_1 = 4.5; orifices a and c.

Figure 11.- Continued.

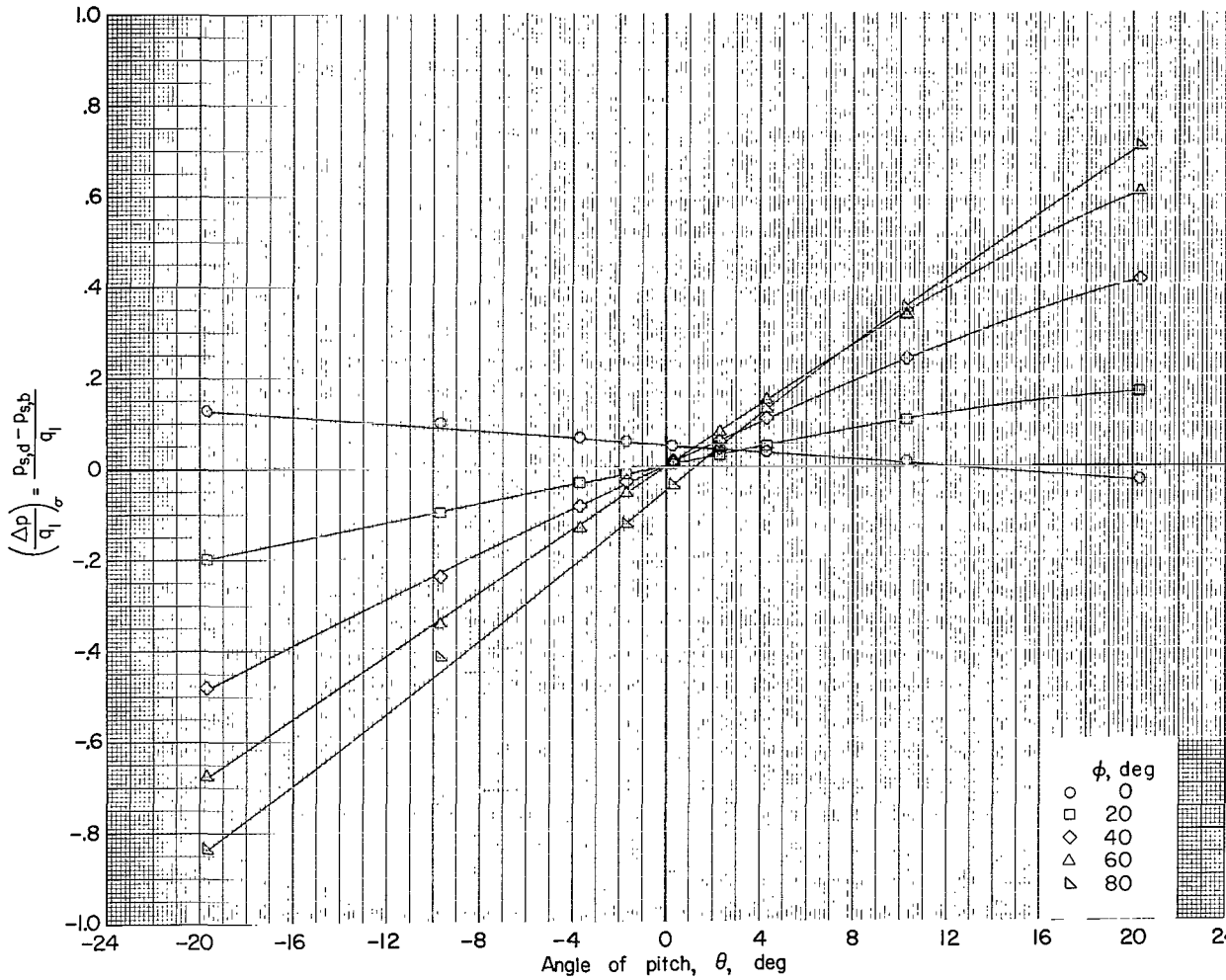

(d) $M_1 = 4.5$; orifices b and d.

Figure 11.- Continued.

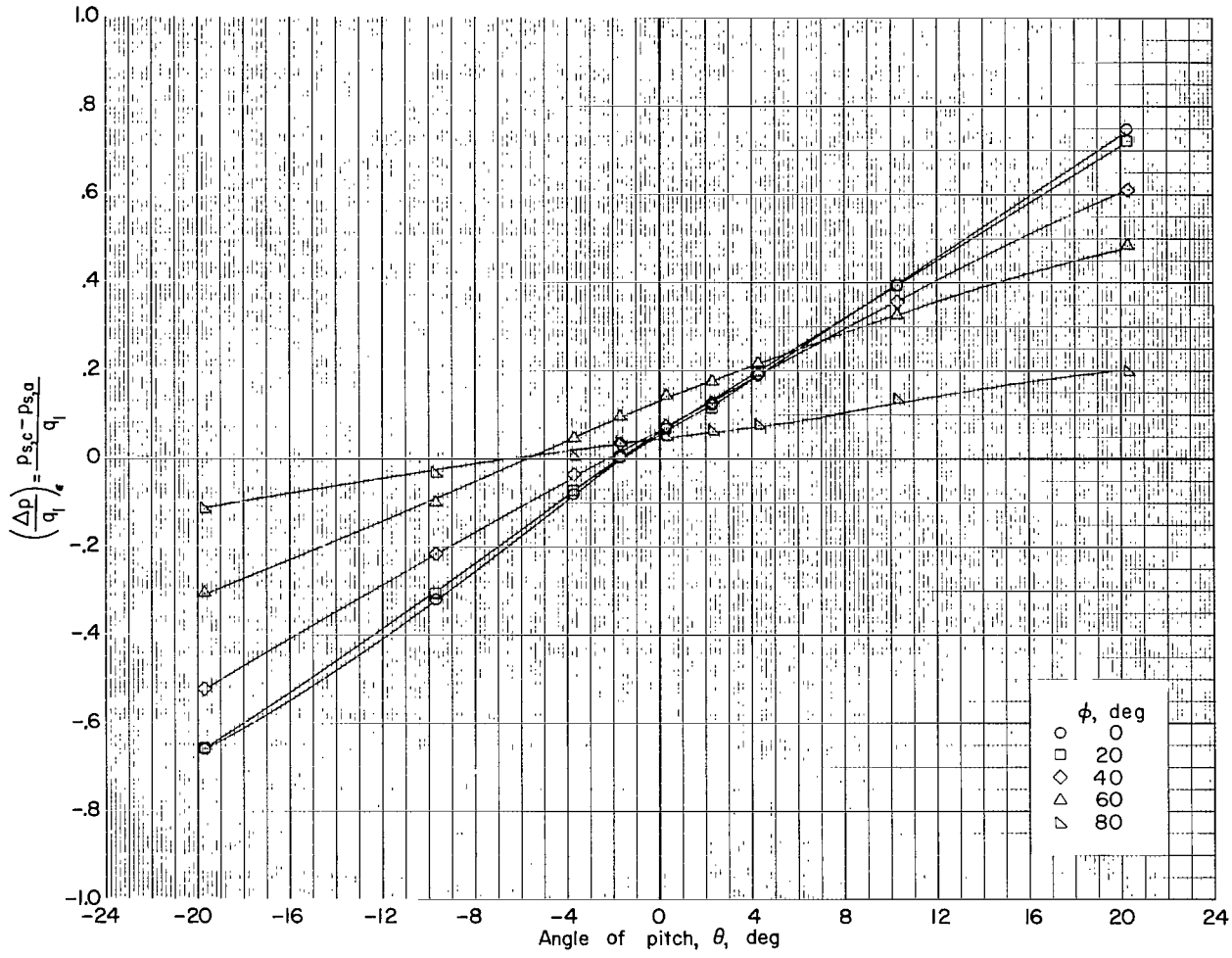

(e) M_1 = 6.0; orifices a and c.

Figure 11.- Continued.

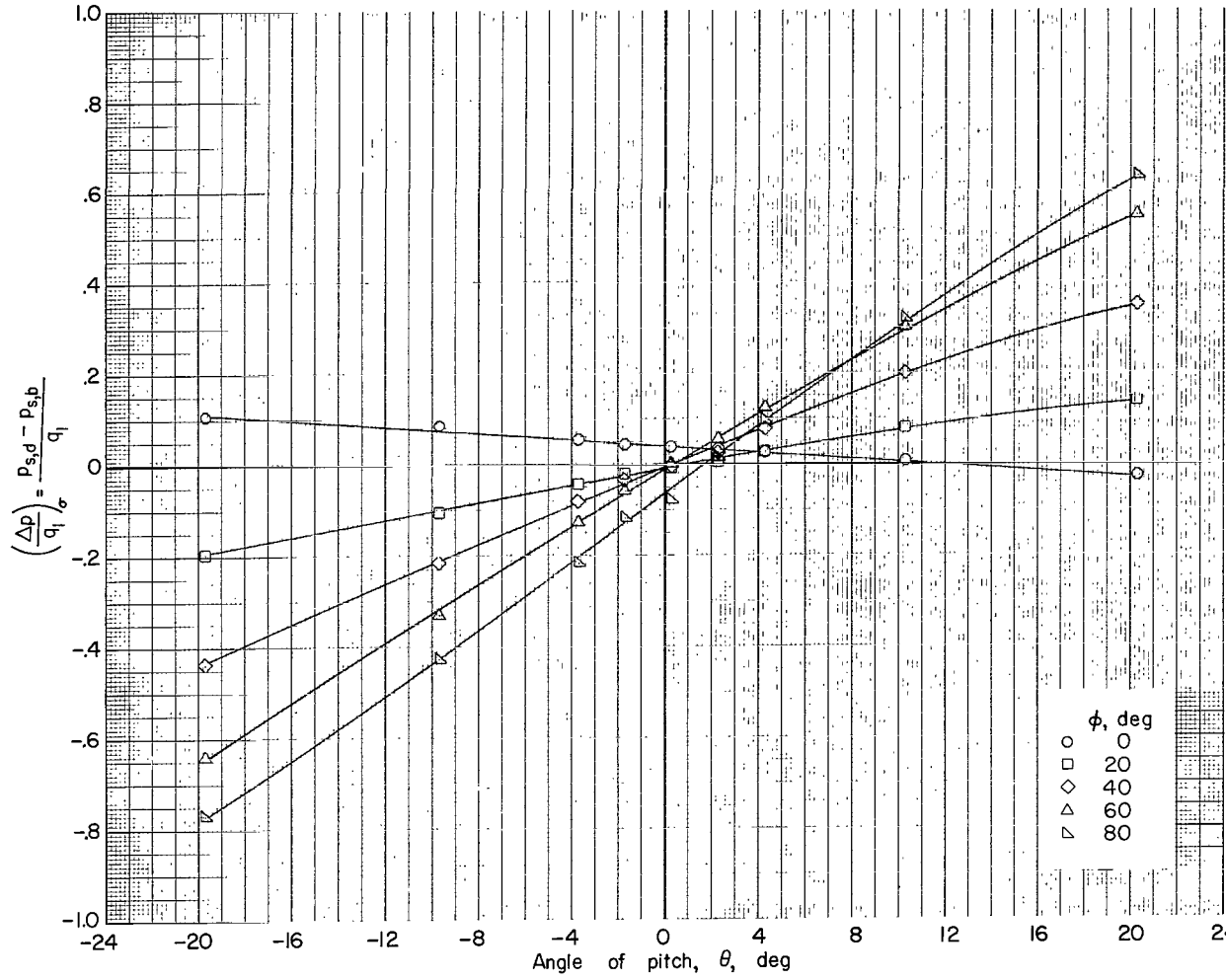

(f) $M_1 = 6.0$; orifices b and d.

Figure 11.- Concluded.

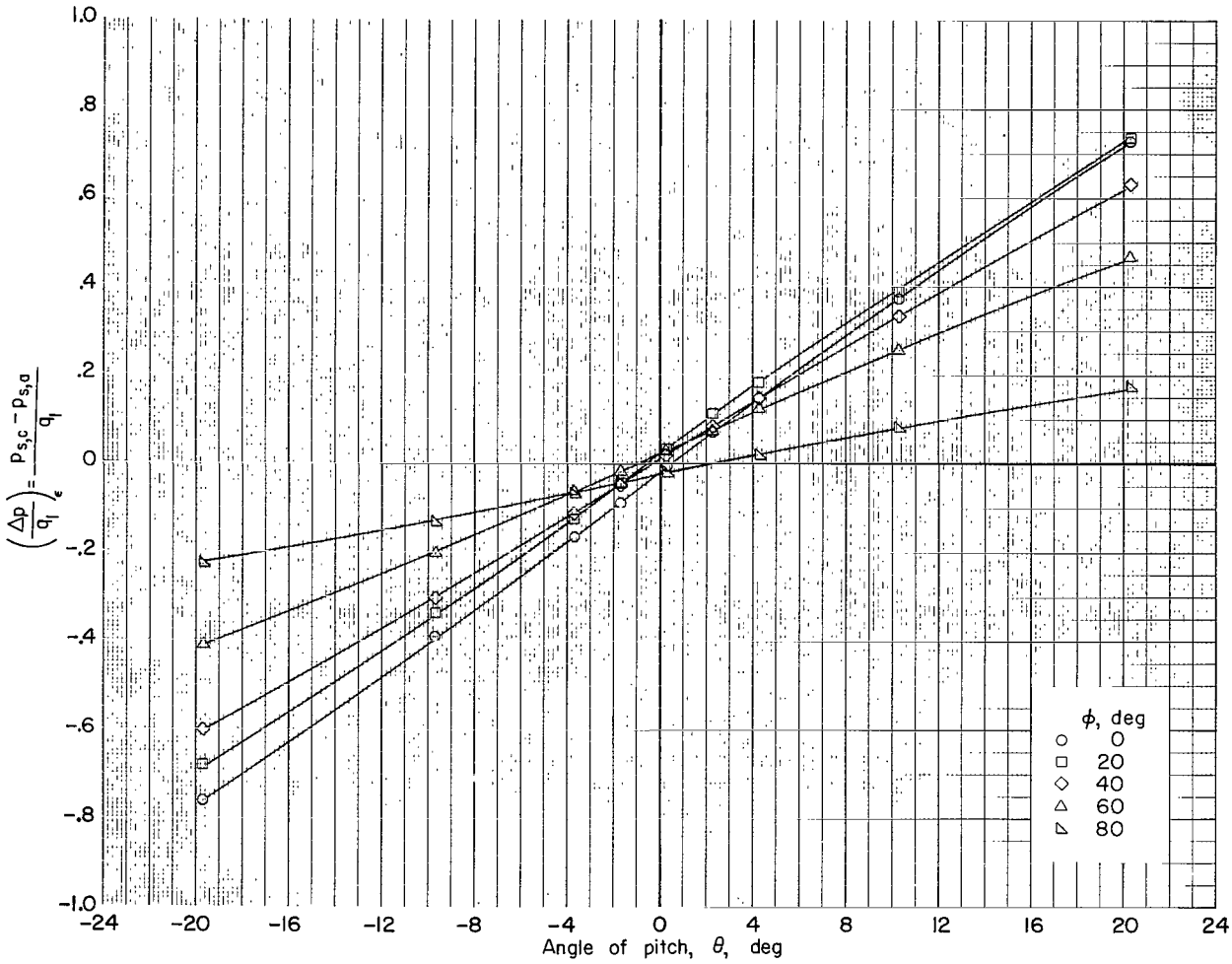

(a) $M_1 = 3.0$; orifices a and c.

Figure 12.- Variation of static pressure differences with angle of pitch. Probe 6.

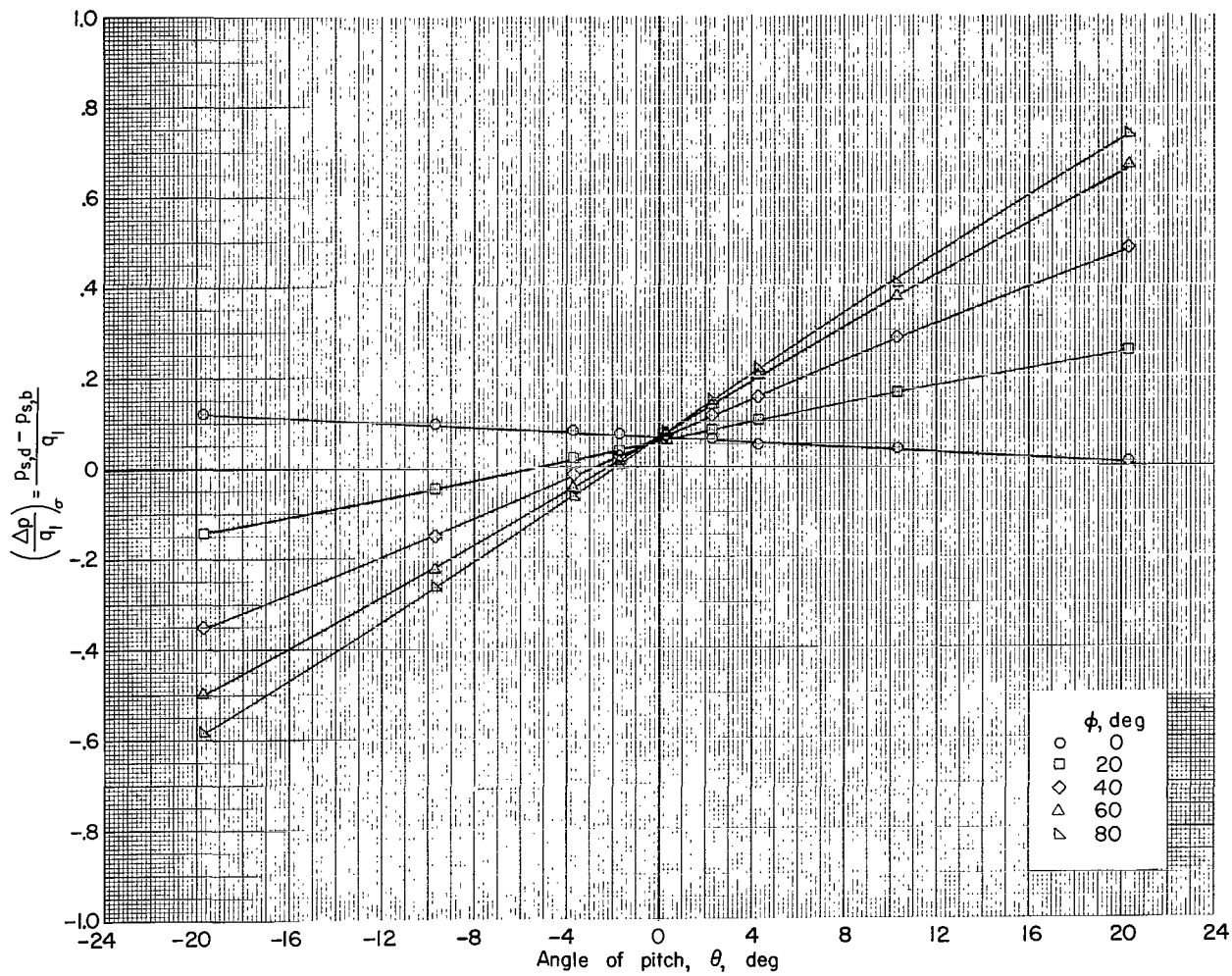

(b) M_1 = 3.0; orifices b and d.

Figure 12.- Continued.

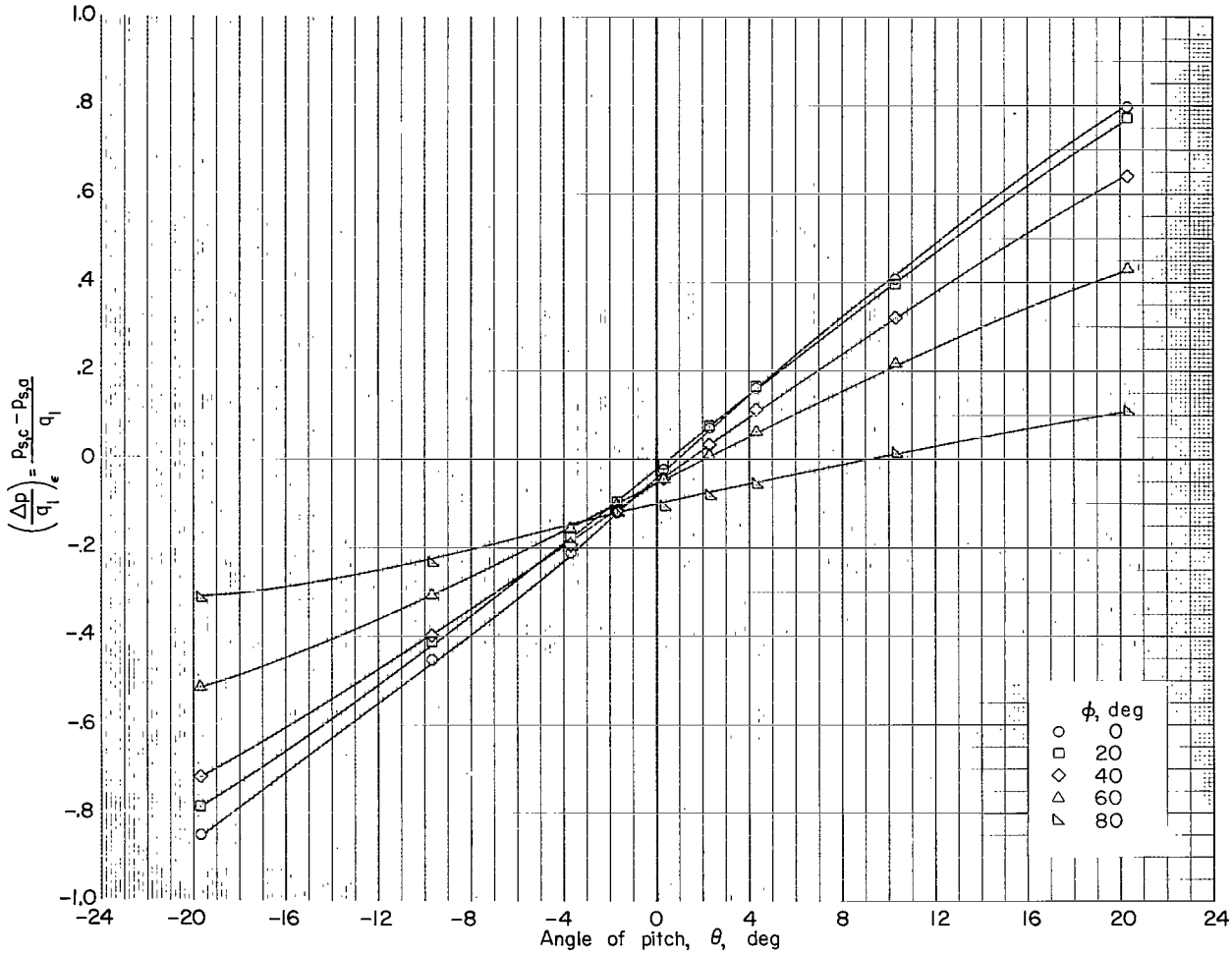

(c) $M_1 = 4.5$; orifices a and c.

Figure 12.- Continued.

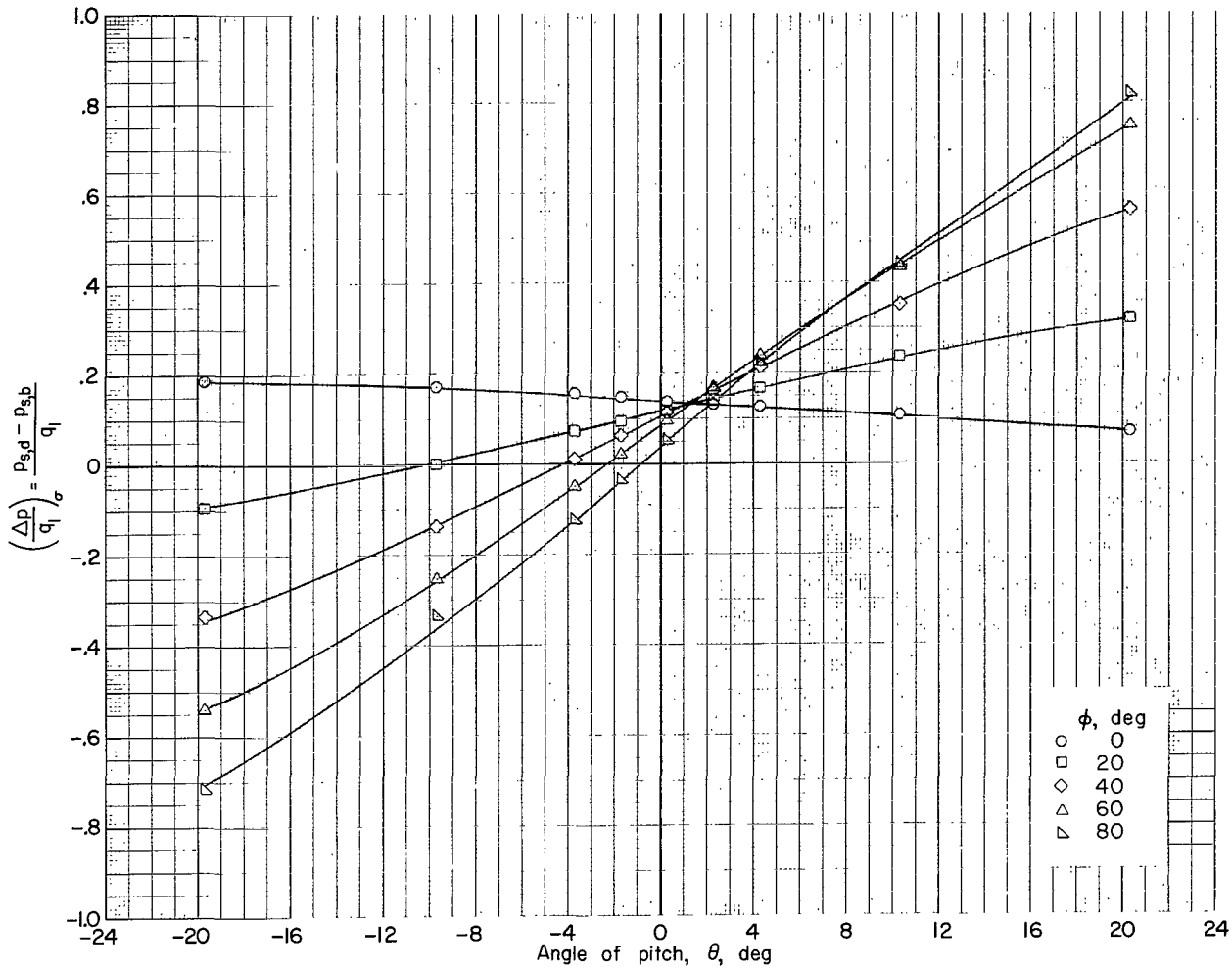

(d) $M_1 = 4.5$; orifices b and d.

Figure 12.- Continued.

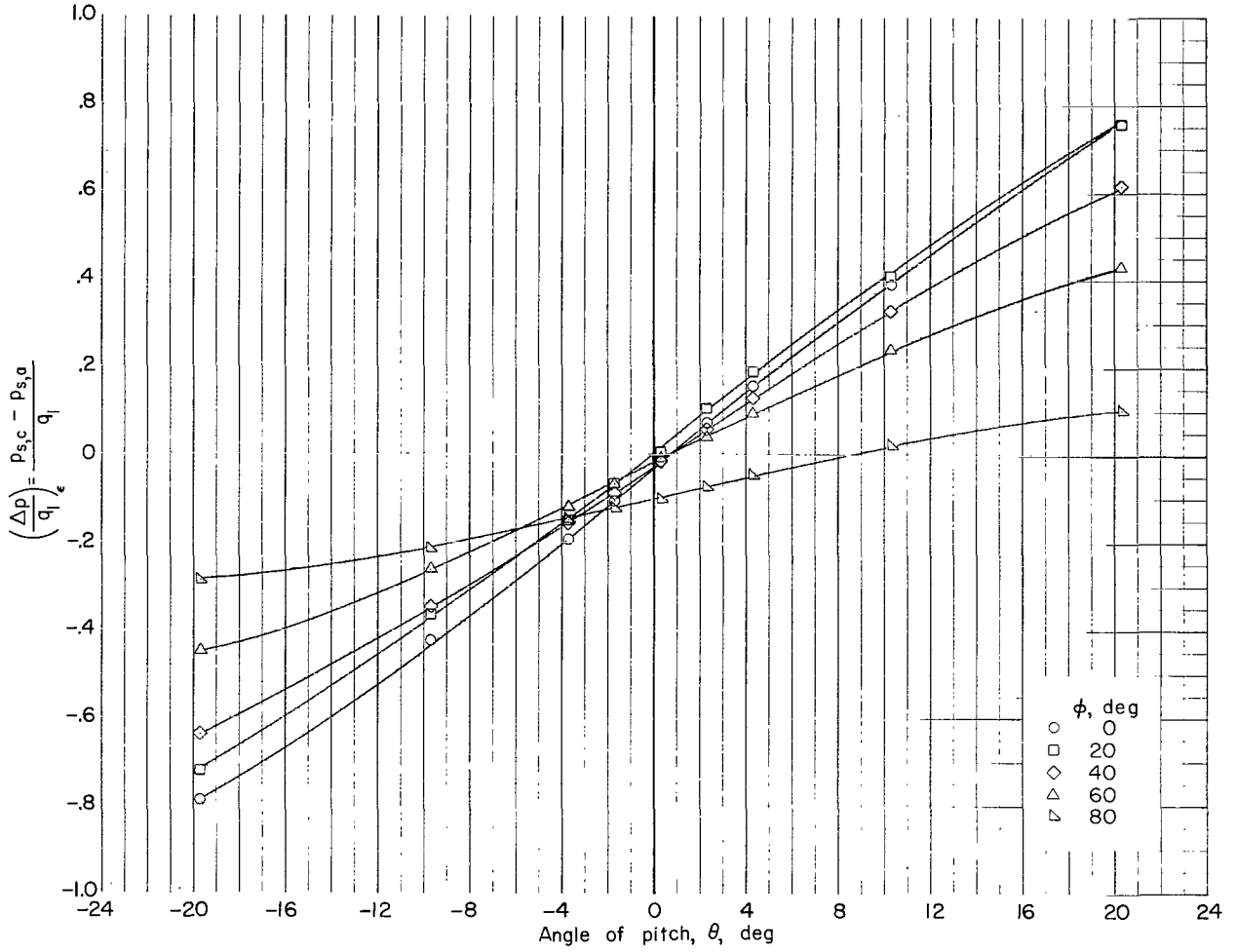

(e) M_1 = 6.0; orifices a and c.

Figure 12.- Continued.

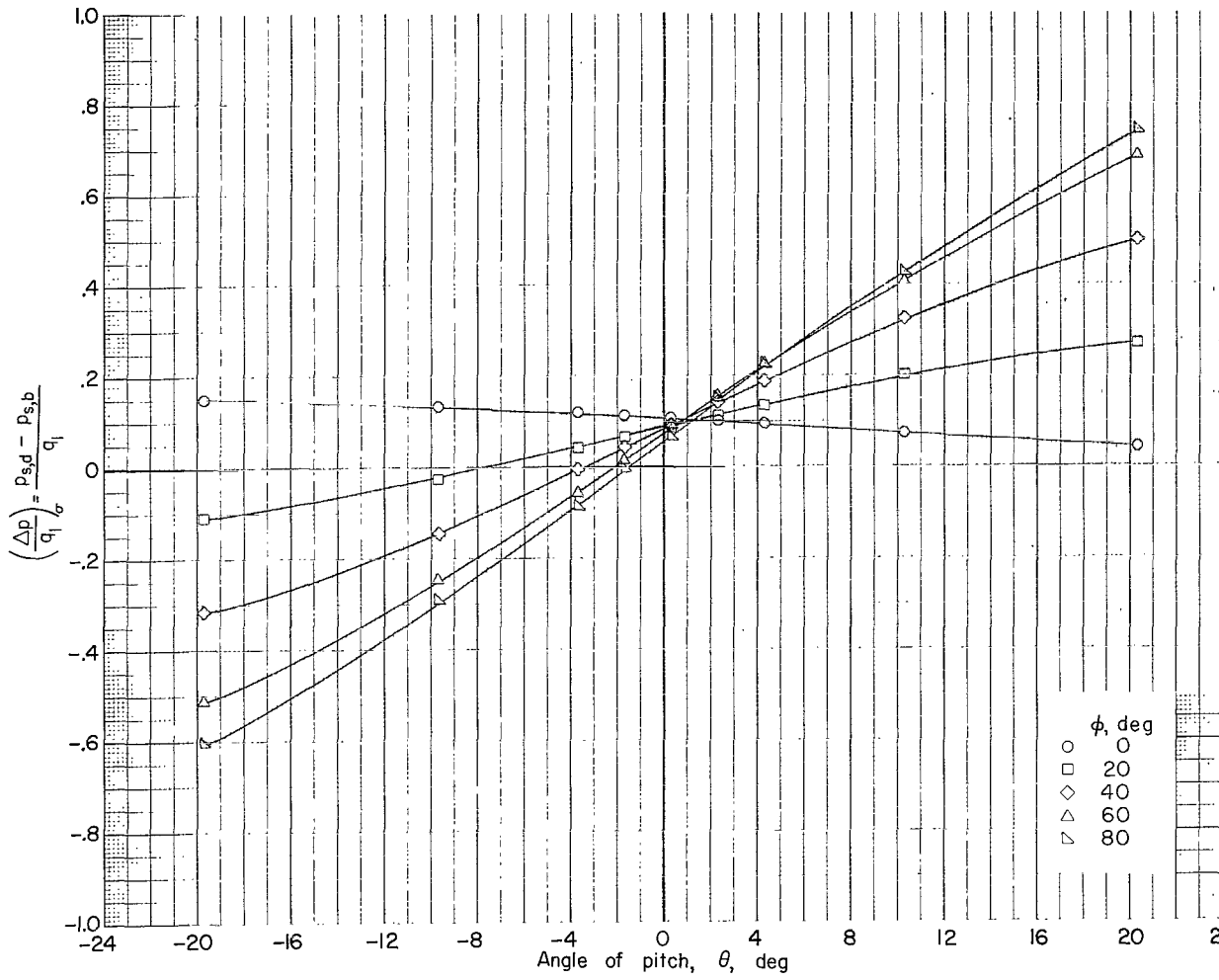

(f) M_1 = 6.0; orifices b and d.

Figure 12.- Concluded.

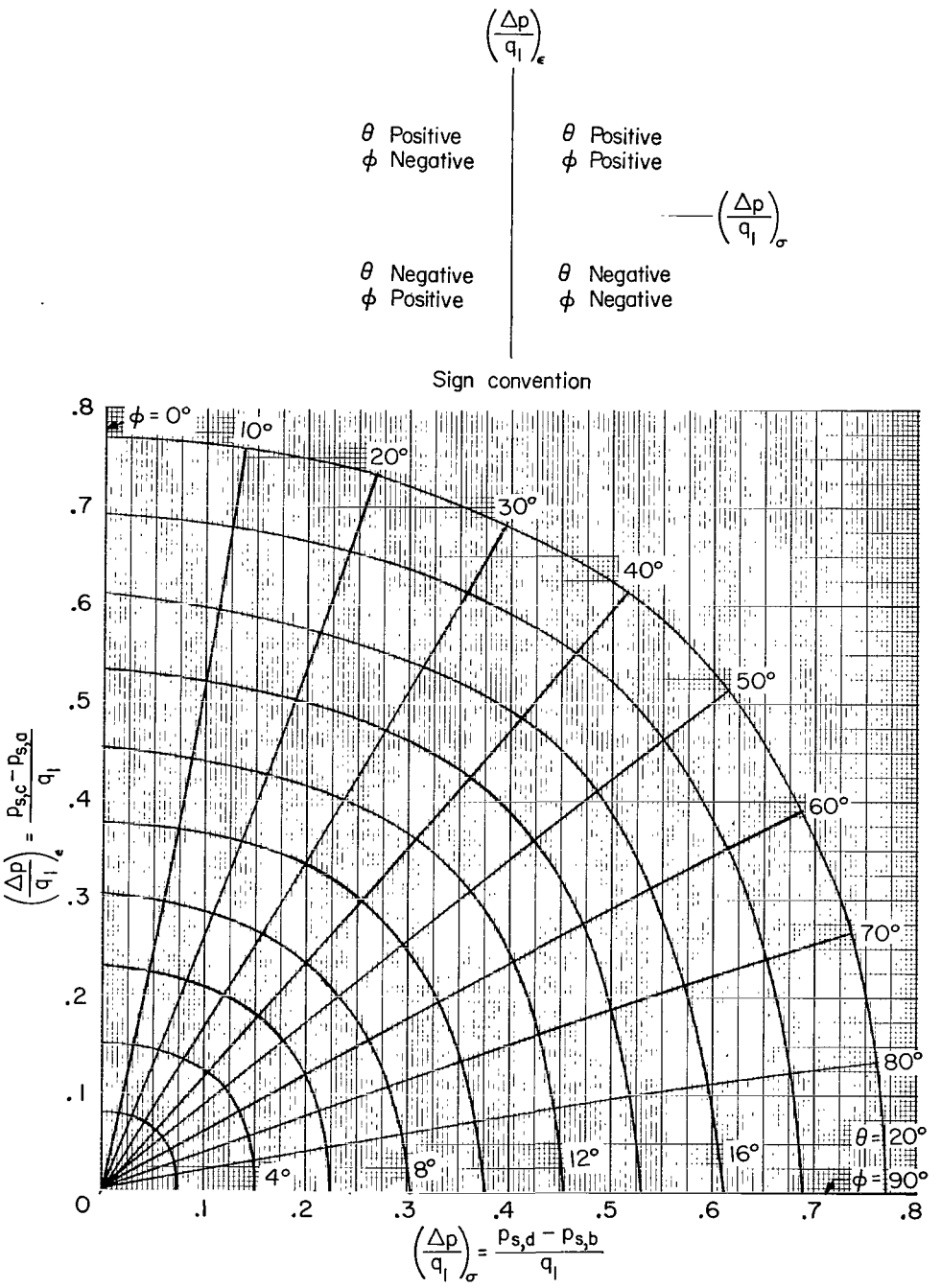

(a) $M_1 = 3.0$.

Figure 13.- Chart for determination of pitch and roll angles. Probe 1.

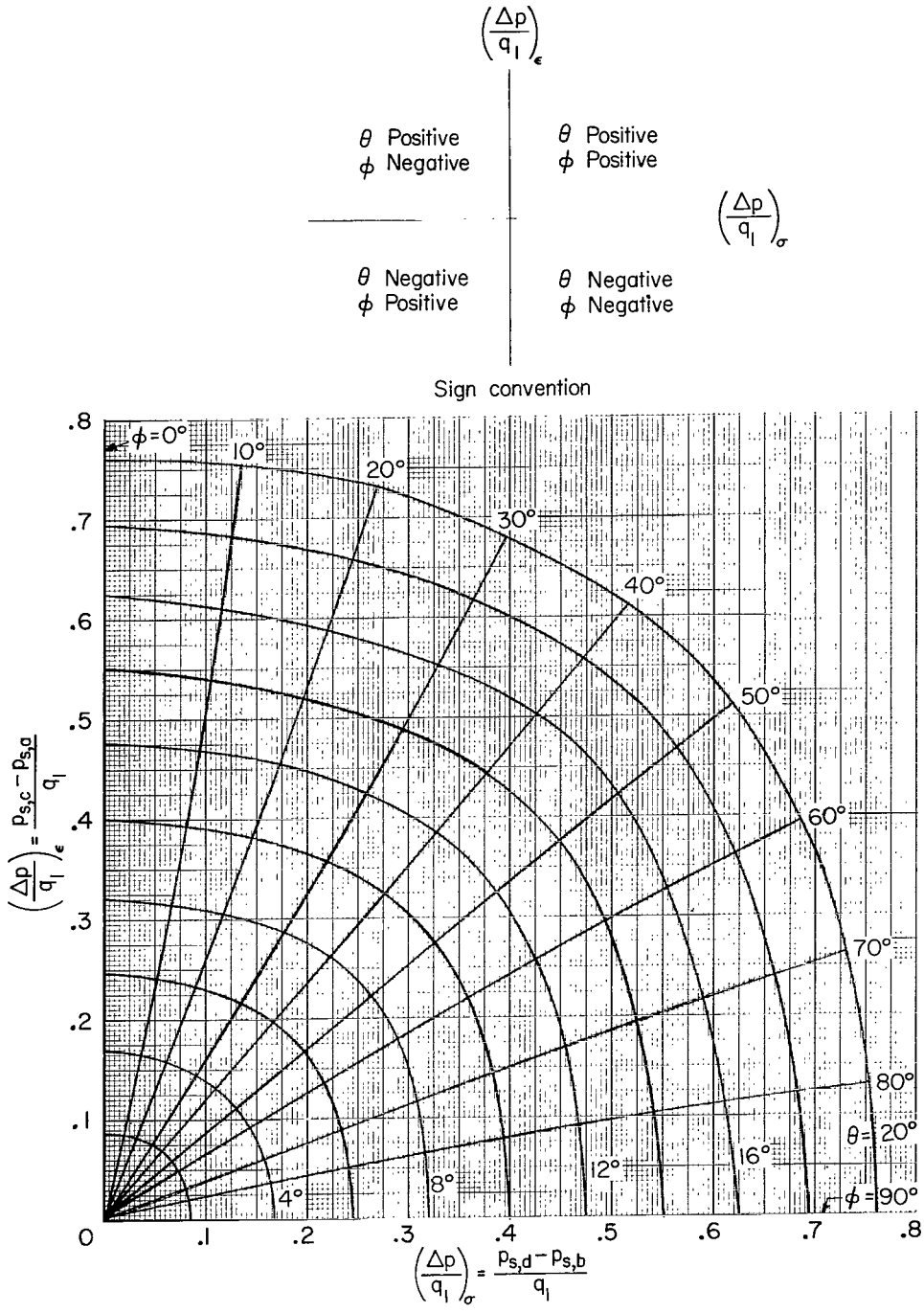

(b) M_l = 4.5.

Figure 13.- Continued.

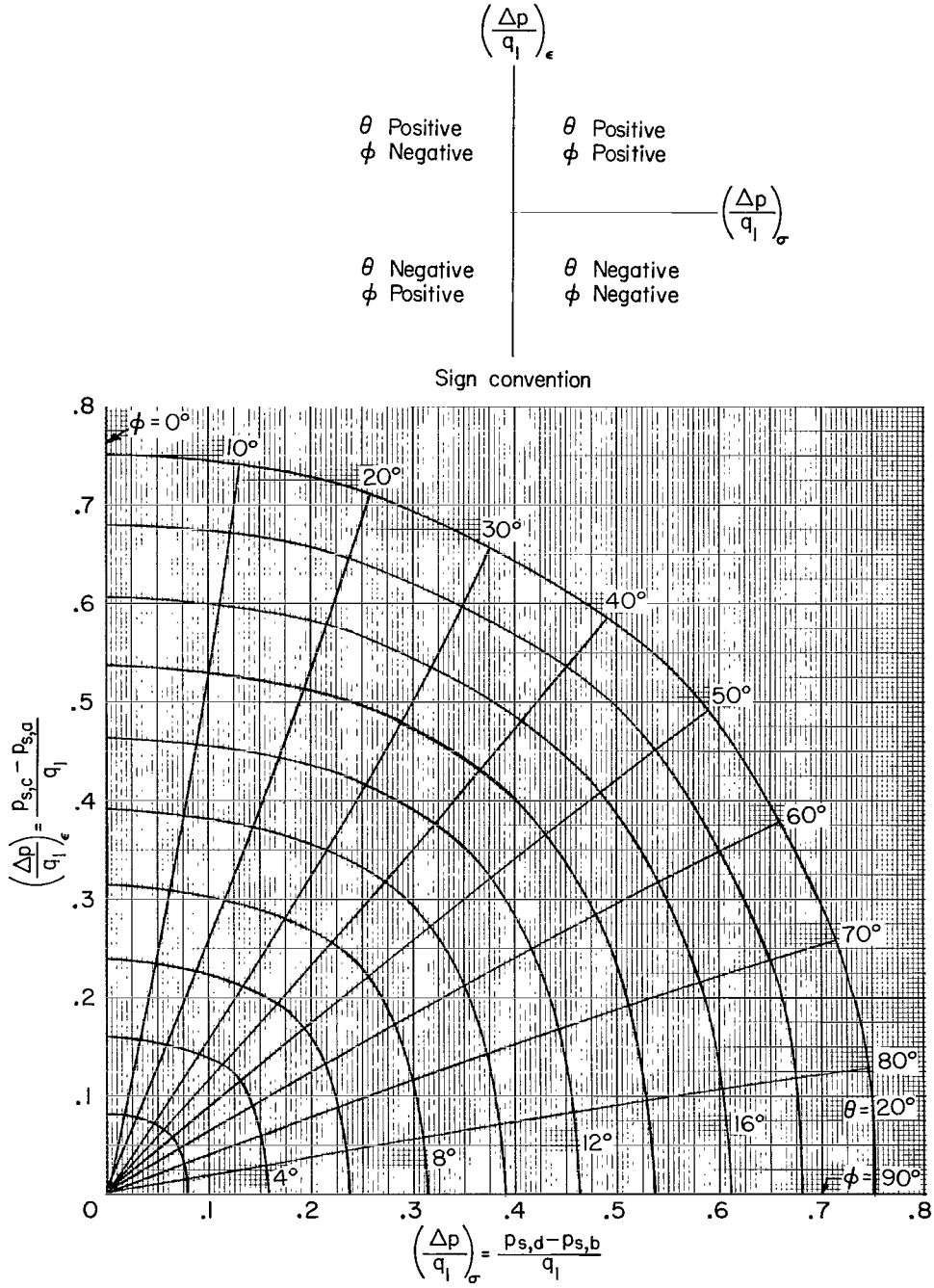

(c) $M_1 = 6.0$.

Figure 13.- Concluded.

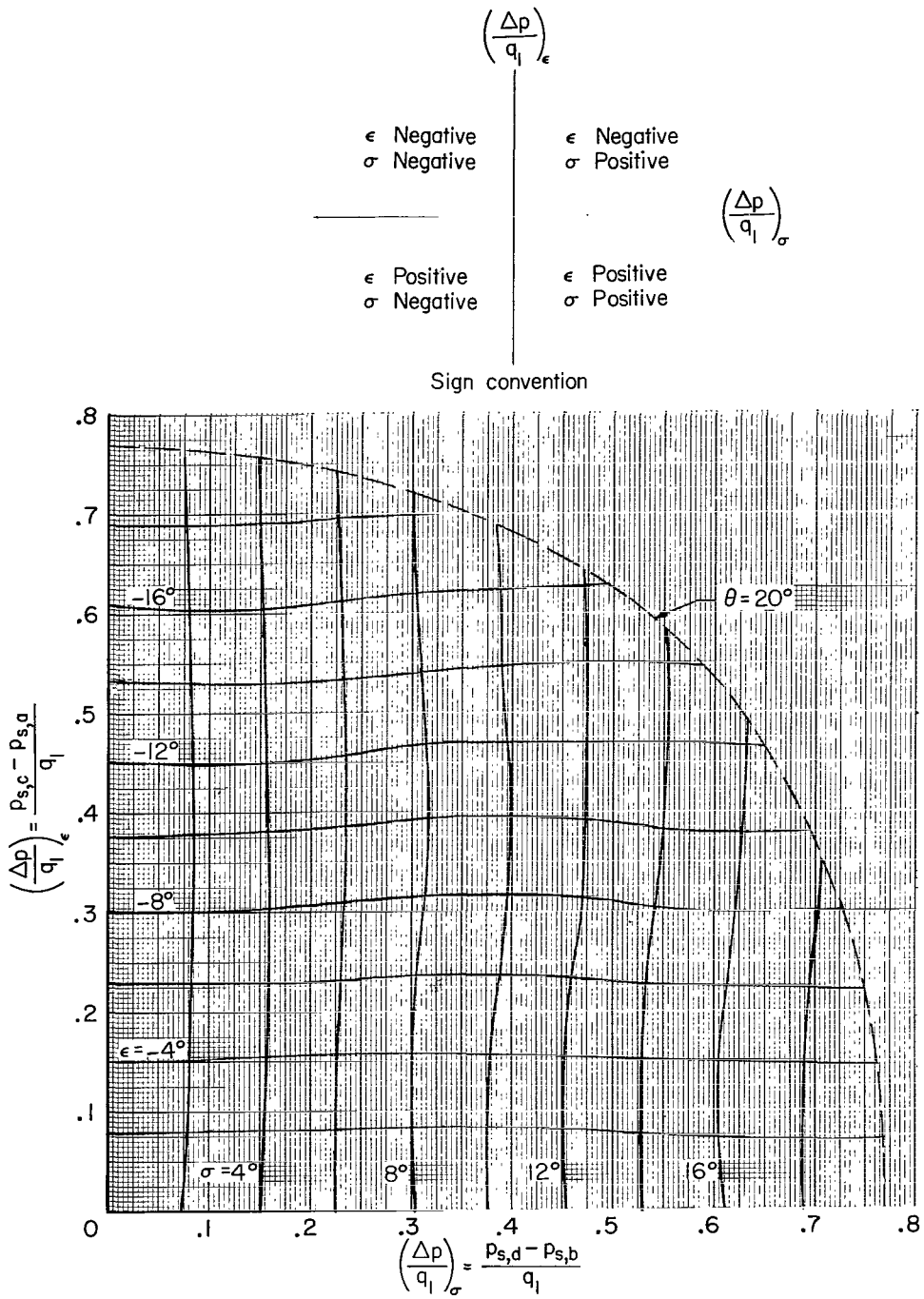

(a) $M_1 = 3.0$.

Figure 14.- Chart for determination of downwash and sidewash angles. Probe 1.

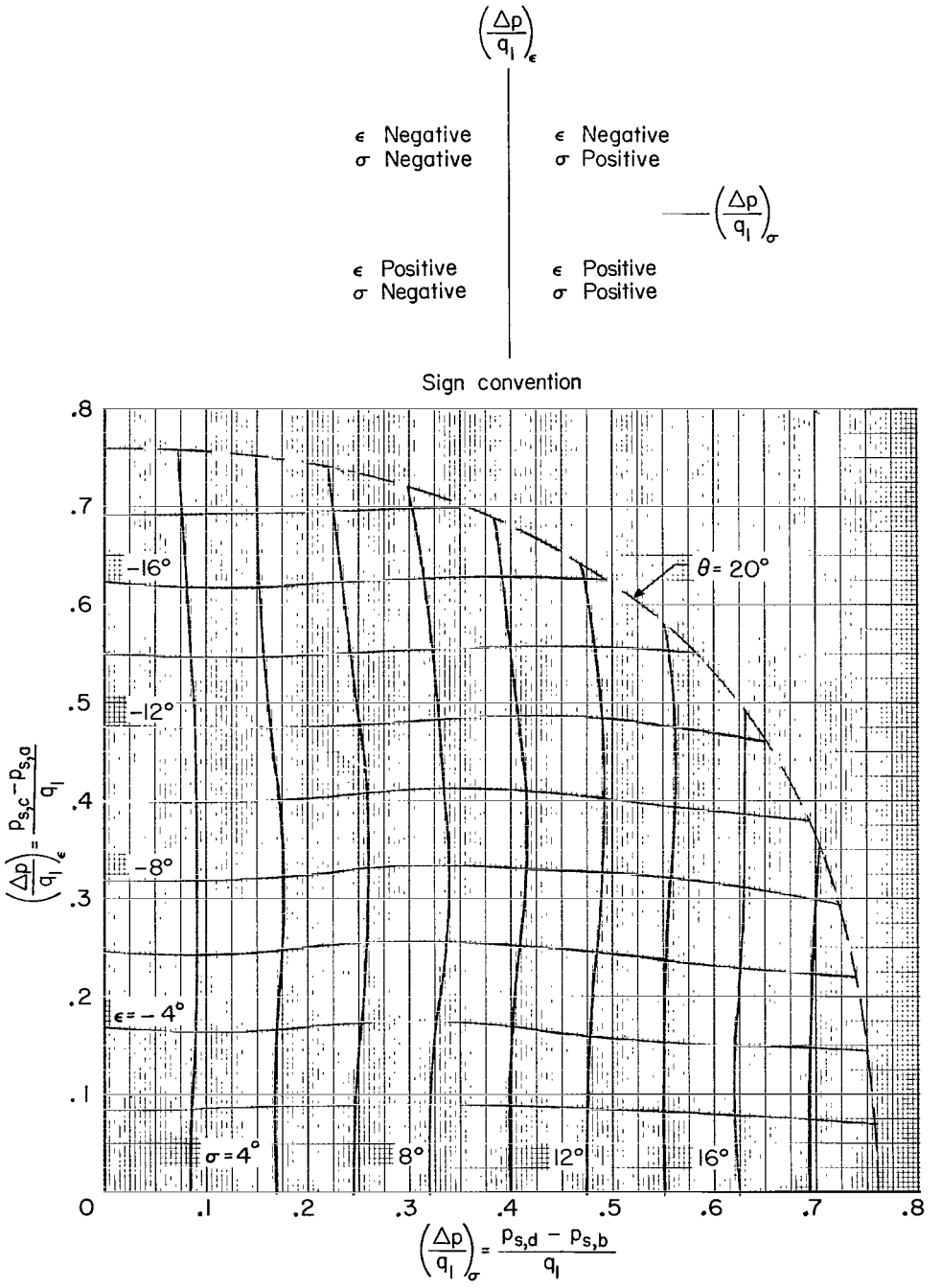

(b) $M_1 = 4.5$.

Figure 14.- Continued.

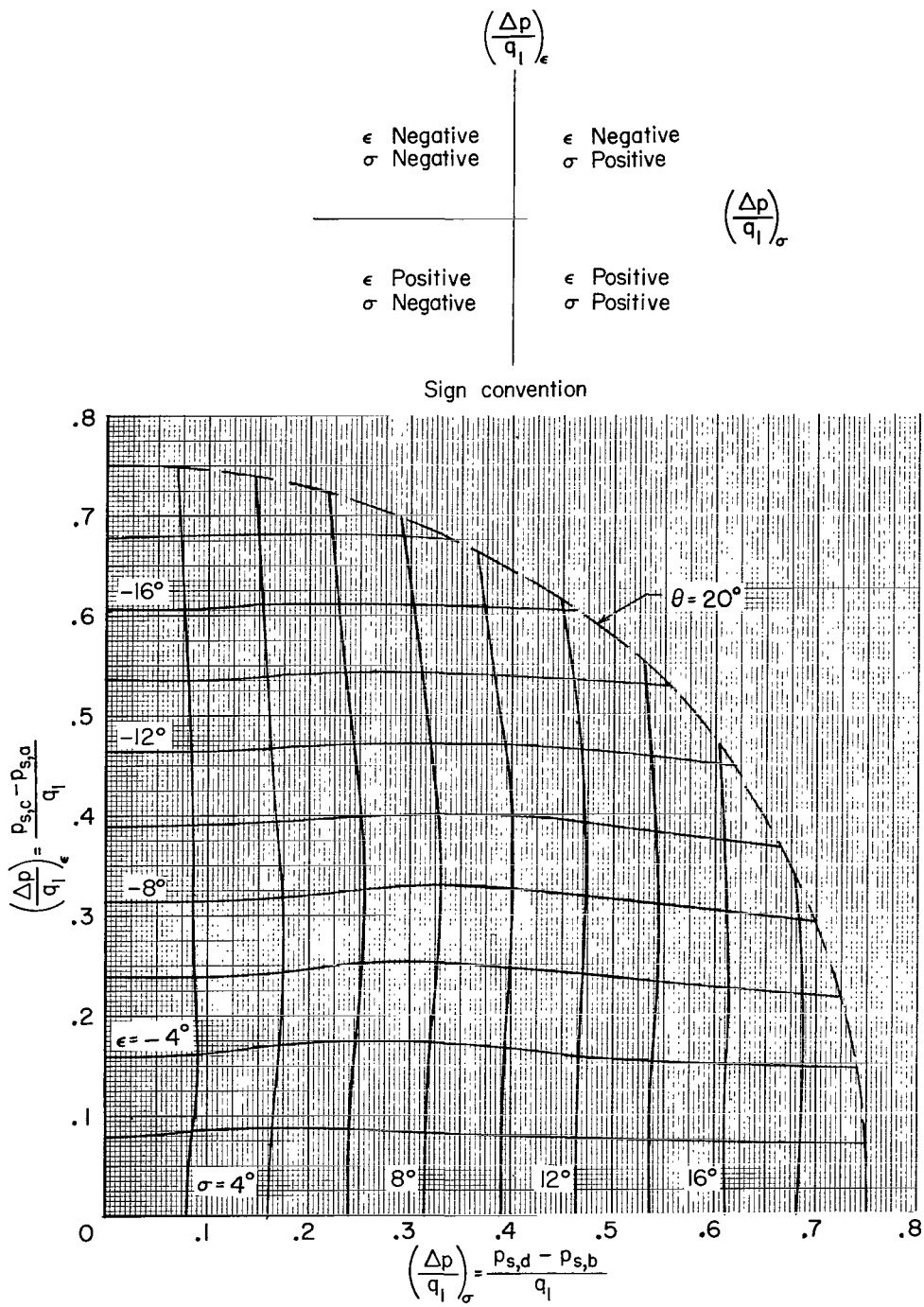

(c) M_l = 6.0.

Figure 14.- Concluded.

3/18/85

"The aeronautical and space activities of the United States shall be conducted so as to contribute . . . to the expansion of human knowledge of phenomena in the atmosphere and space. The Administration shall provide for the widest practicable and appropriate dissemination of information concerning its activities and the results thereof."

—NATIONAL AERONAUTICS AND SPACE ACT OF 1958

NASA SCIENTIFIC AND TECHNICAL PUBLICATIONS

TECHNICAL REPORTS: Scientific and technical information considered important, complete, and a lasting contribution to existing knowledge.

TECHNICAL NOTES: Information less broad in scope but nevertheless of importance as a contribution to existing knowledge.

TECHNICAL MEMORANDUMS: Information receiving limited distribution because of preliminary data, security classification, or other reasons.

CONTRACTOR REPORTS: Technical information generated in connection with a NASA contract or grant and released under NASA auspices.

TECHNICAL TRANSLATIONS: Information published in a foreign language considered to merit NASA distribution in English.

TECHNICAL REPRINTS: Information derived from NASA activities and initially published in the form of journal articles.

SPECIAL PUBLICATIONS: Information derived from or of value to NASA activities but not necessarily reporting the results of individual NASA-programmed scientific efforts. Publications include conference proceedings, monographs, data compilations, handbooks, sourcebooks, and special bibliographies.

Details on the availability of these publications may be obtained from:

SCIENTIFIC AND TECHNICAL INFORMATION DIVISION

NATIONAL AERONAUTICS AND SPACE ADMINISTRATION

Washington, D.C. 20546